



ISKENDERUN TECHNICAL
UNIVERSITY
INSTITUTE OF GRADUATE STUDIES

**MASTER
THESIS**

**DESIGN AND PROTOTYPE
APPLICATION OF THE
AUTONOMOUS AND PORTABLE
HYDROGEN GENERATOR SYSTEM
SUPPORTED BY SODIUM
BOROHYDRIDE**

Feride Cansu ISKENDEROGLU

DEPARTMENT OF MECHANICAL
ENGINEERING

JANUARY 2022





**DESIGN AND PROTOTYPE APPLICATION OF THE AUTONOMOUS
AND PORTABLE HYDROGEN GENERATOR SYSTEM SUPPORTED BY
SODIUM BOROHYDRIDE**

Feride Cansu İSKENDEROĞLU

**THE THESIS OF MASTER OF SCIENCE
IN
THE DEPARTMENT OF MECHANICAL ENGINEERING**

**THE GRADUATE EDUCATION INSTITUTE
OF ISKENDERUN TECHNICAL UNIVERSITY**

JANUARY 2022

The thesis study, which named “DESIGN AND PROTOTYPE APPLICATION OF THE AUTONOMOUS AND PORTABLE HYDROGEN GENERATOR SYSTEM SUPPORTED BY SODIUM BOROHYDRIDE” prepared by Feride Cansu İSKENDEROĞLU, was accepted with UNITY OF VOTE / MULTIPLE VOTE as a MASTER'S THESIS in the Mechanical Engineering Department of Iskenderun Technical University by the following jury.

Supervisor: Assoc. Prof. Dr. Mustafa Kaan BALTACIOĞLU

Department of Mechatronic Engineering, Iskenderun Technical University

I approve/disapprove that this thesis is a Master's Thesis in terms of scope and quality.

.....
.....

Chairman: Assoc. Prof. Dr. Hüseyin Turan ARAT

Department of Mechanical Engineering, Sinop University

I approve/disapprove that this thesis is a Master's Thesis in terms of scope and quality.

.....
.....

Member: Assist. Prof. Dr. Çağlar CONKER

Department of Mechatronic Engineering, Iskenderun Technical University

I approve/disapprove that this thesis is a Master's Thesis in terms of scope and quality.

.....
.....

Thesis Defense Date: 31/01/2022

I certify that the thesis, accepted by the board of jury, titled above was reviewed, approved and fulfills the requirements for the award of degree of the Master of Science.

.....

Assoc. Prof. Dr. Ersin BAHCECI
Director of Graduate Education Institute

ETHICAL STATEMENT

In this thesis study, which I prepared in accordance with the Thesis Writing Rules of the Iskenderun Technical University's Graduate Education Institute;

- It is my responsibility to ensure that the thesis should be same as the original copy when viewed on the computer screen, since no changes can be made on the thesis by the Council of Higher Education (Yükseköğretim Kurulu);
 - All the data, information and documents, that I presented in this thesis, were obtained within the framework of academic and ethical rules;
 - All the information, documents, evaluations and results, that I presented in this thesis, were presented in accordance with the scientific ethics;
 - All the works, that used in this thesis, were cited with making appropriate references,
 - All the data, that used in this thesis, were not made any changes,
 - The work, that have presented in this thesis, is original,
- I declare that the above items are true. Otherwise, I declare that I accept all forfeiture that may arise against me.

İmza

Feride Cansu İSKENDEROĞLU

...../...../.....



"I believe that water will one day be used as a fuel, that hydrogen and oxygen, which constitute it, used alone or simultaneously, will provide an inexhaustible source of heat and light of an intensity that coal cannot have."

The Mysterious Island, Jules Verne



DESIGN AND PROTOTYPE APPLICATION OF THE AUTONOMOUS AND
PORTABLE HYDROGEN GENERATOR SYSTEM SUPPORTED BY SODIUM
BOROHYDRIDE

(M. Sc. Thesis)

Feride Cansu İSKENDEROĞLU

ISKENDERUN TECHNICAL UNIVERSITY
ENGINEERING AND SCIENCE INSTITUTE

January 2022

ABSTRACT

In this experimental thesis, it is aimed to design and prototype a hydrogen generator working with sodium borohydride to provide lightly and more efficient hydrogen gas production. For this purpose, a prototype with both a compact structure and autonomous control is produced, and unlike the hydrogen generators available in the literature, it works with solid sodium borohydride dosing logic. In addition, a cheap, efficiently and environmentally friendly alternative catalyst solution is sought for hydrogen production instead of costly and high yielding noble metal catalysts used in the sodium borohydride's hydrolysis reaction. A high metal content slag byproduct is used to synthesize this catalyst alternative. Catalysts synthesized using slag; Performance tests were carried out using various parameters, for example, catalyst concentration, component ratios, reaction temperature. Considering the Co-B catalyst studies in the literature, it was seen that the hydrogen gas production rate rise in the range of 5 and 10 times. The best performances were demonstrated by acid-treated slag catalyst samples supplemented with 40% and 50% Co-B with preheating at 50 °C with catalyst hydrogen production rates of approximately 65 L/min.g in 25 minutes. The prototype, controlled by Adunio Uno, consists of 4 different compartments, the water and catalyst mixture was injected onto solid sodium borohydride with water pumps and nozzles. Thus, fuel wastage is reduced by 15%; this is achieved by using multiple fuel chambers instead of a single fuel chamber. In addition, with the use of slag, catalyst costs are reduced by 25% and 35%. The test results of the catalyst samples were compared and discussed with the optimum liquid injection amount and optimum mixing percentages. The performance analyzes of the prototype and catalysts were completed utilizing 20 ml of distilled water and 2 g of NaBH₄. These results were showed the prototype has a relatively consistent hydrogen gas stream of around 17.5 L/min and the total flow is 343.46 L for 20 min. As a result; the tightness and performance tests of the prototype were investigated using different catalyst samples during 1 hour, and the results were investigated in depth. The average flow rate of this 4-part autonomous generator is approximately 3.00 L/min.g_{catalyst} during 1 h. In the working cycle, the soft ripples have spied on the hydrogen-produced amount from time to time.

Key Words : Sodium Borohydride, Hydrogen, Renewable Energy, Autonomous Systems, Portable Power Generator

Page : 94

Supervisor : Assoc. Prof. Dr. Mustafa Kaan Baltacıoğlu

SODYUM BOROHİDRİT DESTEKLİ OTONOM VE TAŞINABİLİR HİDROJEN JENERATÖR SİSTEMİ TASARIMI VE PROTOTİP UYGULAMASI

(Yüksek Lisans Tezi)

Feride Cansu İSKENDEROĞLU

İSKENDERUN TEKNİK ÜNİVERSİTESİ
LİSANSÜSTÜ EĞİTİM ENSTİTÜSÜ

Ocak 2022

ÖZET

Bu deneysel tezde, daha hafif ve verimli hidrojen gazı üretimi sağlamak için sodyum borhidrür ile çalışan bir hidrojen jeneratörü tasarlamak ve prototiplemek amaçlanmıştır. Bu amaçla hem kompakt yapıya sahip hem de otonom kontrole sahip bir prototip üretilmiş olup, literatürde bulunan hidrojen jeneratörlerinden farklı olarak katı sodyum borhidrür dozajlama mantığı ile çalışmaktadır. Ayrıca hidrojen üretimi için sodyum borhidrürün hidroliz reaksiyonunda kullanılan yüksek verimli pahalı asal metal katalizörler yerine ucuz, verimli ve çevre dostu alternatif bir katalizör çözümü aranmaktadır. Bu katalizör alternatifini sentezlemek için yüksek metal içerikli bir cüruf yan ürünü kullanılır. Cüruf kullanılarak sentezlenen katalizörler; Performans testleri, bileşen oranları, katalizör konsantrasyonu, reaksiyon sıcaklığı gibi bir dizi farklı parametre kullanılarak gerçekleştirilmiştir. Literatürdeki Co-B katalizör çalışmaları dikkate alındığında hidrojen üretim hızının 5 ile 10 kat arasında arttığı gözlemlenmiştir. En iyi performanslar, 25 dakikada yaklaşık 65 L/dk. katalizör hidrojen üretim oranları ile 50 °C'de ön ısıtma ile %40 ve %50 Co-B ile desteklenmiş asitle muamele edilmiş BFS katalizör numuneleri ile gösterildi. Adunio Uno tarafından kontrol edilen prototip, 4 farklı bölmeden oluşuyor, su ve katalizör karışımı, su pompaları ve nozullar ile katı sodyum borhidrür üzerine damlatıldı. Böylece yakıt israfı %15 oranında azaltıldı; bu, tek bir yakıt odası yerine birden fazla yakıt odası kullanılarak elde edilir. Ayrıca cüruf kullanımı ile katalizör maliyetleri %25 ve %35 oranında azalmaktadır. Katalizör numunelerinin test sonuçları, optimum sıvı enjeksiyon miktarı ve optimum karışım yüzdeleri ile karşılaştırılmış ve tartışılmıştır. Prototipin deneyleri 2 g NaBH₄ ve 20 ml distile su kullanılarak gerçekleştirilmiştir. Prototip, nispeten sabit isteğe bağlı hidrojen akış hızları (yaklaşık 17,5 L/dk) gösterdi ve toplam akış 20 dakika boyunca 343.46 L'dir. Sonuç olarak; Prototipin sızdırmazlık ve performans testleri, 1 saatlik çalışma sürelerinde farklı katalizör numuneleri kullanılarak araştırılmış ve sonuçlar derinlemesine incelenmiştir. Bu 4 parçalı otonom jeneratörün ortalama akış hızı, 1 saat boyunca yaklaşık 3.00 L/dk.katalizördür. Çalışma döngüsünde, zaman zaman üretilen hidrojen miktarında yumuşak dalgalanmalar gözlemlenmiştir.

Anahtar Kelimeler : Sodyum Borhidrür, Hidrojen, Yenilenebilir Enerji, Otonom Sistemler, Taşınabilir Güç Jeneratörü

Sayfa Adedi : 94

Danışman : Doç. Dr. Mustafa Kaan Baltacıoğlu

ACKNOWLEDGMENTS

I want to thank to my thesis advisor, Assoc. Prof. Dr. Mustafa Kaan Baltacıođlu, who trusted and supported me, respected my ideas from the very first moment, additionally, give with professional advice and helped me move forward, helped me open my own way and have new experiences. I am thinking to it has been a pleasure to work with him (but I know it has been a real challenge for him). All-time, I will be most grateful for all valuable advice and his brotherhood that he has given me throughout my education. Furthermore, I shall also thank to the financial and moral support of Prof. Dr. Ertuđrul Baltacıođlu. I wish to thank the dissertation committee members. Assoc. Prof. Dr. H. Turan ARAT and Assist. Prof. Dr. ađlar Conker, for their time and efforts on my dissertation. It is an honor for me to have them as my committee members. Also, I want to thank my valuable academicians whom I had find a chance to work with; H. Turan ARAT, ađlar Conker, M. Hakan Demir and H.Hüseyin Bilgi. I would like to thank my spiritual sisters (Dr. Ariana Baldinelli, Rya Yalın, Yađmur Budak, Ayşenur Ertan, Betl HOTMAN, Şebnem Akar) and my whole family who have supported, believed, loved and respected my ideas since the first day we met. I wish to thank my black box Başak Gndz, Sedat, Soner and Sema İskenderođlu who reminded me of my dreams and supported me when I fell, got tired and gave up.

I wish to dedicate this thesis to my mom and my father, Ayşe and Cemalittin İskenderođlu, for their support, endless love, sacrifice and encouragement for the duration of my life, for always being behind me, respecting all my decision, allowing me to build myself .

My Dear Atatrk! Today, the Republic you founded, the principles and reforms you made, your vision and leadership, and thanks to you; I was able to come to these days with alone as a free, modern, secular Turkish scientist and woman whose true mentor is science, in this geography where I belong. I am grateful to you and I am on your leave until I die.

I have completed the first milestone towards becoming the scientist I have dreamed of since my childhood. Everything is just beginning...

TABLE OF CONTENTS

	Page
ABSTRACT	iv
ÖZET	v
ACKNOWLEDGMENTS	vi
TABLE OF CONTENTS.....	vii
LIST OF TABLES.....	x
LIST OF FIGURES	xi
LIST OF PICTURES	xiv
LIST OF SYMBOLS AND ABBREVIATIONS	xv
1. INTRODUCTION.....	1
2. LITERATURE SUMMARY	5
2.1. Autonomous Systems.....	5
2.2. Energy Production	5
2.3. Power Supply Types for Portable Application	6
2.4. Fuel cells and Battery Systems for Nonstationary Applications.....	8
2.4.1. Fuel cell applications of UAVs	13
2.5. Hydrogen Energy	13
2.5.1. Hydrogen energy storage types	15
2.6. Sodium Borohydride (NaBH ₄)	20
2.6.1. Catalysts	22
2.6.2. Blast furnace slag	25
2.7. Development of the Hydrogen Generators	27
3. MATERIALS, EXPERIMENTAL METHOD, SETUP, TEST RIG AND PROTOTYPE DESIGN	29

	Page
3.1. Materials	29
3.1.1. Chemical materials	29
3.1.2. Tools and apparatus	32
3.1.3. Glass materials	34
3.1.4. Prototype material and electronic apparatus	35
3.1.5. Characterization devices	41
3.2. Experimental Method, Setup and Test Rig	43
3.2.1. Experimental method of the BFS-Co-B catalysts synthesis	43
3.2.2. Experimental setup and test rig of the hydrolysis reactions of the NaBH ₄	45
3.2.3. Experimental setup and test rig of the hydrogen generator prototype	47
3.3. Prototype Design.....	48
3.3.1. 3D design and analysis of hydrogen generator	49
3.3.2. Autonomous control card design and writing control system algorithms	51
4. RESULTS	54
4.1. Characterization Analyses of BFS Catalysts	54
4.1.1. XRD characterization analyses	54
4.1.2. SEM characterization analyses	57
4.2. Performance Analyses of BFS Catalysts	59
4.2.1. Performance impact of HCl acid on BFS powder and BFS catalysts on hydrolysis reaction performance	59
4.2.2. Performance impact of Co nano powder % quantity on hydrolysis reaction performance	60
4.2.3. Performance impact of the catalyst quantity on hydrolysis reaction performance	64
4.2.4. Performance impact of the NaBH ₄ quantity on hydrolysis reaction performance	66

	Page
4.2.5. Performance impact of the temperature on hydrolysis reaction performance	68
4.2.6. Performance impact of the PVA coating on hydrolysis reaction performance	70
4.3. Performance Results of Prototype Design	73
4.3.1. Manual performance experiments of the prototype	73
4.3.2. Autonomous performance experiments of the prototype	74
5. DISCUSSIONS	77
5.1. Discussions of BFS Catalysts	77
5.2. Discussion of Hydrogen Generator Prototype	79
6. CONCLUSIONS	81
REFERENCES	83
RESUME	92
INDEX	95

LIST OF TABLES

Table	Page
Table 2.1. Comparing of battery technologies and fuel cell systems	7
Table 2.2. Detailed comparing of battery and PEMFC and hydrogen tank system with same nominal power	9
Table 2.3. Detailed comparing of fuel cell types	11
Table 2.4. Comparing of UAV projects working with fuel cell systems	13
Table 2.5. Comparing of hydrogen storage technologies	18
Table 2.6. The hydrogen gas production features of Co-based catalysts.....	24
Table 2.7. Chemical compound of the BFS powders.....	26
Table 3.1. Technical features of the NaBH ₄ chemical powder	29
Table 3.2. Technical features of the Co micron powder	30
Table 3.3. Chemical compound of the BFS	31
Table 3.4. Technical features of the plexiglass	35
Table 3.5. Technical features of the water solenoid valve - 12V - 1/2"	36
Table 3.6. Technical features of the nozzle	37
Table 3.7. Technical features of the piezo buzzer	39
Table 5.1. The comparison of some Co-based catalysts' hydrogen gas production performance	77
Table 5.2. Comparing of the BFS catalysts samples experimental analysis	78

LIST OF FIGURES

Figures	Page
Figure 2.1. The features of the hydrogen gas.....	14
Figure 2.2. Hydrogen energy using areas	14
Figure 2.3. Source, way and decarbonisation measure of hydrogen energy production	16
Figure 2.4. Transportation and storage options of hydrogen energy	16
Figure 2.5. Hydrogen storage types, their advantages and disadvantages.....	17
Figure 2.6. Hydrogen storage types, their hydrogen capacity and temperature for H ₂ release	19
Figure 2.7. Lewis structure and 3-D structure of Sodium Borohydride chemical powder	20
Figure 2.8. Some support materials for catalyst production	23
Figure 3.1. X-ray Fluorescence analysis of GBFS that are used in thesis	31
Figure 3.2. The flow chart of the preparation steps of the Co-B-BFS(-) catalyst.....	43
Figure 3.3. The flow chart of the preparation steps of the BFS(+) powder.....	44
Figure 3.4. The flow chart of the preparation steps of the Co-B-BFS(+) catalysts.....	45
Figure 3.5. Experimental setup flow chart	46
Figure 3.6. The test rig of the hydrogen generator system	48
Figure 3.7. The design of the hydrogen generator system	49
Figure 3.8. The 3D design of the hydrogen generator system	50
Figure 3.9. The design of the autonomous control system	51
Figure 4.1. XRD peak profiles of the Raw BFS powder	54
Figure 4.2. XRD peak profiles of the 40% Co-B-BFS(-) catalyst	55
Figure 4.3. XRD pattern of 1M HCl acid treated BFS sample	56
Figure 4.4. XRD peak profiles of the 40% Co-B-BFS(+) catalyst	56

Figures	Page
Figure 4.5. (a) SEM image of the Raw BFS powder	58
Figure 4.5. (b) SEM image of the Co-B-BFS(-) catalyst	58
Figure 4.6. (c) SEM image of the BFS(+) powder	58
Figure 4.6. (d) SEM image of the Co-B-BFS(+) catalyst	58
Figure 4.7. The hydrolysis reaction performance analyses of the Raw BFS, the Co-B-BFS(-) and the Co-B-BFS(+) catalysts samples	59
Figure 4.8. The total volume of hydrogen gas of the Raw BFS powder, the Co-B-BFS(-) and the Co-B-BFS(+) catalysts samples	60
Figure 4.9. The hydrolysis reaction performance analyses of the 20% Co-B-BFS(-), 30% Co-B-BFS(-), 40% Co-B-BFS(-) and 50% Co-B-BFS(-) catalysts samples.....	61
Figure 4.10. The total volume of hydrogen gas of the 20% Co-B-BFS(-), 30% Co-B-BFS(-), 40% Co-B-BFS(-) and 50% Co-B-BFS(-) catalysts samples.....	62
Figure 4.11. The hydrolysis reaction performance analyses of the 20% Co-B-BFS(+), 30% Co-B-BFS(+), 40% Co-B-BFS(+) and 50% Co-B-BFS(+) catalysts samples	63
Figure 4.12. The total volume of hydrogen gas of the 20% Co-B-BFS(+), 30% Co-B-BFS(+), 40% Co-B-BFS(+) and 50% Co-B-BFS(+) catalysts samples.....	64
Figure 4.13. The performance analysis of the impact of the catalyst quantity on hydrolysis reaction	65
Figure 4.14. The performance impact of the catalyst quantity on the total volume of hydrogen gas	66
Figure 4.15. The performance analysis of the impact of the NaBH ₄ quantity on hydrolysis reaction	67
Figure 4.16. The performance impact of the NaBH ₄ quantity on the total volume of hydrogen gas	68
Figure 4.17. The performance analysis of the impact of the preheating temperature on hydrolysis reaction variation	69
Figure 4.18. The impact of the preheating temperature on the total hydrogen gas	70

Figures	Page
Figure 4.19. The performance analysis of the impact of the PVA coating on hydrolysis reaction	71
Figure 4.20. The impact of the PVA coating on the total hydrogen gas	72
Figure 4.21. The hydrogen gas production flowrate of the Co Nano powder hydrolysis reaction	73
Figure 4.22. The total hydrogen production of the Co Nano powder hydrolysis reaction	74
Figure 4.23. The working flowrate performance of the Co nano powder catalyst in the 4-part autonomous hydrogen generator	75
Figure 4.24. The working flowrate performance of the Co-B-BFS(+) catalyst in the 4-part autonomous hydrogen generator	76

LIST OF PICTURES

Pictures	Page
Picture 2.1. Sodium borohydride powder	21
Picture 2.2. BFS Production in the Iron-steel factory	25
Picture 3.1. Alicat M-series gas mass flow meter	33
Picture 3.2. PT-100 thermocouple	33
Picture 3.3. Arduino Uno Rev3	34
Picture 3.4. Water solenoid valve - 12V - 1/2"	36
Picture 3.5. Rainbird van spray nozzle	37
Picture 3.6. One way 5V relay module	37
Picture 3.7. 1/4W 330R resistor	38
Picture 3.8. 16x2 LCD display - blue display with I2C solder	38
Picture 3.9. Piezo buzzer.....	39
Picture 3.10. Voltage regulator-LF33CV	39
Picture 3.11. MQ2 type gas sensor	40
Picture 3.12. High precision temperature sensor	40
Picture 3.13. Malvern panalytical EMPYREAN (3rd generation) XRD device	41
Picture 3.14. Thermo fisher scientific apreo S LoVac SEM device	42
Picture 3.15. The granulated raw BFS and the raw BFS supported different %Co-B catalysts	44
Picture 3.16. The 1M HCl-BFS and the 1M HCl-BFS supported different %Co-B catalysts	45
Picture 3.17. Hydrogen gas production system test rig	47
Picture 3.18. A part of the autonomous control system working algorithm	52
Picture 4.3. The impact of environmental conditions on the uncovered NaBH ₄ powder and on the NaBH ₄ /BFS catalyst powder covered with PVA	72

LIST OF SYMBOLS AND ABBREVIATIONS

The symbols and abbreviations that used in this study are presented below with their descriptions.

Symbols	Descriptions
H₂	Hydrogen
H₂O	Water
HCl	Hydrochloric acid
NaBH₄	Sodium borohydride
O₂	Oxygen
OH⁻	Hydroxide
Co	Cobalt
B	Bor
h	hour
L/min	Liter per minute
L/min.g_{catalyst}	Liter per minute*gram of catalyst

Abbreviations	Descriptions
BFS	Blast furnace slag
BFS(-)	Raw/non-acid treated blast furnace slag
BFS(+)	1M HCl acid treated blast furnace slag
GBFS	Granule blast furnace slag
PAFC	Phosphoric acid fuel cell
PCFCS	Proton ceramic fuel cells
PEMFC	Proton exchange membrane fuel cell
PVA	Polyvinyl alcohol
SEM	Scanning electron microscope
SOFC	Solid oxide fuel cell
XRD	X-Ray diffraction

1. INTRODUCTION

Since the beginning of the 21st century, the development in the aerospace sector has accelerated. In addition, autonomous technologies and energy storage solutions play a key role in strategic defence systems such as unmanned aerial vehicles (UAVs), submarines and military portable technologies [1]. The energy demand, that is providing by traditional energy sources, creates some problems such as inadequate power supply for the autonomous and portable systems which are rapidly developing. Today, the energy required for the task periods of the systems is supplied from the batteries. For developing technologies, the batteries are insufficient, their weights are increased the energy consumption of the systems and created transportation problems. One of the developed systems to supply the energy required is the fuel cell systems. Fuel cells, which can operate in light, quiet and grid-independent environments, provide an alternative way to obtain the energy required by portable applications [2]. In this way, autonomous systems that can be used for durable, a long mission time and more demanding missions, can be produced [3]. In these autonomous systems, the energy required of either the electronic system or the whole system can be supplied from the fuel cells. However, the fuel cells are used in the full efficiency in reducing energy and emissions, when some of their disadvantages are eliminated.

The main disadvantage to use the fuel cells is that the hydrogen used as fuel in applications cannot be supplied to the system with a simple and safe way. The compressed hydrogen tank that is one of the hydrogen storage methods, the system applications of these tanks create a few disadvantages such as weight, safety, volume and energy density of systems are reduced.

One of the safest way to hydrogen storage are using the solid-state metal hydride tanks or chemical compounds such as sodium boron hydride (NaBH_4) [4]. The NaBH_4 that uses often in recent studies, has become a popular H_2 source, due to the advantages such as high hydrogen storage capacity, producibility as needed, and non-flammable or non-explosive [5]. All over the world, studies to make hydrogen production from sodium boron hydride more efficient have gained intensity. However, the design and prototype of portable systems where hydrogen can be produced from this chemical is very scarce. According to the findings of studies conducted in recent years, fuel cells constitute an alternative option in terms of producing durable, long-term and autonomous systems that can be used for demanding tasks

[3]. Most of these studies are based on the more efficient and faster production of H_2 from the $NaBH_4$ hydride. The designs of hydrogen reactor and auxiliary equipment should be developed by considering systemic conditions such as weight, volume and aerodynamic structure in portable applications as well as in defence system applications such as UAV and submarine. While most reactor designs are unsuitable for autonomous system applications, the $NaBH_4$ solutions are generally used in designed systems.

Principles and Objectives of the Thesis

Two major aims were addressed in this thesis:

Inexpensive and efficient catalyst synthesis to be used in the hydrolysis of $NaBH_4$

This thesis is to prepare new catalysts for $NaBH_4$ hydrolysis reaction, which is a solution to the new, safe, environmentally friendly, inexpensive, efficient, practical, stable and easy to use hydrogen storage problem, based on the use of solid-state $NaBH_4$ for portable applications. Although the hydrolysis reaction of $NaBH_4$ is based on a simple reaction, it has been the subject of many chemical studies in the literature. The usage area of $NaBH_4$ is limited because the catalysts used in the reaction are very expensive. This situation has forced many researchers to work on the synthesis of cheap catalysts to be able to use them in this reaction. In the one part of this thesis, a study has been made for a new usage area that will contribute to the recycling of the blast furnace slag (BFS) by-product. This by-product has harmed the environment by creating storage problems because of is a most produced as the by-product in the world. There is no study in the field of energy dependent on the recovery, recycling and reusing of the BFS waste product. In addition, there has not any study seen in the literature; the slag by-product as catalyst support. The usability of the slag by-product in catalyst synthesis for the $NaBH_4$ hydrolysis reaction is explained in detail along with the thesis. In addition, it is aimed to reduce environmental pollution and increase added value production with an efficient and environmentally friendly catalyst design that will be used in hydrogen production dependent on the recycling and reusing of BFS waste product. It is expected that the results of the study will be positive since it is a by-product with high metal content. Briefly, the slag, which is a by-product, was treated in hydrochloric acid by the impregnation method. Various catalyst samples were synthesized by loading Co nano powder on both raw slag powder and acid-treated slag powder. Performance analyses

of the Co-B catalysts that are supported with the BFS by-product, were examined exhaustively. These analyzes were carried out by using the BFS by-product both its base form and its treated form with HCl acid that by using the impregnation-chemical reduction method. These performance analyses of the Co-B catalyst samples were examined in three different types of BFS, that are the Raw BFS, the Co-B-BFS (non-treated) and the Co-B-BFS(+). Then the impacts of these Co-B catalyst samples were analyzed on hydrogen production from the solid-state sodium boron hydride (NaBH_4) hydrolysis reaction, in this thesis. The impacts on the hydrolysis reaction of NaBH_4 of certain parameters, for example, the content of raw BFS, the HCl acid treatment on the raw BFS, the Co % quantity and the pre-temperatures were explored. The impact on hydrolysis reactions was analyzed by using different parameters such as temperature, percentages of Co, amounts of catalyst and amounts of NaBH_4 . SEM and XRD analyzes were made and researches were carried out on the morphology of the samples, particle structures, and the impact of acid treatment. As a result, optimization of the acquired parameters, the powder mixtures were obtained the high efficiently Co-B-BFS catalysts for the solid state. NaBH_4 hydrolysis reaction. Moisture and gas barrier issues of solid-state NaBH_4 , prevent by some solutions.

Development of autonomous and portable hydrogen generation system prototype

An innovative design that will reduce the weight and volume of traditional systems and the development of autonomous prototype systems are important for defence technologies. Studies on the autonomous operation of these prototypes are very few in literature. Within the scope of this thesis, a new design of the hydrogen generator prototype, which has been developed for fuel cell systems used in portable applications, is focused on. An autonomous prototype that can be used in all kinds of applications, light, small volume and working with solid NaBH_4 was obtained. The steps involved in designing and prototyping an autonomous hydrogen generator are described. The base of this prototype is designed as an autonomous hydrogen generator, that is using hydrides for hydrogen/fuel cells applications. The energy required for applications will be provided from hydrogen gas which is produced with the use of hydrides that have high hydrogen storage capacity in the catalytic hydrolysis reaction . This catalytic hydrolysis reaction occurs between water, the sodium boron hydride and the catalyst . Detailed information about catalysts is given in the thesis.

The hydrogen gas released as a result of the hydrolysis reaction, then it is transferred to the fuel cell system. The required amount of water, catalyst and hydride was calculated considering the 1 hour duty period of the fuel cell. These calculations were used in the prototype design. Instead of a single reaction chamber, more than one reaction chamber was designed. In this way, it is planned to prevent the use of excessive chemicals. According to the findings obtained from other studies in the literature, some usage problems such as unstable hydrogen production in mobile applications, one-time service life, heavy or large volume storage system and short duty time can be avoided by using the produced prototype. The design of this system consists of water tank, liquid pump, fuel tank, reaction chamber and control unit. This design provides high energy density, inexpensive design, low cost, high applicability and fast use, refilling or cleaning.

As a result of the study, a small prototype design was built, examined and characterized, details about the operating system and performance of a portable and autonomous prototype with 4 parts and 1 hour hydrogen production capacity are given. Briefly, the dimensional design of the prototype was made using the parameters obtained from the catalyst sample analysis. The autonomous operation algorithm of the system, which works with the plug-and-plug principle, has 4 segments, consists of fuel unit, water-catalyst unit, equipment unit and control unit, is designed depending on pressure change or time. Thanks to the interface to be prepared with the autonomous working algorithm Arduino microcontroller control card and an open source software program such as C++ , the system's self-decision mechanism will be created depending on pressure or time. As the ultimate goal, the first prototype of a new autonomous hydrogen compatible with portable applications to be developed for individual use was manufactured with plexiglass material. Leakage and parameter tests of the hydrogen generator were carried out. One-hour trial experiments were conducted using the catalysts produced in the first chapter of autonomous operation experiments. By using solid state NaBH_4 powder in the designed system, the problems of increasing the low hydrogen storage capacity in systems using aqueous solutions, low gravimetric H_2 storage capacity and unstable hydrogen production are prevented. In addition, the decrease in system efficiency seen in cartridge systems has been prevented. Then this design can be developed for more big-scale uses.

2. LITERATURE SUMMARY

2.1. Autonomous Systems

The first autonomous technologies that come to mind are the robotic device technologies that communicate with each other on the production lines of factories operating in the manufacturing sector. Autonomous systems stand out as an important element of today and future technologies, in terms of production efficiency and product quality with the impact of Industry 4.0. In the near future, the developments in autonomous systems will evolve to a level that will be able to carry out all the necessary operations smoothly and efficiently, without the need for human-based commands, with the observations and outputs made within their own analysis and predictions. Autonomous technologies are one of the areas of technology that are expected to develop rapidly in the next 10-15 years. These technologies, which have important features that minimize human errors, are widely used today, thanks to their fast and high accuracy rates and instant decision support systems. Since the beginning of the 21st century, developments in the defence, space and aviation sectors have gained momentum. The usage areas and importance of autonomous technologies in these sectors are increasing with the developments in artificial intelligence technology. Developing countries as well as countries of tech giant companies, that want to benefit from the facilities offered, have started to make significant investments by preparing strategies for artificial intelligence and autonomous systems. These autonomous technologies that are developed with investments, play a key role in strategically important domestic and national defence systems such as unmanned aerial vehicles (UAV), submarines and military portable technologies [1]. For this reason, independent and environmentally friendly energy production ways have a strategic importance for the development and continuity of use of these applications.

2.2. Energy Production

Energy needs are increasing day by day, because of the rapid growth in world population, industry and technology. So, energy is one of the essential necessities for any society whose economic development and industrialization. As a result of activities such as increased urbanization and energy consumption, the climate change that develops as a result of global warming's impact and arises, thus, is one of the biggest environmental problems in 20th

century.

There are in existence two main and various lower production ways to satisfy the energy demand. This energy demand is supplied from renewable energy and non-renewable energy sources. However, greenhouse gases, which are the leading roles in global warming, are mostly released when energy is produced using non-renewable energy sources. According to the energy statistics report published by IEA, energy production and consumption activities constitute one-third of the greenhouse gas formation [6]. Accordingly, energy production and consumption activities have strategic importance in examining global warming problem that is a dangerous atmospheric issues and climate change problem that is a big environmental change issue. In consequence of this situation, energy system activities are undergoing a transformation across the world. Profound changes will necessitate in the energy production, distribution and consumption for avoiding climate change. As a result of the reactions against the country's policies, a common vision has been created on a new sustainable and supportable energy economy dependent on natural, clean and ecological fuel source as the energy source. Numerous countries request alternative energy solutions for supply the energy demands while they keep on decreasing their reliance on petroleum products. Renewable energy sources such as solar, wind, hydrogen, hydropower, biomass, geothermal and ocean energy; are at the forefront of these alternative energy solutions. Renewable energy sources have gained great importance due to can provide sustainable energy services with their features such as being inexhaustible, sustainability, ecological awareness and supply of energy security. The potential of renewable energy sources is enormous as far as meets the world's energy demand for many years. After all, renewable energy sources that are currently viewed as significant and fast-growing, are expected to play a vital role especially in energy production [2]. The storage of this generated energy creates big problems for non-stationary uses, mobile and portable applications. For this reason, studies on energy storage as well as energy production methods are great importance for these technologies.

2.3. Power Supply Types for Portable Application

Today, the energy needs of these systems are mostly supported by lithium-ion polymer batteries. For the energy needs of developing technologies, traditional energy sources such as lithium batteries and other battery technologies are insufficient to be the power source of

rapidly developing autonomous and portable systems. The system weights and charging times of these technologies are disadvantageous. Traditional systems need improvement in terms of payload and energy efficiency. However, traditional technologies increase the energy consumption of the systems, create problems such as transportation problems, and shorten their duty times and ranges. In Table 2.1, a detailed comparing of primary, secondary types batteries and fuel cells, which can use as power supply ways for portable technologies, is made.

Table 2.1. Comparing of battery technologies and fuel cell systems [7]

	PRIMARY BATTERIES		SECONDARY BATTERIES		FUEL CELLS
Types	Alkaline	Zn-C	Ni-Cd	Li-ion polymer	PEMFC
Energy Density (Wh/L)	122-263	120-152	50-150	185-220	240
Specific Energy Density (Wh/kg)	66-99	55-77	40-60	100-158	360
Features	High energy density	Low current drain, Disposable power supply	Recharge-able power supply	Self-discharge Memory effect	- Semi-permanent power supply - High energy density and efficiency - Low response characteristic
	Works as the galvanic or voltaic cell while produces electricity		Works as the galvanic or voltaic cell while discharging produces electricity and works as the electrolytic cell while consumes electricity		Works as the simple galvanic or voltaic cell while produces electricity

Table 2.1. (continue) Comparing of battery technologies and fuel cell systems [7]

	Irreversible cell reaction	Reversible cell reaction	Reversible cell reaction
Features	Non-rechargeable	Rechargeable	Energy can produce continuously
	Needs the active materials. Ex.: Leclanche cell or Dry cell, Lithium cell.	Usable repeatedly by recharge Ex.: Lead storage battery, Lithium-ion cell	Fuels should be supplied continuously. It doesn't store energy.
Uses	Watches, Transistors, radios, ect.	In electronic. equipment, automobile equipment, personal equipment (digital cameras, laptops, flash light, etc.)	Space Vehicles, Drone, Submarines, energy source, etc.




Primary batteries, secondary batteries and fuel cells are galvanic cells or voltaic cells that directly produce electricity. And all of them do it by using electro chemical reactions. Like a battery, a fuel cell uses anodes, cathodes and electrolytes plates to produce electricity. This is the basis of all batteries and fuel cells. In both, low voltage DC cells are combined in series to produce higher voltage and power [8,9]. Also, unlike batteries, fuel cells do not need to be recharged, they are need to supporting with fuelling as the H₂ and O₂ gases. The anode and cathode are metal materials while in a battery, but, in fuel cells, they are from occur gases such as H₂ and O₂ [10]. According to the findings of studies conducted in recent years, fuel cells constitute an alternative option in terms of producing autonomous systems that can be used for durable, long-term and demanding tasks [3]

2.4. Fuel cells and Battery Systems for Nonstationary Applications

Fuel Cell is an electrochemical device that combines hydrogen and oxygen to produce electricity that water and heat are as its by-product. One of the more common types of fuel

cells is the proton exchange membrane or the polymer electrolyte membrane (PEM). This type of fuel cells has a wide use in different ways; such as residential use, transportation system, military applications and defending systems [11]. PEMFC systems are systems that use hydrogen and oxygen as fuel. And as a product they bring heat, water and energy to the environment. The resulting products do not have carbon footprint and are therefore called clean and renewable energy systems. In Table 2.2., a detailed comparing of the battery system and PEMFC & Hydrogen system, which could use as a 200 W power supply for portable technologies, is given.

Table 2.2. Detailed comparing of battery and PEMFC and hydrogen tank system with same nominal power [12,13]

		 + 	
	PEMFC	Hydrogen Tank (9 L, 1.5 MPa)	Battery
Nominal Power :	200 W	-	200 W
Nominal Voltage:	15 V	-	12 V
Nominal Current:	13.3 A	-	13.3 A
Stack Weight (kg):	0.65	3.1	12.08
System Size (mm):	140*110*108	167*520	228*138*206
System Weight (kg):	1.19	3.1	17.3

In autonomous/autonomous systems produced for the defence, space and aviation sectors, the energy needed by the electronic systems or the entire system is provided by fuel cells. Fuel cells can provide clean, efficient, high power density electrical energy by using only hydrogen and ambient air; it is light, silent, zero-emission, which can also operate in off-grid environments, and due to these features, it is used with high efficiency to reduce fossil energy consumption, energy loss and emissions. Fuel cell technology allows to overcome the limitations of conventional battery/battery technology. With its features such as being able

to refill its fuel in minutes, having a higher energy/mass ratio, and producing light and clean energy, it significantly reduces the downtime of the system and significantly extends its duty times and ranges. Therefore, fuel cells are an alternative energy source in providing the energy required for defence systems, off-grid applications and military or personal portable equipment applications where system weight and portability are important [14,15]. In Table 2.3., a detailed comparing table of fuel cell types is given [16].



Table 2.3. Detailed comparing of fuel cell types

TYPE	<u>PROTON EXCHANGE MEMBRANE FUEL CELL (PEMFC)</u>		<u>PHOSPHORIC ACID FUEL CELL (PAFC)</u>	<u>DIRECT ALCOHOL FUEL CELL (DAFC)</u>		<u>ALKALINE FUEL CELL (AFC)</u>	<u>MOLTEN CARBONATE FUEL CELL (MCFC)</u>	<u>SOLID OXIDE FUEL CELL (SOFC)</u>
TYPE	<i>Low-Temperature PEMFC (LT-PEMFC)</i>	<i>High-Temperature PEMFC (HT-PEMFC)</i>	<i>PAFC</i>	<i>Direct Methanol fuel cell (DMFCs)</i>	<i>Direct ethanol fuel cell (DEFCs)</i>	<i>AFC</i>	<i>MCFC</i>	<i>SOFC</i>
FUEL	Hydrogen (H ₂)	H ₂	H ₂	Liquid methanol-water solution	Liquid ethanol-water solution	H ₂	Methane	Methane
CATALYST	Platinum supported on carbon	Platinum/Ruthenium supported on carbon	Platinum supported on carbon	Platinum/Platinum/Ruthenium supported on carbon	Platinum/Platinum/Ruthenium supported on carbon	Nickel/ Silver supported on carbon	Nickel Chromium (NiCr)/ Lithiated nickel (NiO)	Nickel-YSZ composite/ Strontium-doped lanthanum manganite (LSM)
NOBLE METAL INCULUDITY	Noble metal	Noble metal	Noble metal	Noble metal	Noble metal	Noble metal / Non-noble metal	Non-noble metal	Non-noble metal
ELECTROLYTE	Solid polymer membrane (Nafion)	Nafion/PBI doped in phosphoric acid	Liquid phosphoric acid (H ₃ PO ₄) in silicon carbide (SiC)	Solid polymer membrane (Nafion)	Solid Nafion/Alkaline media/Alkaline-acid media	Potassium hydroxide (KOH) in water solution/ Anion exchange membrane (AEM)	Liquid alkali carbonate (Li ₂ CO ₃ /Na ₂ CO ₃ /K ₂ CO ₃) in Lithium aluminate (LiAlO ₂)	Solid yttria-stabilized zirconia (YSZ)
ELECTRICAL EFFICIENCY	40% - 60%	50% - 60%	36% - 45% (85% with cogeneration)	35% - 60%	20% - 40%	60% - 70%	55% - 65% (85% with cogeneration)	55% - 65% (85% with cogeneration)
OPERATING TEMPERATURE	60 °C - 80 °C	110 °C - 180 °C	160 °C - 220 °C	Ambient - 110 °C	Ambient - 120 °C	Below zero - 230 °C	600 °C- 700 °C	800 °C - 1000 °C
CHARGE CARRIER	Hydrogen Ion (H ⁺) (proton)		Hydrogen Ion (H ⁺) (proton)	Hydrogen Ion (H ⁺) (proton)	Hydrogen Ion (H ⁺) (proton)	Hydroxyl ion (OH ⁻)	Carbonate ion (CO ₃) ₂ ⁻	Oxygen Ion (O ₂ ⁻)
QUALIFIED POWER (W)	100 W - 500 kW		> 10 MW	100 kW - 1MW		10 kW - 100 kW	100 MW	> 100 MW
USES	Vehicles, small generators, small applications		Power plants, combined heat & power	Vehicles, small applications		Outer space	Power plants, combined heat & power	Power plants, combined heat & power

Table 2.3. (continue) Detailed comparing of fuel cell types

TYPE	<u>PROTON CERAMIC FUEL CELL (PCFC)</u>	<u>ZINC-AIR FUEL CELL (ZAFCS)</u>	<u>DIRECT FUEL CELL (DFCS)</u>			<u>BIO FUEL CELL (BFCS)</u>	
TYPE	<i>PCFC</i>	<i>ZAFC</i>	<i>Direct Borohydride fuel cell (DBFC)</i>	<i>Direct Formic acid fuel cell (DFAFC)</i>	<i>Direct carbon fuel cell (DCFC)</i>	<i>Enzymatic fuel cell (BFC+)</i>	<i>Microbial fuel cell (BFC++)</i>
FUEL	Methane	Zinc	NaBH ₄	Liquid formic acid (HCOOH)	Solid carbon (coal, coke, biomass)	Organic matters (glucose)	Any organic matter (glucose, acetate, waste-water)
CATALYST	Nickel	Non-noble metal oxides (such as manganese oxide - MnO ₂)	Gold/ Silver/ Nickel/ Platinum supported on carbon	Palladium/ Platinum supported on carbon	Graphite or carbon-based material/ Strontium-doped lanthanum manganite (LSM)	Biocatalyst supported on carbon	Biocatalyst supported on carbon/ Platinum supported on carbon
NOBLE METAL INCULUDITY	Non-noble metal	Non-noble metal	Noble metal / Non-noble metal	Noble metal / Non-noble metal	Non-noble metal	Non-noble metal	Noble metal / Non-noble metal
ELECTROLYTE	Protonic/ Zirconia	Liquid alkaline	Solid Nafion/Anion exchange membrane (AEM)	Solid Nafion	Solid yttria-stabilized zirconia (YSZ)/Molten carbonate/Molten hydroxide	Ion exchange Membrane/Membrane-less	Ion exchange membrane
ELECTRICAL EFFICIENCY	55% - 65%	30% - 50%	40% - 50%	30% - 50%	70% - 90%	30%	15% - 65%
OPERATING TEMPERATURE	700 °C - 750 °C	Below zero - 60 °C	20 °C - 85 °C	30 °C - 60 °C	600 °C - 1000 °C	20 °C - 40 °C	20 °C - 60 °C
CHARGE CARRIER	Hydrogen Ion (H ⁺) (proton)	Hydroxyl ion (OH ⁻)	Sodium ion (Na ⁺)	Hydrogen Ion (H ⁺) (proton)	Oxygen Ion (O ₂ ⁻)	Hydrogen Ion (H ⁺) (proton)	
QUALIFIED POWER (W)							
USES							

2.4.1. Fuel cell applications of UAVs

Therefore, the UAV systems, including portable applications, need alternative energy sources and new solutions to reduce their weight, volume and production costs, and to increase their energy efficiency. In Table 2.4, various international UAV projects provides a comparative table of flight times for compressed H₂ and liquid H₂ used as energy sources. Therefore, the search for different hydrogen storage technologies continue rapidly. Efficient, safe, environmentally friendly and cost-effective H₂ storage technologies are a popular field of study.

Table 2.4. Comparing of UAV projects working with fuel cell systems [17]

PROJECT NAME	YEAR	ENDURANCE (hour)		FEATURES OF MODELS			
		without load	with load	H₂ tank (CH₂) capacity	PEMFC capacity (W)	Load capacity (kg)	MTOW (kg)
HYCOPTER-1 (HES)	2015	4	2.5	120 g storage H ₂	200	1	5.2
HYCOPTER (HES)	2018	3.5	-	5-9-12 L	1500	2.5	15
H2QUAD400 (ENERGYOR)	2015	3.75	2	-	-	0.4	6.3
HYDRONE1550 (MMC)	2016	2.5	-	9 L	1800	5	22
HYDRONE1800 (MMC)	2016	-	4	9 L	1800	5	-
JUPITER-H2	2017	3	2	3 L	650	1.25	-
LH2 MULTI-ROTORS	2019	12	-	6 L	800	-	-

2.5. Hydrogen Energy

Because of the fast decrease of petroleum product holds, the world is moving towards a hydrogen-based economy that is the most important alternative fuel of the 21st century. Hydrogen gas, which is a clean, low emission, harmless to the ecosystem, compressible,

high thermal efficient, productive and consumption gas, is regard as the energy carrier of years to come [14]. In Figure 2.1, the features of hydrogen gas are listed.

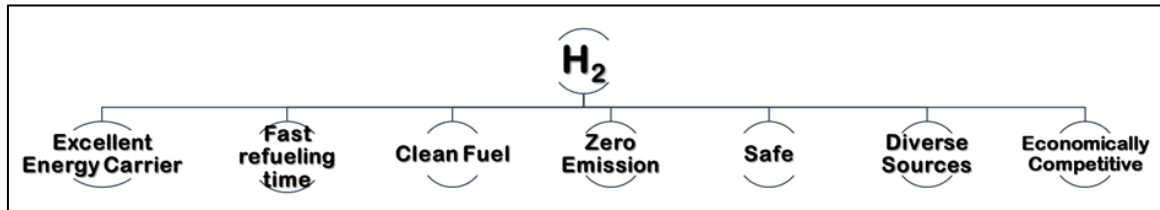


Figure 2.1. The features of the hydrogen gas

Hydrogen gas should be supplied to the system simply and safely, in order to use as a fuel in system applications. The developed technologies have technical problems such as the safe production, delivery and storage of both gas and liquid hydrogen. So, hydrogen gas has a form that is able to leak from its storage tank, when it is desired to be gaseous stored. This leak can be creating a danger besides causing economic costs. Hydrogen storage's cheap, easy and safe would to be from primary factors that will influence the hydrogen economy of years to come [14,18].

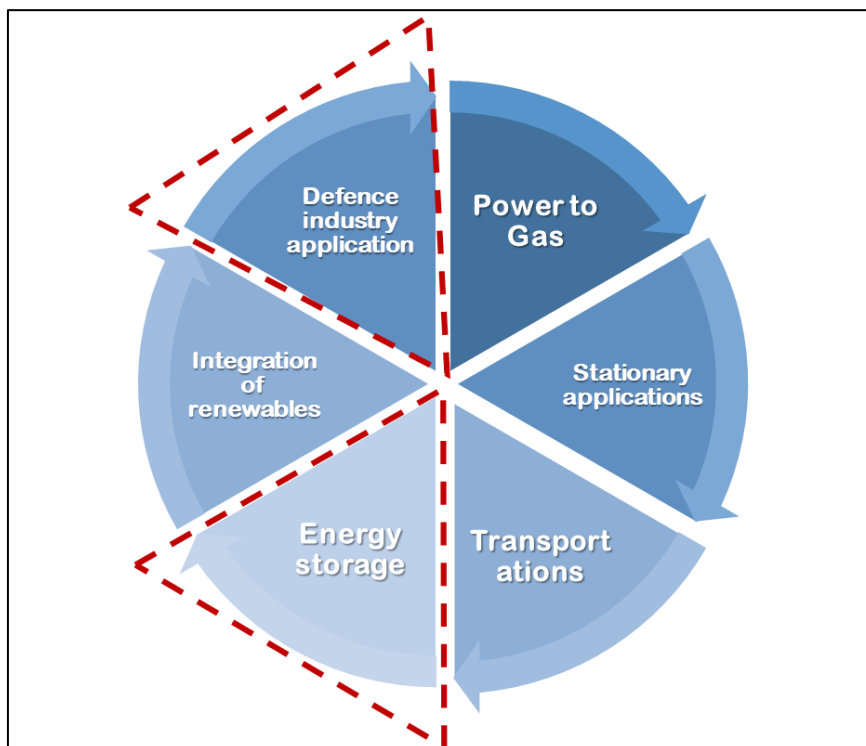


Figure 2.2. Hydrogen energy using areas

In Figure 2.2, the using areas of hydrogen energy are shown. Hydrogen and fuel cells have various using areas, that are including transportation, commercial, industrial, residential and portable applications. Hydrogen and fuel cells can be used in a variety of applications such as the Power to Gas systems, Heat and power systems; backup power systems; portable power systems for transportation applications (airplanes, automobiles, trains and ships); auxiliary power systems for special defence systems applications (UAV, submarines and rockets) and can be integrated into systems to store and activate renewable energy [19].

2.5.1. Hydrogen energy storage types

Alternative hydrogen storage technologies are being developed for the solution of important technical problems such as the transmission and storage of hydrogen in fuel cell applications. Hydrogen technologies are used as energy storage technology in fuel cell technologies, which also play a key role in energy conversion and storage technologies. However, in fuel cell applications, some disadvantages such as the inability to supply hydrogen to the system in a simple and safe way must be eliminated in order to use hydrogen as a fuel [15].

Although hydrogen production and storage techniques are costly today, these costs are expected to decrease in the coming years. Hydrogen is a light and volatile gas with a high energy content. For this reason, the hydrogen desired to be stored in gaseous state can easily leak/-has a structure that can leak- from the tank in which it is stored, the leakage that may occur may create danger as well as causing economic costs. The cheap and easy storage of hydrogen is one of the main factors that will affect the hydrogen economy in the future [20]. In Figure 2.3, the source, way and decarbonisation measure of hydrogen energy production are listed. Also, transportation and storage options of hydrogen energy are listed in Figure 2.4.

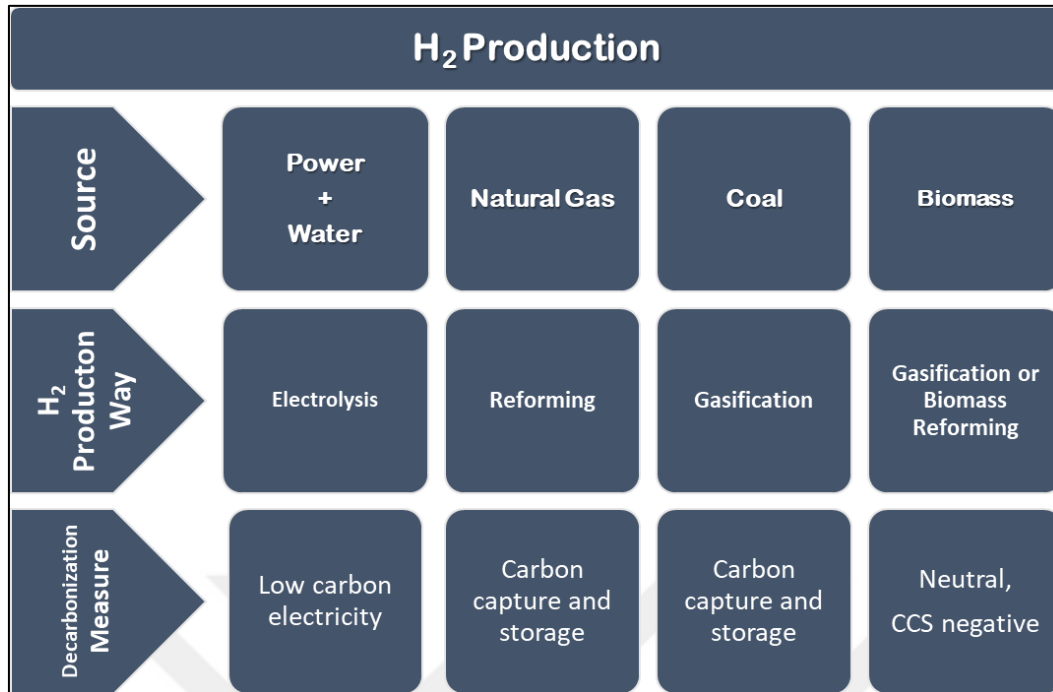


Figure 2.3. Source, way and decarbonisation measure of hydrogen energy production

The hydrogen storage technologies selected for fuel cell applications continue to be developed. In addition to autonomous technologies, energy storage solutions are of great importance for technological applications in the defense, space and aviation sectors.

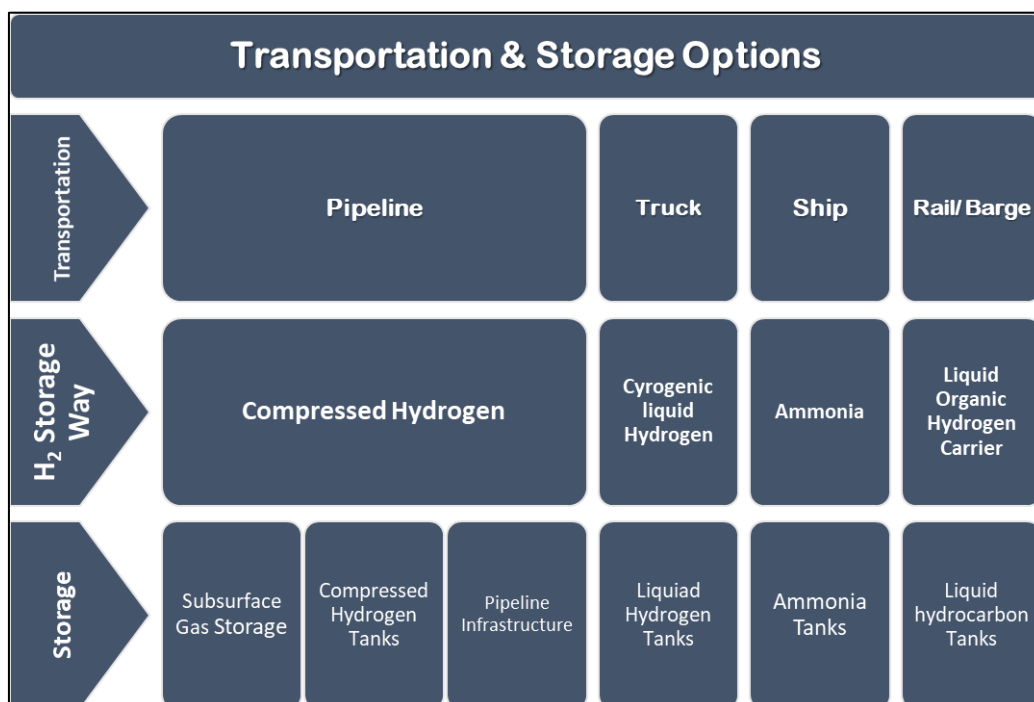


Figure 2.4. Transportation and storage options of hydrogen energy

Technical problems such as the transmission and storage of H₂ are among the most important problems in fuel cell applications and these problems are of great importance in industrial applications. Using liquid, compressed or metal hydride hydrogen tanks in fuel cell systems used in application where the system's energy density is critical, provides disadvantages with regards to volume, safety or weight, and reduces the energy/mass ratio considerably [21,22].

Storage Type	Advantages	Disadvantages
Gas storage • Compressed hydrogen	High efficiency, convenient, mature technology.	Expensive cylinder and the immature technology of fast filling.
Liquid storage • Liquid hydrogen	High liquid density and storage efficiency.	Large consume of energy and time, low temperature.
Carbon nanotubes • Gaseous hydrogen	Highly porous structure and particular interaction between carbon atoms and gas molecules	Immature technology and hydrogen capacity depends on many factors
Chemical storage (metal hydride) • MgH ₂ NaH, NaBH ₄	High safety, high purity of hydrogen, good reversible cycle performance, large volume of hydrogen density.	Absorbing impurities, reducing the hydrogen capacity and the lifetime of tank.
Physical storage (metal organic framework) • Porous coordination, network	Highly porous, high uptake of H ₂ and specific surface areas.	Hydrogen storage temperature is far below operating temperature.

Figure 2.5. Hydrogen storage types, their advantages and disadvantages [23]

When hydrogen gas is used in system applications, it needs high pressures, large volumes, low temperatures or advanced storage techniques. This is because it is a high energy content but extremely light and volatile gas [24].

Table 2.5. Comparing of hydrogen storage technologies [7]

<i>H₂ Storage Technology</i>	<i>H₂ Storage density (% by weight)</i>	<i>Features</i>
<i>Compressed tank</i>	2.50 - 4.00 (300 - 700 bar)	<ul style="list-style-type: none"> - Low storage density and high charge pressure - Difficult to refill in an off-grid area
<i>Liquefied tank</i>	5.00 - 7.00	<ul style="list-style-type: none"> - High gravimetric storage density - Extremely low temperature (253 C°) for cooling
<i>Metal hydride</i>	2.30 - 3.00	<ul style="list-style-type: none"> - Good storage security but low gravimetric storage density
<i>Chemical hydride (NaBH₄)</i>	3.55 - 10.80	<ul style="list-style-type: none"> - High H₂ storage density - H₂ extraction possible at room temperature - Good storability and easy usability

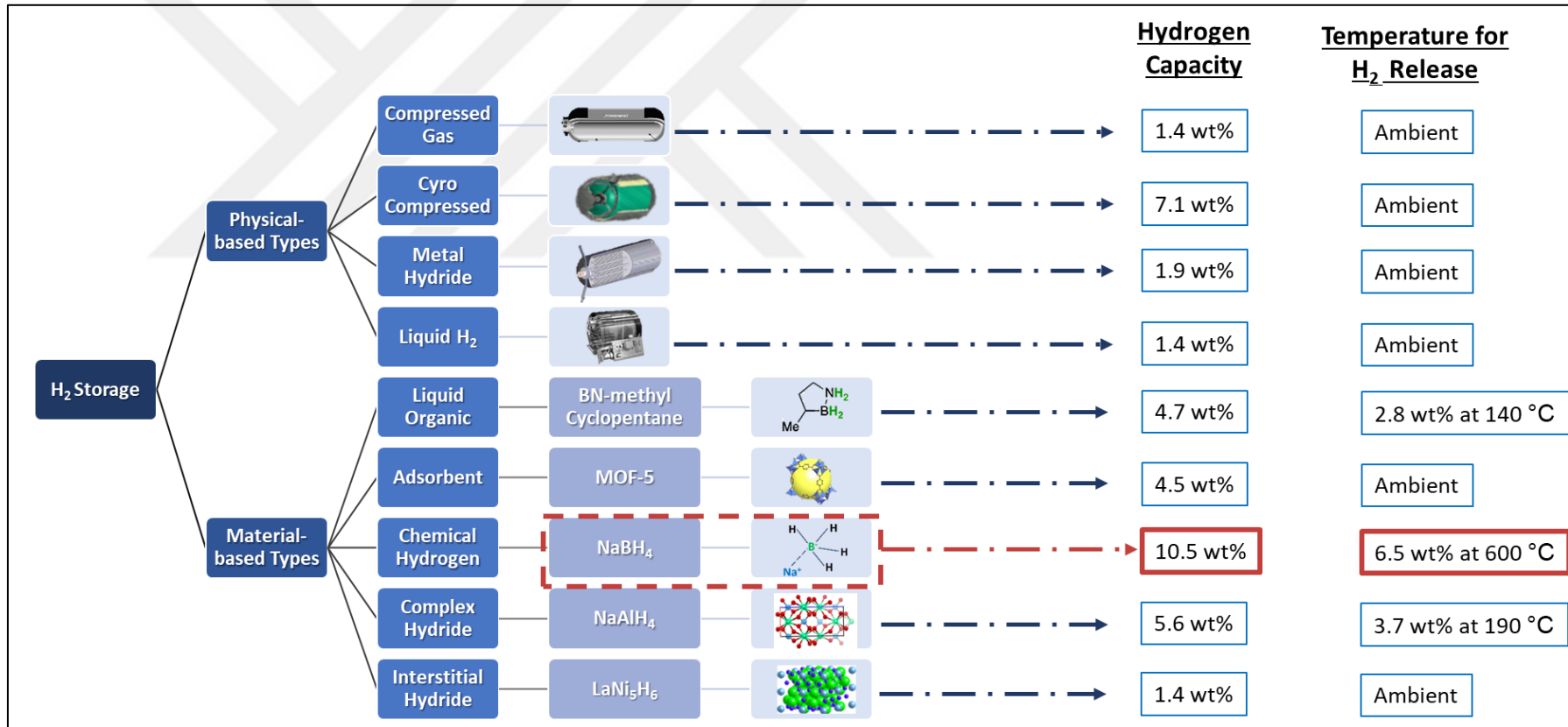


Figure 2.6. Hydrogen storage types, their hydrogen capacity and temperature for H₂ release

Hydrogen storage technologies that are efficient, safe, environmentally friendly and cost-effective, are a popular workplace. Especially, using liquid, compressed or metal hydride hydrogen tanks in fuel cell systems used in application where the system's energy density is critical, provides disadvantages with regards to volume, safety or weight, and reduces the energy/mass ratio considerably.

2.6. Sodium Borohydride (NaBH_4)

Boron is an important source of wealth for Turkey, which has 72.2% of the world's boron mineral reserves [25]. However, boron without added value cannot contribute to the country's economy to the desired extent, and it may even cause a negative impact on the import/export balances of imported industrial products produced with boron mine exported as raw material. In Figure 2.7., the Lewis structure and 3-D structure of Sodium Borohydride chemical powder are shown.

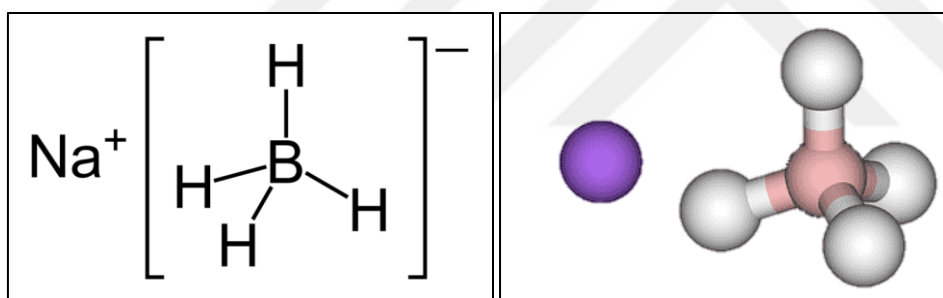


Figure 2.7. Lewis structure and 3-D structure of NaBH_4 chemical powder

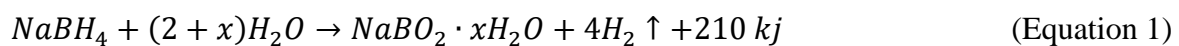
The safest ways to store hydrogen are to use solid-state metal hydride tanks or chemical compounds such as NaBH_4 [4]. Sodium boron hydride is the most efficient type of hydride that uses chemical methods to store and produce hydrogen. The fact that NaBH_4 is a catalytic reaction, it can store high hydrogen in its content, it is lighter than pressurized/compressible tanks and the flexibility of the hydride in hydrogen production provides many advantages and therefore has opened a new era in hydrogen storage and production technology. The use of NaBH_4 has been one of the important research areas in aviation applications and fuel cell technologies. Boron-based materials, especially NaBH_4 ; for many years, they have become a potential solution in energy storage technologies because they have H_2 storage capacity, are more economically advantageous, and do not have problems such as storage and

transportation. Boron-based materials constitute a serious option for many fuel cell applications and are frequently mentioned in every field of fuel cell technology [26].



Picture 2.1. Sodium borohydride powder

The stabilized NaBH_4 solution is practical, suitable, effective and reduces safety concerns for high purity hydrogen storage [27]. NaBH_4 has many advantages such as having a catalytic reaction, high hydrogen storage capacity, lighter and flexibility in hydrogen production. The hydrogen storage capacity of the boron-based materials is very high. Therefore, especially NaBH_4 powder, which is one of the boron-based materials, have turned into a frequently used material in the energy storage for many years [5,28]. In special applications like aeronautical applications that have long operating times and have to working away from the energy sources, the energy demand supplies from the hydrogen, is gain very big advantage. The NaBH_4 based hydrogen production systems have more benefits rather than the heavy metal hydride or pressure tanks like the hydrogen storage systems [4,29]. The hydrogen content percentage and the theoretical hydrogen storage capacity percentage of NaBH_4 are 10.6 % and 10.8 % by weight, respectively. That is an easy-to-use hydride and has a stable hydrogen production, when compared to other chemical hydrides. [30]. The different catalysts and reaction parameters are tried in the hydrogen production studies based upon the NaBH_4 's hydrolysis reaction, that is given the equation as below:



2.6.1. Catalysts

Many of the NaBH_4 studies are based upon faster and more efficient gas production from the hydrolysis reaction of NaBH_4 . In addition, the high activity and long-lasting catalysts synthesis is one of the objectives. It is incredibly valuable the hydrogen gas supply, that is quickly and sustainably with small quantities of chemicals are using during the hydrolysis processes, both academically and industrially.

The impacts of various transition metal catalysts, that used in catalytic hydrolysis reaction of the NaBH_4 , are investigated on hydrogen production. The hydrogen production's increase observes with the addition of catalysts to the reaction. Today, in line with the researches on NaBH_4 , the most successful catalyst type in hydrolysis of NaBH_4 is the catalyst types containing noble metals. Although noble metals that are Pt, Ru and Pd based are used in the NaBH_4 's hydrolysis studies [31–33], it is observed that the catalytic activity is increased, and because of their high cost and rarity, their production for industrial applications is constrained. In the studies, transition metal (such as Fe, Cu, Ni, Co) catalysts, that are high catalytic activity and being less costly, have more advantages than noble metals, considering when used in NaBH_4 reactions. So, this metals are expected that are used as a catalyst in more studies [34–36]. The previous studies, that have the hydrolysis reaction of NaBH_4 , based upon obtain of hydrogen gas, have been conducted using various catalysts such as Co-Ni, Co-P, Ni-B, Ni-P and Ni-Co-B catalysts, catalyst and Co-supported catalysts [37–39], Ni-based catalysts [40], Cu-Co catalyst, Co-WB catalyst, Pd modified catalyst [41–43], Pt [32,44], Ru and Ru-Ni alloy catalysts [33], Co-B nanocatalyst [26]. In the production studies of high efficiency and low costs catalysts made with noble metal catalysts, especially Co-B catalysts has high catalytic activity and stability in the hydrolysis of NaBH_4 [14]. The metal-containing catalysts used as catalysts in hydrogen production reactions from NaBH_4 have high catalytic activity. A new catalyst is able to produce for use as a catalyst in these hydrogen production reactions from industrial waste such as clay which contains high amounts of metal and is rich in content [36,45–48].

Support materials

Support materials have an important place among the components needed in the catalyst design. One of the most important reasons for using support materials is that the active

ingredients provide the required surface area for adsorption and catalytic reactions.

In addition, it improves the mechanical properties of the catalyst and provides longer use. Catalyst particles are added on the catalyst support to increase the impact surface of the catalyst used in the hydrolysis of NaBH_4 . An ideal catalyst support should have a large surface area, high conductivity or a high degree of graphitization, a suitable pore structure to provide mass transport, and desired functional groups on its surface so that metal particles can be easily attached to their surface [49]. Generally, materials with high mechanical and thermal resistance such as Al_2O_3 , SiO_2 , ZrO_2 , Pt, Co, Ni are used as reinforcement. While preparing these catalyst designs, many porous materials such as Al_2O_3 [50], SiO_2 [51], TiO_2 [52–54], activated carbon [36], clays [45,49,55], zeolite [56,57] and ceramics [58] can be used as support components. Enhancers are substances that increase the activity and stability of the catalyst with auxiliary properties by adding small amounts to the catalytic structure in order to assist the active ingredient and support.

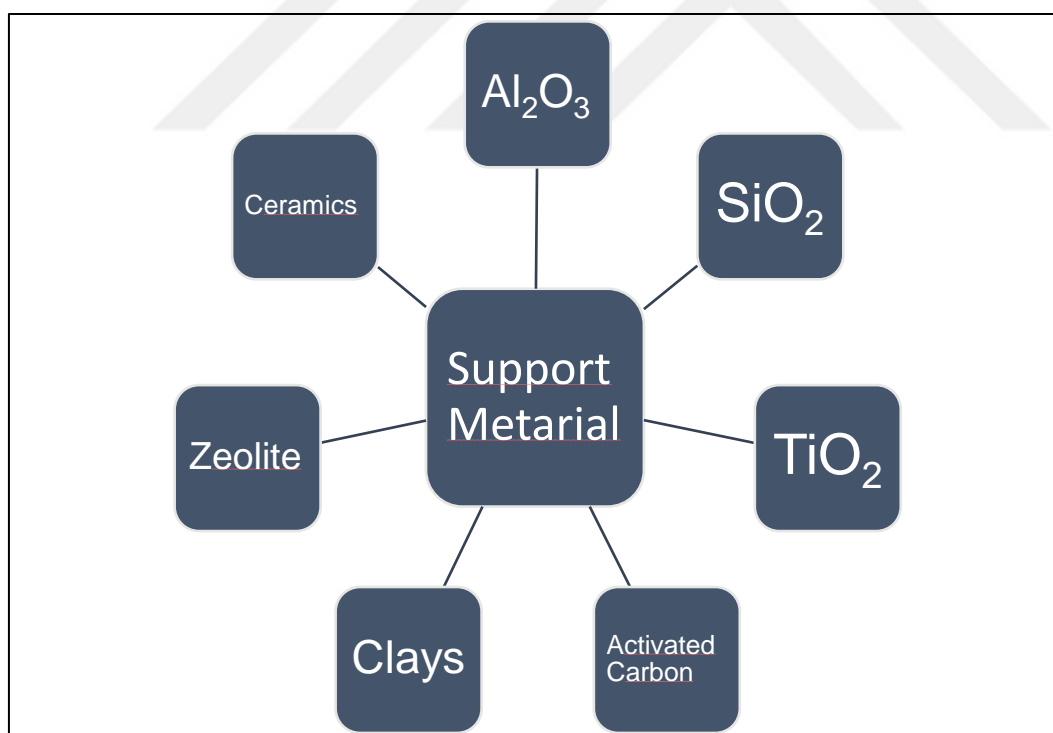


Figure 2.8. Some Support Materials for Catalyst production

Clay is preferred as a support material due to it has different pore size (low, high and meso), high structural and thermal strength. In the study using Co -B catalysts supplemented with acid-modified sepiolite clay as the support material, the maximum hydrogen gas production

rate of the hydrolysis reaction with these catalysts is approximately 3 times higher than the maximum hydrogen gas production rates of the acid-treated sepiolite clay-supported Co-B catalysts. The catalyst samples obtained from the hydrolysis reactions of NaBH_4 . According to the performance results of catalyst that made with clay, are the nature harmless, easy to process, inexpensive, efficient, reusable, and as contribute to recycling. [49].

Table 2.6. The hydrogen gas production properties of Co-based catalysts

<i>Catalyst's type</i>	<i>NaBH₄</i> <i>(wt %)</i>	<i>Hydrolysis</i> <i>temperature</i> <i>(°C)</i>	<i>Hydrogen</i> <i>production rate</i> <i>(L/min.g_{catalyst})</i>	<i>References</i>	
<i>Co powder</i>	-	1	25	0.13	[30]
<i>Co-Cu-B</i>	7	25	2.81	[59]	
<i>Co-B</i>	-	20	30	2.75	[60]
<i>Co -B</i>	AT (Attapulgit Clay)	5	25	3.35	[45]
<i>Co -B</i>	AT (Attapulgit Clay)	5	25	1.27	[45]
<i>Co -B</i>	TiO₂	1	30	12.50	[52]
<i>Co -B</i>	Al₂O₃	1	30	11.65	[52]
<i>Co -B</i>	CeO₂	1	30	10.39	[52]
<i>Co</i>	SiO₂	5	40	8.70	[61]
<i>Co -B</i>	SiO₂-AC	5	25	0.40	[61]
<i>Co -B</i>	MWCNTs	20	30	5.10	[62]
<i>Co -B</i>	Graphane	8	50	56.61	[63]
<i>Co -B</i>	Carbon black	10	25	8.03	[64]
<i>Co -B</i>	Modified AC	1	27	10.29	[65]
<i>Co -Ce-B</i>	CSAC	5	25	16.42	[36]
<i>Co -B</i>	Acid treated sepiolite clay	5	30	1.49	[49]

Based on the literature studies, it can be expected that the slag by-product will be an alternative as catalyst support material, since its content is similar to clay and contains more metal.

- i. Amorphous and crystalline Co_2B samples produced by the researchers were used as catalysts in the hydrolysis reaction of NaBH_4 . These amorphous Co_2B catalysts have a higher H_2 production rate than catalysts produced by calcination under air or under Ar at 500°C . Amorphous Co_2B with NaBH_4 solution has 1% w/w concentration, H_2 production rate is 1.1 L/g catalyst . Min [66].
- ii. Fuel powder containing solid NaBH_4 , NaOH and Al particles were used in the hydrolysis reaction. The optimized mix produces 1778 ml of hydrogen/g of mix in 100% yield in 50 minutes at 323 K. As a result of their studies, when the catalytic promoter catalyst $\text{BNi}_2 / \text{Al}(\text{OH})_3$ is added in the hydrolysis process, an increase in the production rate is observed [67].
- iii. Some NaBH_4 hydrolysis experiments made with some catalysts such as and Ni-Co - P- Al_2O_3 . The results of this studies show that Al_2O_3 catalysts have a positive effect on the efficiency of hydrogen production [68].

2.6.2. Blast Furnace Slag

Blast furnace slag is a by-product produced in high quantities during iron production in blast furnaces in iron and steel plants.



Picture 2.2. BFS production in the Iron-steel factory

Slag, which is a major source of waste, is a complex of lighter-than-metal oxides and silicates and accumulates on the surface due to the difference in density and is defined as a by-product formed when metals or metal-containing ores are melted. During the reduction interaction of 1 ton of metal between 1450 °C and 1550 °C, around 200-600 kg of slag are produced [69].

Usually, the 'BFS powder content' more than 95 % occur of impure parts that are from coal, limestone and iron metal. Substances such as limestone and dolomite reduce iron oxides and turn them into molten raw iron. The temperature of the molten slag collected in the upper part of the furnace is between 1400-1600 °C, which is very close to the temperature of the raw iron collected in the lower part of the furnace. The slag is collected by sweeping from the upper surface of the furnace over time. Ca-Al-Mg silica glasses with glassy structure are formed by rapid cooling of the molten slag with jet water engines. If the molten blast furnace slag is suddenly cooled with the help of water, a fine-grained glassy structure is obtained [70]. The chemical compounds of BFS that produced in different countries are given in Table 2.6.

Table 2.7. Chemical compound of the BFS powders [70,71]

Chemical Compounds (%)	USA	SOUTH AFRICA	TURKEY	CHINA
CaO	29-50	30-40	34-41	40.43
SiO₂	30-40	30-36	34-36	30.18
Al₂O₃	7-18	9-16	13-19	10.77
Fe₂O₃	0.1-1.5	-	0.3-2.5	0.64
MgO	0-19	8-21	3.5-7	7.91
MnO	0.2-1.5	-	1-2.5	-
S⁻²	0-2	1-1.6	1.2	-
SO₃	-	-	-	3.21
Na₂O	-	-	-	0.28
K₂O	-	-	-	0,56
Na₂O + 0.658 K₂O	-	-	-	0.01

Classification is made according to BFS alkalinity indexes. The simplest alkalinity index is a CaO/SiO₂ ratio has greater than 1 [72]. The hydraulic activity of BFS depends on the

degree of basicity. When BFS is used with alkaline activators, its hydraulic activity increases [70,73]. An increase in mechanical strength was observed as Al_2O_3 content increased in BFS with a constant alkaline ratio. In case of low quantity of CaO in BFS, low mechanical properties are compensated by high alumina reinforcement. With the increase of MgO amount up to 8-10 %, a slight increase in mechanical properties is observed, but with further increase in this ratio, the mechanical properties are adversely affected [73]. In addition, it was stated that the hydraulic activity increased as the CaO, Al_2O_3 and MgO content increased, and the hydraulic activity decreased as the SiO_2 content increased. By creating a high alkaline environment, the ratio of the quantity of CaO and MgO to the quantity of SiO_2 by mass is greater than 1. Thus, the hydraulic activity of BFS can be increased [70,73].

In Turkey, a large part of the steel production is done by the the of scrap/electric arc furnace technology. The consist of BFS by-product, that obtained in Turkish steel factories, is occurred Al_2O_3 (12.94 %), SiO_2 (39.66 %), CaO (34.20 %), Fe_2O_3 (1.58 %), MgO (6.94 %), SO_3 (0.72 %) Na_2O (0.20 %), K_2O (1.44 %), in accordance with literature informations [70,74,75].. Large storage areas, that are create the pollution of soil, water and air, are filling with waste products, and thus effect on the environment and the human health's negatively. Also, if the slag by-product is not used or reutilised, as well as the disposal' costs are rising daily, when the raise on production in the steel-iron industries A lot of associations have been doing different examinations for the reusing of waste products such as dust, sludge and slag occurred in results of the steel-iron process. Also, they want to draw attention as part of the zero-waste project that effects the all industry. The amount, disposal cost of the waste products and the using energy are decreased when the reusing of the BFS. Therefore, both environmental and economic earnings will be accomplished with slag recycling [69].

2.7. Development of the Hydrogen Generators

In the H_2 generator studies in the literature, NaBH_4 solutions are used in the designed reactors or many problems are observed in the solid NaBH_4 cartridge applications.

- i. A developed high-density hydrogen generator has been evaluated by Kim et al for stable, sustainable hydrogen production and start-stop system to affirm the commercialization possibility of hydrogen generator. According to the performance assessments, the hydrogen production efficiency of the system is 89.9%, the hydrogen generator

gravimetric is 739.1 W h / kg and the volumetric specific energy densities are 272.8 W h / L. The hydrogen storage density of the system is 5.1% by weight; in addition, it is 1.44 times higher than conventional hydrogen generators using NaBH₄ aqueous solution. The control of the production rate is enhanced by a working control algorithm system that measures the hydrogen production rate with a pressure sensor attached to the reactor pressure. This pressure value is determined by considering the volume and flow rate of the hydrogen gas quantity need for the fuel cell's optimum operating condition. The hydrogen generator, that is designed in a cylindrical structure by researchers of this study, have placed in the hull of a UAV. The size of this hydrogen generator ,which has 5.5 kg weight, are 358 mm length and 230 mm diameter [76].

- ii. In 2016, Okumuş et al., in this study, a generator with a reactor volume of 11 cm³, a hydrogen production rate of 5.4 L/min and a lifetime of 10 times was designed using a special Co-based catalyst . It is sufficient to feed a fuel cell system, which has capable of producing capacity 218 W power, has 50-cells. The system's energy density is 325 Wh/kg and the full system has 7.5 kg weight [77].
- iii. In 2015, Kim et al. A hydrogen generator system for a 100 W fuel cell was designed by A hydrogen generator system is designed using the separation of solid state NaBH₄ and HCl concentration. In this study, the system's the gravimetric value of the hydrogen density was measured as the highest value when solid state NaBH₄ and 4.0 N HCl solution were used together. The hydrogen efficiency of the system was 95% and the hydrogen production rate of the system was measured as 650 ml/min [78].

3. MATERIALS, EXPERIMENTAL METHOD, SETUP AND TEST RIG AND PROTOTYPE DESIGN

3.1. Materials

3.1.1. Chemical materials

The slag by-product substance, needs to go through certain chemical processes and be treated by certain synthetic compounds and chemical material, to be utilized as a catalyst support material. The extra pure Co nano powder, NaBH_4 powder and HCl acid solution were from the Turalab Ltd. and the Nanografi Co.Ltd. Also, HCl acid, NaBH_4 and Co nano powder are other chemical materials used in preparing new catalyst synthesis from BFS slag for using in the NaBH_4 reaction.

NaBH_4 powder

The NaBH_4 chemical powder (extra pure) was purchased from Tekkim Ltd. and the Turalab Ltd.. The NaBH_4 is 98.5% pure and contains 0.05% Si and 0.005% Fe. The NaBH_4 chemical powder was used as the H_2 storage and H_2 production material in the synthesis of the BFS catalysts, in the NaBH_4 reaction and in the Hydrogen generator prototype.

Table 3.1. Technical features of the NaBH_4 chemical powder

Molar mass	37,83 g/mol
Appearance	white crystals hygroscopic
Density	1,07 g/cm ³
Melting point	400 °C (752 °F; 673 K)(decomposes)

HCl acid solution

The HCl acid (extra pure) solution was supplied from the Turalab Ltd.. The HCl acid used in preparing new catalyst synthesis from BFS slag for using in the NaBH_4 reaction.

Cobalt (Co) micron powder

The Cobalt (Co) Micron powder was supplied from the Nanografi company. The Co Micron powder is 99.99% pure and has a size of 1 μm . The Co Micron powder was used as catalyst support material in the synthesis of the BFS catalysts, also, was used as a catalyst in the H_2 generation from NaBH_4 reaction that are using in the Hydrogen generator prototype .

Table 3.2. Technical features of the Co micron powder

Purity	99.99 %
Particle Size	1 μm
Cas	7440-48-4
Density	8.92 g/cm^3
Boiling Point	2900 $^\circ\text{C}$
Melting Point	1495 $^\circ\text{C}$
Coeff. Of Expansion @ 20$^\circ\text{c}$	12.5×10^{-6}
Electric Resistivity	6.24 microhm-cm
Crystal Structure	Hexagonal
Form	Powder
Applications	Alloys, Customer Manufacturing, Industrial- general

Granulated blast-furnace slag (GBFS)

In this thesis, the catalyst support material is obtained from the raw granulated blast-furnace slag (GBFS) by-product. The GBFS by-product was procured from the Iron-Steel Factory, Iskenderun, Hatay. The fines of the grinding of BFS are such that 92 % can be sifted out a 30 mm sifter. The GBFS' X-ray Fluorescence (XRF) analysis by using the Malvern Mastersizer 2000 device was made. The X-ray Fluorescence analysis and particle size distribution are given in Figure 3.1.

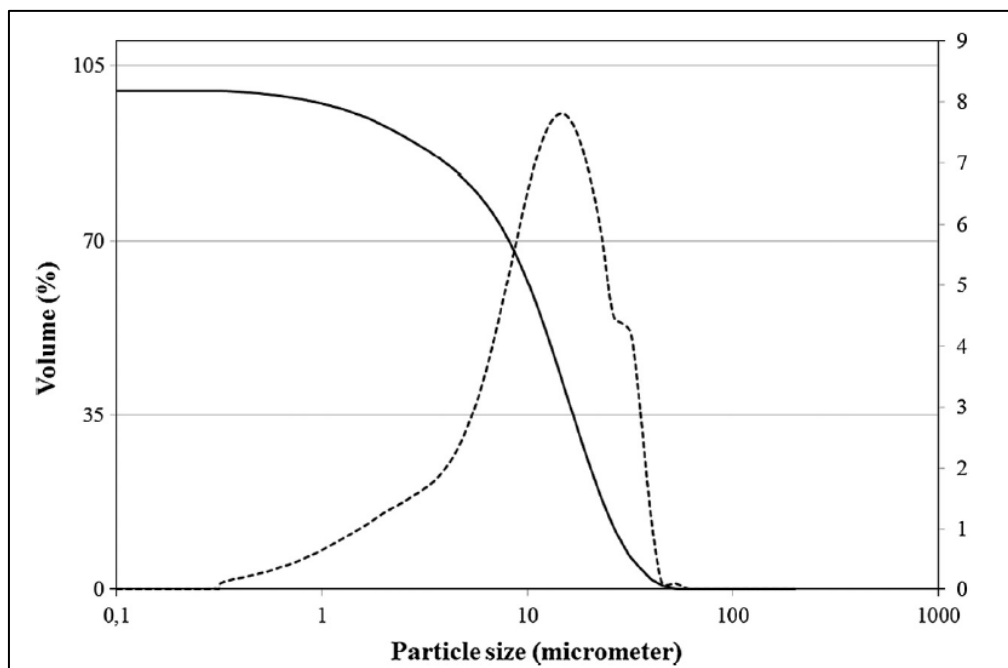


Figure 3.1. X-Ray Fluorescence analysis of GBFS that are used in thesis [70,74,79]

In Table 3.3., the XRF analysis results of the synthesised GBFS's chemical compound were given. In this characteristic, an amorphous hump has observed at around 30° , it has probative the presence of huge amounts of glass content. The 99 % of GBFS content has a vitreous material, also, it has a specific surface area which is $540 \text{ m}^2/\text{kg}$. [70,74,79,80].

Table 3.3. Chemical compound of the BFS [70,74,80]

Chemical Type	Chemical Compound (%)
CaO	36.25
SiO₂	43.08
Al₂O₃	11.34
Fe₂O₃	0.74
MgO	6.10
MnO	-
S⁻²	0,51
SO₃	0.60
Na₂O	0.28
K₂O	0.75
Na₂O + 0.658 K₂O	0.77

3.1.2. Tools and apparatus

Digital precision balance (0.001)

In this study, a digital laboratory balance with an accuracy of 0.001 g was used. In this way, the chemical powders used were measured with high precision, allowing for high accuracy work.

Oven

In this study, an oven was used to production of new catalysts powder synthesis.

Magnetic stirrer with heater

In this study, a magnetic stirrer with heater was used to obtain a homogeneous mixture.

Dehumidifier

In the study, it is used to prevent the water vapor released due to the dehumidifier reaction out of going to the fuel cell together with the hydrogen gas.

Alicat mass flow meter

In this study, Alicat M-Series Gas Mass Flow Meter shown in Figure x was used. This flowmeter was chosen because it can measure more than 98 types of gases over a wide flow range. In addition, it can simultaneously measure both the volumetric flow of the gas, the mass flow of the gas, and the temperature and pressure values of the gas. The measurement accuracy is between 0.01% and 100% of full scale.



Picture 3.1. Alicat M-series gas mass flow meter [81]

PT-100 thermocouple

Since temperature differences are an observable and important factor in reactions, temperature sensors and thermocouples are used to determine the total heat transfer coefficients. The main difference between PT100 sensors and thermocouples is that Pt100 sensors have a high accuracy rate, whereas thermocouples have a fast response time. In this thesis, the reason for choosing PT100 thermocouples is faster data acquisition [82].



Picture 3.2. PT-100 thermocouple

Arduino uno

Arduino Uno is a microcontroller board based on the ATmega328P and contains everything needed to support the microcontroller. It has 14 digital input/output pins (6 of which can be used as PWM outputs), 6 analog inputs, a 16 MHz ceramic resonator (CSTCE16M0V53-R0), a USB connector, a power jack, an ICSP header and reset button. It is very simple to use, you just need to connect it to a computer with a USB cable or run it with an AC to DC adapter or battery to get started. Arduino is an easy to use microcontroller, it's using is very common in both the hobby and professional project market. Arduino uses a simple C-derived programming language that has limited instruction sets. Thus, it allows to easily create interface circuits, write programs, and control motors and lights. So, therefore, becomes more user-friendly [83–85].



Picture 3.3. Arduino uno rev3 [86]

3.1.3. Glass materials

- 250 mL 4-necked flask
- 25-50-500 mL beakers
- Petri dishes of 120x20 mm
- Petri dishes of 100x20 mm

- 100- and 50-mL measuring tapes
- 120 mm funnel
- 40 cc sample jar

3.1.4. Prototype material and electronic apparatus

Plexiglass

Poly-methyl-methacrylate (PMMA), called plexiglass, is a low-weight and break resistant transparent thermoplastic homopolymer that finds widespread application in various fields. In order to achieve high specific strength, traditional metal parts used in applications are replaced with polymers in products. In addition to the fact that they are generally available and sold in different thicknesses, sizes and shapes such as sheets, rods or tubes, it can likewise be formed to suit specific designs. Plexiglas is preferred in prototype projects due to its features such as the lightweight, the dimensional stability, the high optical clarity and the high resistance to impact, weather, UV lights, chemical material.

Table 3.4. Technical features of the plexiglass

Density:	1.17	g/cc
Ultimate tensile strength (UTS):	48–76	MPa
Elastic modulus (Tensile):	1800–3100	MPa
Poisson's ratio:	0.35–0.4	
Thermal conductivity:	0.167–0.25	W/m.K
Specific heat capacity:	1466	J/kg-K

Solenoid valve

In this study, a one-way solenoid valve, which has two 1/2" outputs and operates with 12 V DC, has a minimum pressure requirement of 0.02 MPa, is used. This solenoid valve can operate at different DC voltages such as 6V DC by opening more slowly. A TIP120 or N-

Channel power FET with 1N4001 flyback diode can be used to drive this valve from a microcontroller pin. An adapter/battery with 12V 1A power is used as power source.



Picture 3.4. Water solenoid valve - 12V - 1/2" [87]

Table 3.5. Technical features of the water solenoid valve - 12V - 1/2"

Working Pressure:	0.02 - 0.8	MPa
Working Temperature:	1 - 75	°C
Response time (open):	≤ 0.15	sec
Response time (close):	≤ 0.3	sec
Actuating voltage:	12V (it would work down to 6 V)	DC
Actuating life:	≥ 50 million cycles	
Weight:	122	gr
Dimensions:	76.2 x 57.15 x 50.8	mm

Nozzle

Rainbird Van Spray Nozzle Rain Bird 1800 series has adjustable nozzles for sprayers and UNI-spray. The stainless-steel screw at the top of the nozzle regulates the spray within a range of 0.9 to 1.2 meters.



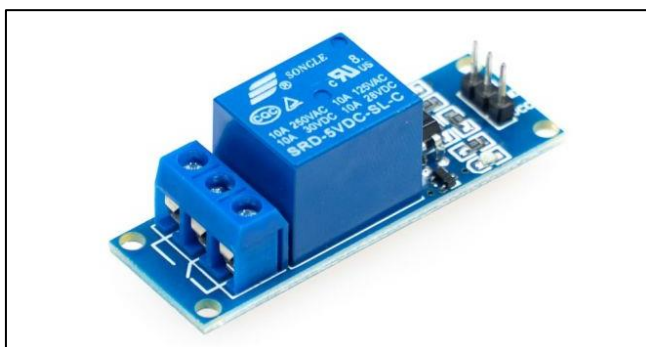
Picture 3.5. Rainbird van spray nozzle [88]

Table 3.6. Technical features of the nozzle [88]

Connection	internal thread
Flow	0.05 to 0,2 m ³ / h
Spray	0.9 to 1.2 m
Operating pressure	1 to 2.1 bar

Relay

1 Way 5V of Relay Module is a relay board. This relay can handle its contacts with 5V by means of a microcontroller board. Relays are triggered with logic 0 (0V) and draws 20 mA of current from microcontroller when triggering.



Picture 3.6. One Way 5V Relay Module [89]

Resistance 330 ohms

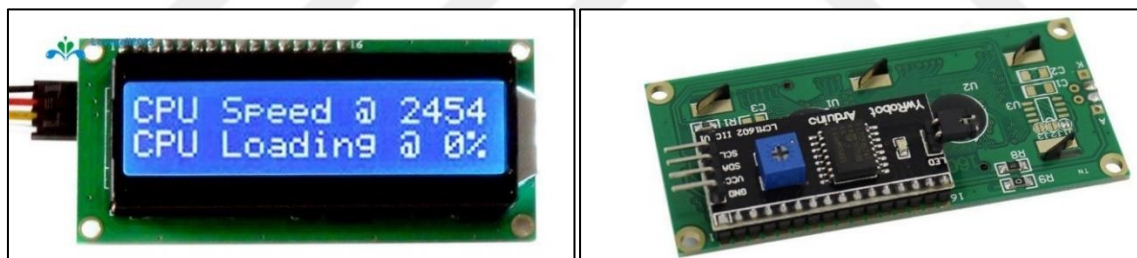
A 330R ohm resistor durable up to energy 0.25W.



Picture 3.7. 1/4W 330R resistor

LCD display

The LCD display module used in this study is 2 lines and 16 characters. It is backlit and has IIC communication interface. An LCD driver can be easily connected to the circuit connection on the Arduino with 4 pins. It allows us to read the values such as flow rate, pressure, temperature occurring in the system as a blank.



Picture 3.8. 16x2 LCD Display- Blue Display with I2C Solder

Buzzer

In this study, a piezo buzzer shown in Figure x was used. Piezo Buzzer is a type of acoustic warning device that works based on piezoelectric principles. It has many usage areas such as alarm, timer, confirmation response alert. Piezo buzzers are highly preferred because they have low cost and high performance. They can react differently from each other according to electric current. Thus, they can produce sounds in different tones at different times.



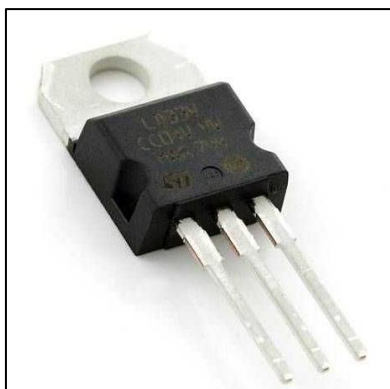
Picture 3.9. Piezo buzzer [90]

Table 3.7. Technical features of the piezo buzzer [90]

Rated Voltage:	12	V DC
Operating Voltage:	8 to 15	V DC
Max. Rated Current:	15 (at 12V DC)	mA
Resonant Frequency:	3.3 +0.5	kHz
Min. Sound Pressure Level:	88 (at 12V DC / 30cm)	dB
Tone Nature:	Continuous	-
Case Material:	ABS	-
Operating Temperature:	-20 to + 60	°C
Store Temperature:	-30 to +70	°C
Weight:	8	g

Voltage regulator-LF33CV

In this study, a voltage regulator shown in Picture 3.10 was used. It is a type of regulator with TO-220 sheath, which is used to reduce the voltage to 3.3V in electronic card circuits.



Picture 3.10. Voltage regulator-LF33CV [91]

Gas sensor

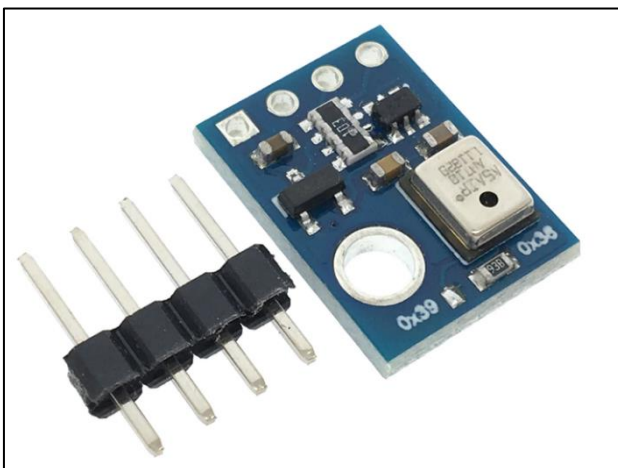
In this study, a gas sensor with a high accuracy was used for measure of hydrogen gas volume. This module has MQ2 type Gas sensor. It uses for detect gasses like Liquid Nature gas (LNG), butane, propane, methane, alcohol, hydrogen and smoke.



Picture 3.11. MQ2 type gas sensor [92]

Pressure and temperature sensor

In this study, a High Precision Digital Temperature and Humidity Sensor module was used. It will measure humidity and temperature changes in the system with high precision.



Picture 3.12. High precision temperature sensor [93]

3.1.5. Characterization devices

The XRD and SEM analyzes are carried out to determine the characterization results of treated and untreated clays.

The X-Ray diffraction device

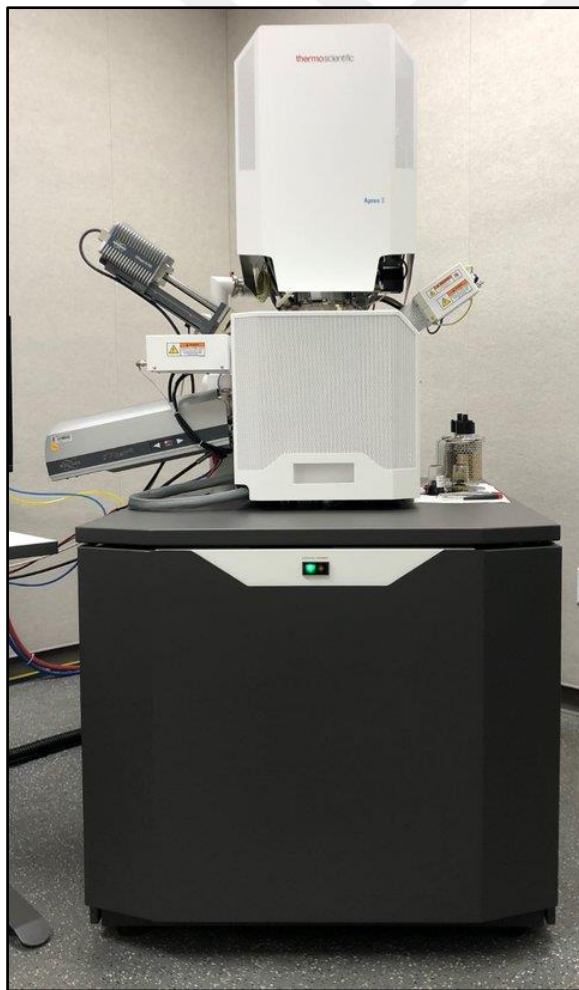
In XRD analyzes carried out to determine the pore structure of slag and synthesized catalysts, İskenderun Technical University, ISTE Center for Science and Technology Studies and Research (ISTE-CSTSR), X-Ray Diffractometer (XRD) Laboratory, “Malvern Panalytical EMPYREAN (3rd Generation) XRD” device used. In this study, Malvern Panalytical EMPYREAN (3rd Generation) brand/model XRD device is shown in Picture 3.13. The working principle of the XRD method device is based on the principle that each crystal phase refracts X-rays in a characteristic pattern depending on their unique atomic arrangement. The XRD investigation technique does not damage the sample during investigation, also, permits investigation of even tiny pieces of sample. The XRD device can measure the thin films and polymers, the amorphous and crystalline materials, quantitative and qualitative analysis of rocks [94].



Picture 3.13. Malvern panalytical empyrean (3rd generation) XRD device [95]

Scanning electron microscopy

In SEM analyzes carried out to examine the morphological structure of slag and synthesized catalysts, İskenderun Technical University, ISTE Center for Science and Technology Studies and Research (ISTE-CSTSR), Scanning Electron Microscopy Laboratory, “Thermo Fisher Scientific Apreo S LoVac SEM” device was utilised. In this study, the working principle of the Scanning Electron Microscope shown in Picture 3.14 is that the electrons detached from the electron source are dropped onto the sample with the help of collector lenses in a column under vacuum. For example, it is based on obtaining information about its topography and chemical compound. This SEM device has a Field Emission Electron Gun and 1 nm image resolution at 1 kV and operates in the 0,2 – 30 kV range [96].



Picture 3.14. Thermo fisher scientific apreo S LoVac SEM device_[97]

3.2. Experimental Method, Setup and Test Rig

3.2.1. Experimental method of the BFS-Co-B catalysts synthesis

Firstly, the chemical impregnation-reduction technique was utilized meanwhile the HCl acid treating process was applied to the Raw GBFS by-product. The impregnation technique, which is utilized, is one of the best catalyst preparation methods. In this method, the support material that has porous structure is mixing with an aqueous solution that has one or more metal compound. Then, other steps of the method such as the waiting a while filtration, washing, drying and reduction are done to this mixture. The catalyst samples prepare using the GBFS(-) and GBFS(+) that were load by different percentages of the Co metal powder. Then, the distilled water and the catalysts such as the Raw BFS, the Co-B-BFS(-) catalyst and the Co-B-BFS(+) catalyst are used to hydrolysis reaction of the NaBH_4 .

Preparing of the Co-B-BFS(-) catalysts samples

Firstly, 20 % amount Co nano powder and 2 g the raw BFS powder were blended for through 30 minutes in 100 ml beaker which has 25 ml of distilled water. This process repeating with another different amounts (30 %, 40 %, and 50 %) Co nano powders. Consequentially, these raw BFS powder, which were added with various amounts percentages Co nano powders, were prepared. These powder sludges were filtered and dried at 110°C in the oven. Thereafter, using 5% NaBH_4 powder, 20 ml distilled water and dried BFS-Co mixtures were reduced with Co ions. Throughout the reduction a black precipitate sludge has occurred, when it was filtered. This filtered black sludge, which was dried in an oven throughout 24 h, after that, it was manually milled. In the Picture 3.15., the stored GBFS catalyst sample powders are shown.

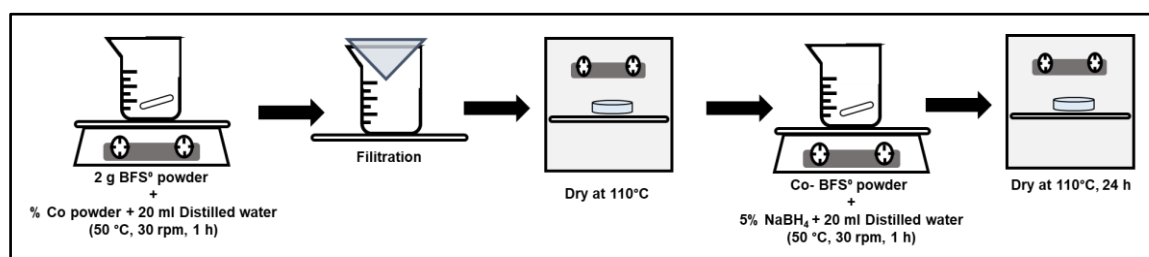
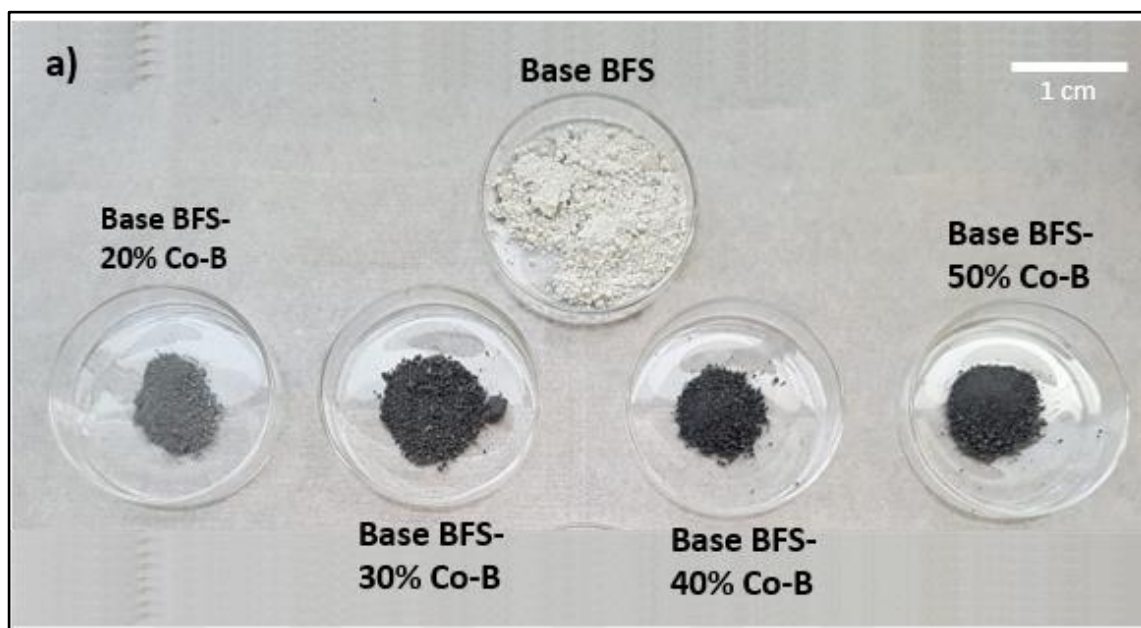


Figure 3.2. The flow chart of the preparation steps of the Co-B-BFS(-) catalyst



Picture 3.15. The granulated raw BFS and the raw BFS supported different % quantity Co -B catalysts

Preparing of the Co-B-BFS(+) catalysts samples

First step, the 1 M HCl solution was added to the 10 g of Raw GBFS powder that is in a 250 ml beaker. Then, second step is this mixture is mixing method that has the 30 rpm velocity, the 50-70°C temperature range and 1 h experiment time on the magnetic stirrer. After that, it was stood during 1-day impregnation time. As a result of this way, slag powder pieces had a void volume and large surface area. Then, the other steps of impetration (filtration, washing, drying(110°C)) method was used 3 times. As a result of, the GBFS(+) material that is treated with HCl acid was prepared.

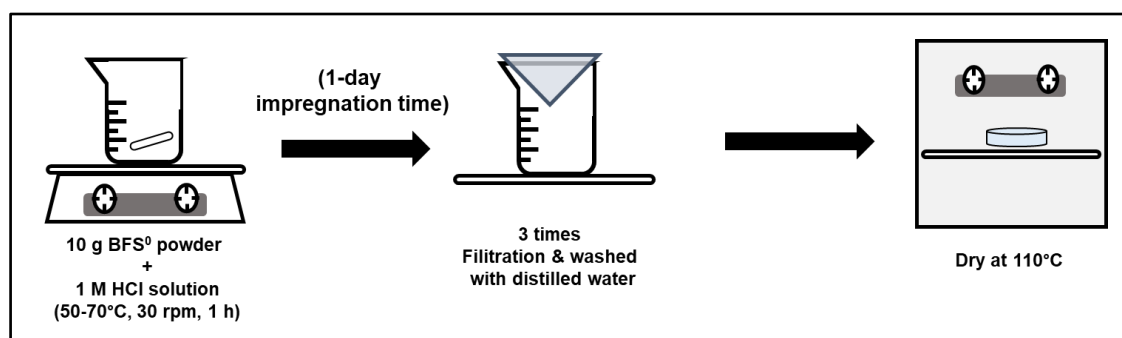


Figure 3.3. The flow chart of the preparation steps of the 1M HCl acid treated Raw BFS powder

The preparation steps of Co-B-BFS(-) catalysts were applied in the same way using the GBFS(+) powder while preparing Co-B-BFS(+) catalysts. In the Picture 3.16., the stored Co-B-BFS(+) catalyst powders are shown.

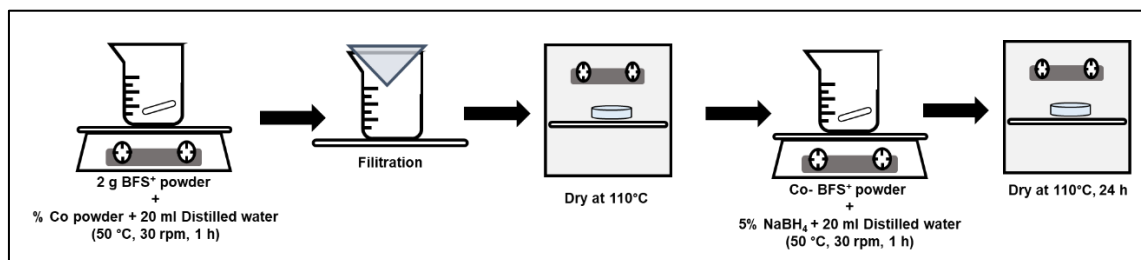
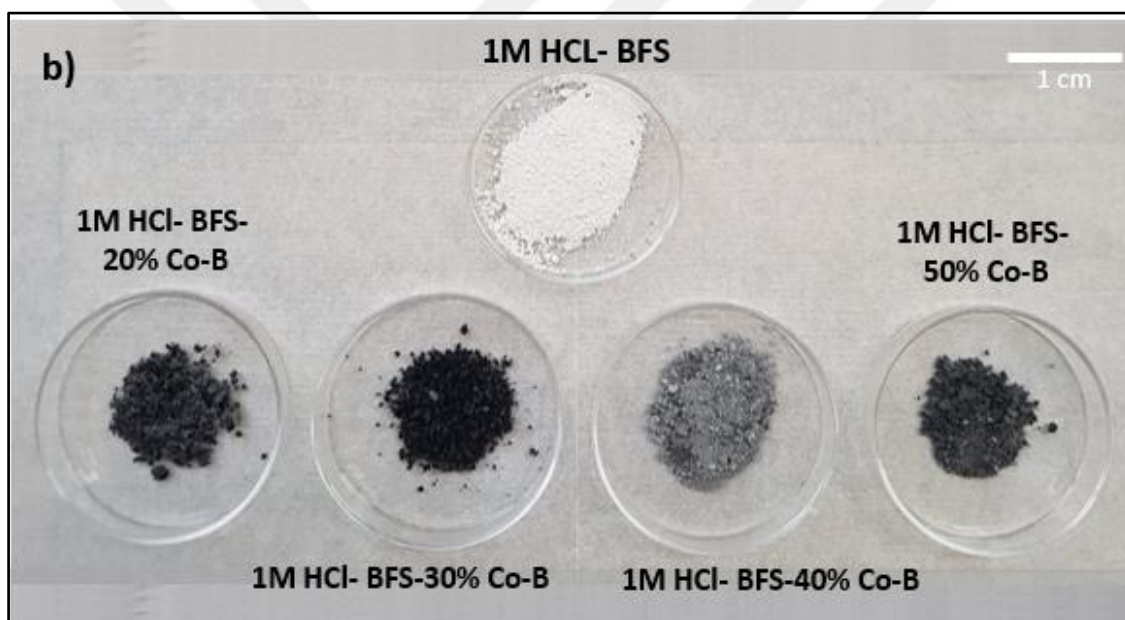


Figure 3.4. The flow chart of the preparation steps of the Co-B-BFS(+) catalysts



Picture 3.16. The acid treated BFS and the acid treated BFS supported different % quantity Co-B catalysts

3.2.2. Experimental setup and test rig of the hydrolysis reactions of the NaBH_4

A reaction vessel with a volume of 250 mL was used in the performance tests of the catalyst samples. This reaction vessel has four necks and a rounded bottom. Each neck is used for a different purpose. A PT100 model thermocouple was used to measure the temperature of the experiment. This thermocouple is fixed to the 1st neck of the reaction vessel, its tightness is strengthened and its connection to the microprocessor is made. A plastic pipe was used to discharge the hydrogen gas released as a result of the reaction to the flowmeter. This pipe is

fixed to the 2nd neck of the reaction vessel, its tightness is strengthened and it is connected to the desiccant. The hydrogen gas produced is first transferred to the dehumidifier. It is aimed to separate the water vapor, which can be released as a result of the reaction and can be discharged together with the gas, from the hydrogen gas. Then, a highly sensitive Alicat brand flowmeter is used in the experimental setup to determine the amount of hydrogen gas produced. The flowmeter was connected to the microprocessor and the hydrogen gas output was recorded throughout the experiment. The reaction model used in this experimental setup is based on the hydrolysis of NaBH_4 to produce hydrogen gas and the catalytic activities of the synthesized catalyst samples. Performance tests of these catalytic hydrolysis reactions were carried out with 20 mL distilled water, 2g NaBH_4 powder and 0.5 g catalyst sample. The powder materials used in the experiment were weighed with a precision scale. The water was measured using a dropping funnel with a tape measure and transferred to the reaction vessel with this funnel. Finally, the data obtained during the experiment were transferred to the microprocessor simultaneously and the results of the experiment were recorded on the computer. The schematic view of the experimental setup used in this study is shown in Figure 3.5.

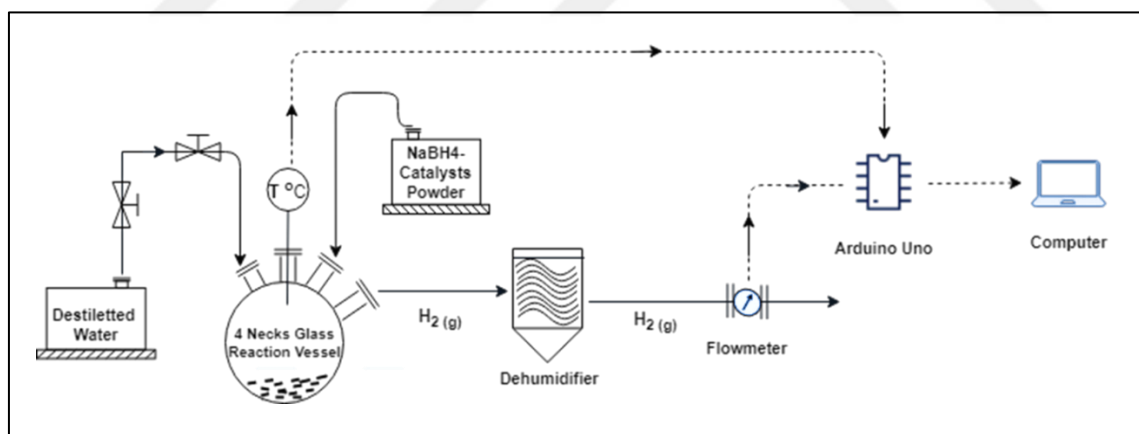


Figure 3.5. Experimental setup flow chart

Performance tests of these catalytic hydrolysis reactions were carried out with the raw BFS powder, the Co-B-BFS(-) catalysts and the Co-B-BFS(+) catalysts sample. The NaBH_4 percentage was optimized at 10 % to be able to produce hydrogen gas in sufficient quantity. Generally, all experiments were started in a 250mL reaction vessel by adding 2g of NaBH_4 powder and 0.5g of catalyst sample from the 3rd neck of the reaction vessel and then adding 20 mL of water from the 4th neck of the reaction vessel. This vessel was sealed tightly with

rubber stoppers and gas sealing Teflon tape. Afterwards, the test vessel was preheated up to 50 °C with the magnetic stirrer-heater. The test temperature was recorded continuously by means of a thermometer. The hydrogen gas produced was separated from the water vapor using a bubble-type dehumidifier. As can be seen in Picture 3.17, all mechanical, electronic and plastic connections of the test system were made and the sealing of all connections was supported. The volume of hydrogen gas produced during the experiment was measured with a flow meter. These experimental data were recorded using a microprocessor. Experiments were repeated at least three times in order to optimize the results.



Picture 3.17. Hydrogen gas production system test rig

3.2.3. Experimental setup and test rig of the hydrogen generator prototype

The water + catalyst mixture was added with the help of a pump to the NaBH_4 particles that are in the fuel reservoir. The reaction is expected to occur rapidly at room temperature. The hydrogen gas produced owing to the fact that the NaBH_4 reaction taking place in the reactor was transferred through the humidifier to the flow meter. The pressure, temperature and production amounts taken from the flow meter collected by the microcontroller were monitored and were realized with an automatic control system for sustainable electricity generation.

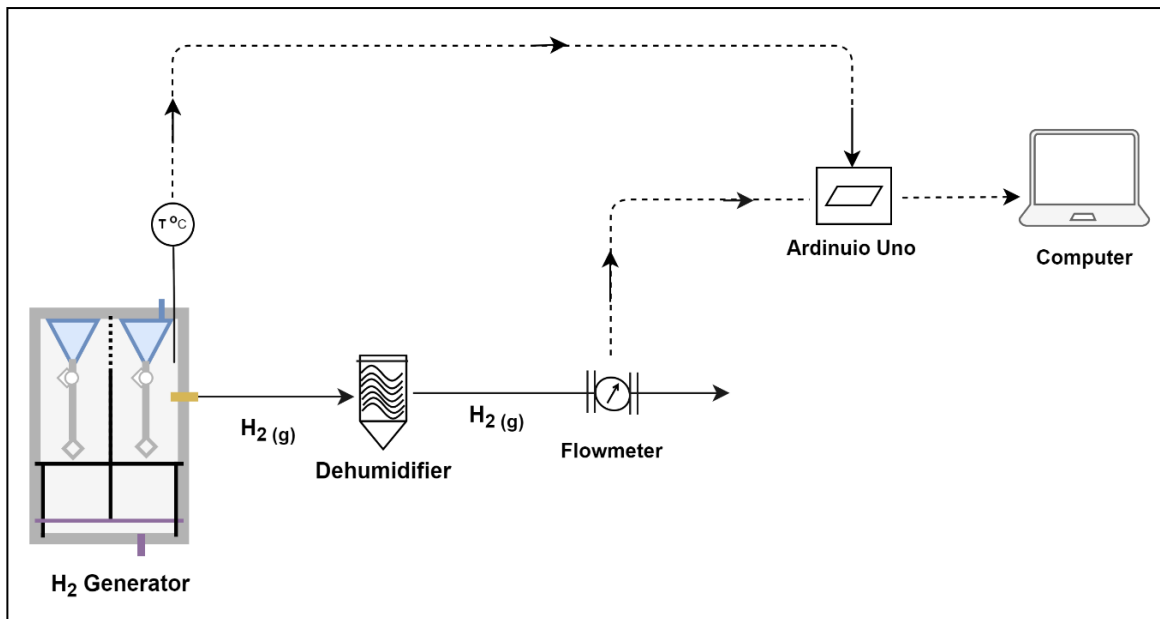


Figure 3.6. The test rig of the hydrogen generator system

The algorithm of the autonomous control system was designed depending on the changes in reactor pressure. A test station was installed in this way; the system tests such as pressure, temperature and the performance of hydrogen production are planned in this system. The electronic operating performance of systems and autonomous systems requirements of the system were also evaluated. After optimal results obtained from these experimental tests, a prototype of the size that were to be integrated into a stack of the fuel cell were prepared. It is planned to conduct performance tests of the generator using the autonomous control system for 1 hour of different working phases and to record the test results.

3.3. Prototype Design

Firstly, hydrogen gas production trials and performance analyzes were carried out by manually controlling the generator system, whose installation was completed. Afterwards, the control card of the analyzed generator was designed, and then autonomous operation trials were carried out on the prototype. The algorithm of the Autonomous control system of the Hydrogen Generator depends on the changes in the reactor pressure. By monitoring the pressure, temperature and production amounts taken from the flow meter collected with the microcontroller, the initiation of the reaction in the next reaction chamber for sustainable

electrical energy production is provided by the automatic control system. In this way, both the system's feedback information was followed and sustainable production was ensured without any problems [98,99]. The generator, in which the autonomous control system was used, was put back into the experimental setup and performance tests were done for various working phases of 1 hour, and the test data were recorded. Consumption values of NaBH_4 and catalysts and system cost were calculated in line with the test results obtained.

3.3.1. 3D design and analysis of hydrogen generator

After calculating the quantity of hydrogen gas needed for supply a fuel cell for 1 hour, the generator's size and volume and its sections were determined depending on the quantity of NaBH_4 powder and water volume required to produce this gas. The quantity of water required to completely dissolve and hydrolyses 2 g of NaBH_4 powder was determined as 20 ml. The first prototype design was made by considering other equipment such as water pump, nozzle, pipe, sensors and Arduino, whose volumes are given in the material section.

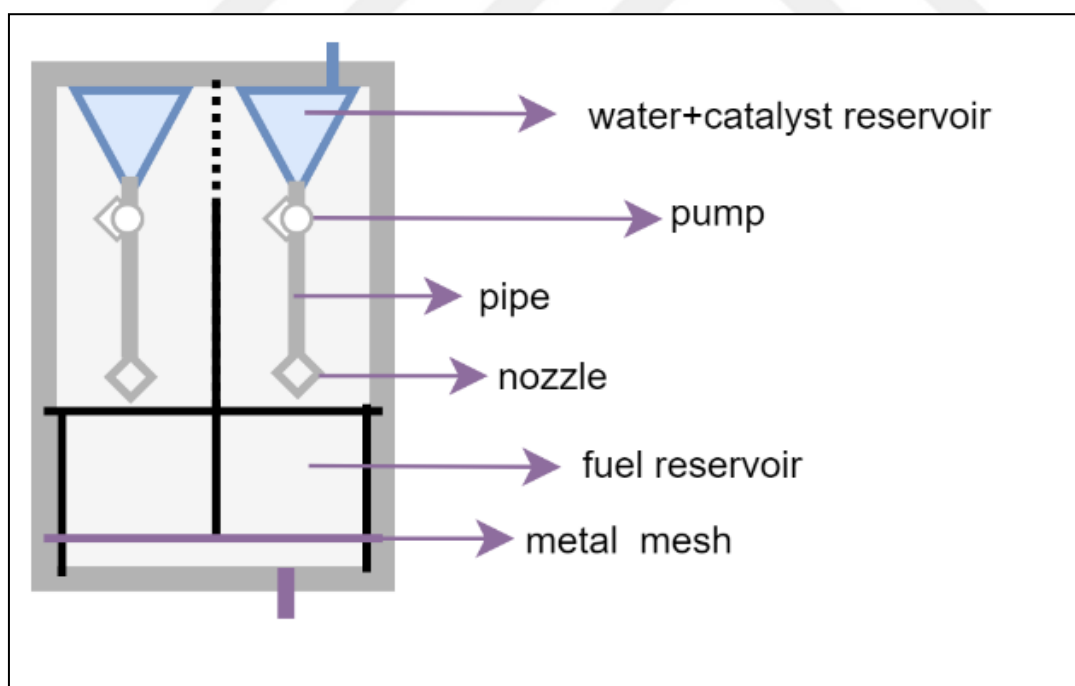


Figure 3.7. The design of the hydrogen generator system

In this study, a four-chamber generator was designed. The design of each of the rooms; It consists of 4 sections, namely the control unit, the water reservoir, the auxiliary equipment section and the NaBH_4 reservoir. The control unit is positioned above these 4 reaction

chambers. The water reservoir consists of a chamber with a conical structure as a mixture of catalyst powder and water. It is aimed to provide the necessary water pressure for the water pump due to the shrinking structure of gravity and the conical structure. The water pump, sensors and other auxiliary equipment are kept away from water and moisture contact in the auxiliary equipment section. Water and catalyst solution, the flow of which is controlled by a water pump, is sprayed on the NaBH_4 powder with the help of nozzles and a homogeneous distribution is achieved. The fuels are discharged from their respective chambers into the reservoir where the reaction takes place. It is explained in detail in the experimental scheme and setup section is shown in Figure 3.7.



Figure 3.8. The 3D design of the hydrogen generator system

The hydrogen generator, whose size and volume were determined, was manufactured using plexiglass material. All connections of the generator were pasted with chloroform adhesive to prevent possible hydrogen leakage, providing a high sealing environment. The first

hydrogen gas production experiments and performance analyzes of the prototype were carried out under manual control. The hydrogen generator prototype manufactured was put instead of the 4-necked glass balloon reaction vessel from the experimental setup used in the hydrolysis experiments of the catalysts, and the experiments were carried out in the same experimental setup and the test results were recorded with the help of Arduino. The hydrogen generator prototype 3D design is shown in Figure 3.8.

3.3.2. Autonomous control card design and writing control system algorithms

Autonomous control card design

The basis of this project is to ensure the continuity of the energy source required for the duty period of the system, depending on the decrease in the gas level in the system. The gas sensor placed in the prototype of the gas sensor measures the hydrogen gas level, activates the water pump when the gas level starts to decrease depending on the situation and enables the reaction in the second reaction vessel to start.

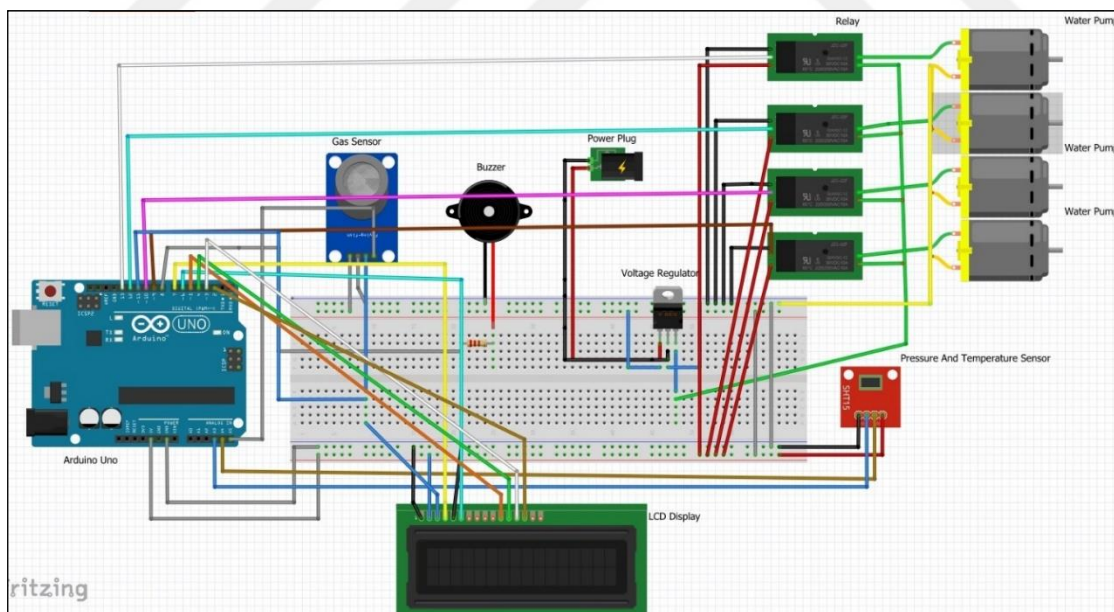


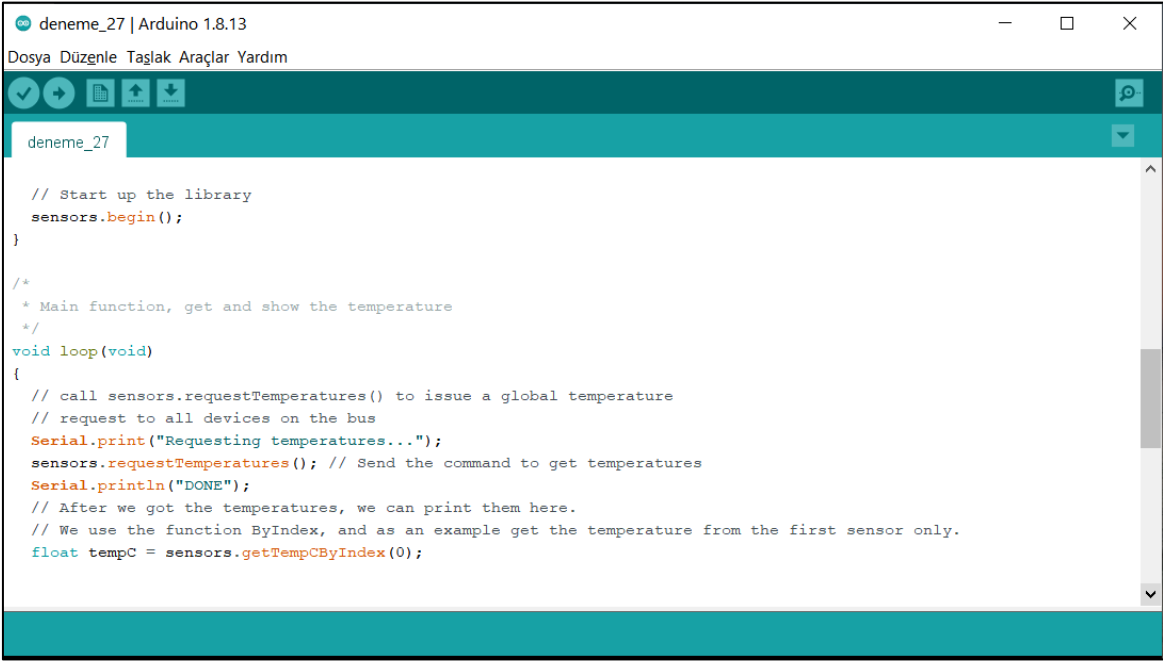
Figure 3.9. The design of the autonomous control system

A temperature and humidity sensor has been added to the prototype to take into account other environmental conditions that may affect the operating performance of the system. With this sensor, it works independently of the system's autonomous control, but they are

programmed to shut down the system when high values are measured. A reference value has been entered for the operation of the system. When the value measured by the gas sensor falls below this reference value, the next water pump will be activated and the reaction will be activated. According to the data coming from the gas sensor, a system mechanism that works automatically by triggering the 220 V water pump with DC 5V has been established. The sensors are connected to the analog input of the Arduino. When the gas level drops according to the values between 0 and 255 read from our sensors, it activates the relay and controls the water flow. Since the water pump works with 12 volts (it can work minimum 6 volts), it is controlled with the help of a relay. The purpose of the relay is to prevent the Arduino used in the system from being burned due to the current. Since this process has a unidirectional working principle, transistor can also be preferred. Values and important information read from the sensors can be read from the LCD screen.

Autonomous control card design and writing control system algorithms

The working algorithm written for the simultaneous monitoring of the autonomous operation and working parameters of the hydrogen generator is implemented using the Arduino board.



```

deneme_27 | Arduino 1.8.13
Dosya Düzenle Taşlak Araçlar Yardım

deneme_27

// Start up the library
sensors.begin();
}

/*
 * Main function, get and show the temperature
 */
void loop(void)
{
  // call sensors.requestTemperatures() to issue a global temperature
  // request to all devices on the bus
  Serial.print("Requesting temperatures...");
  sensors.requestTemperatures(); // Send the command to get temperatures
  Serial.println("DONE");
  // After we got the temperatures, we can print them here.
  // We use the function ByIndex, and as an example get the temperature from the first sensor only.
  float tempC = sensors.getTempCByIndex(0);
}

```

Picture 3.18. A part of the autonomous control system working algorithm

The system is programmed using the 1.6.3 version of the Arduino software and the ATmega328 programming language. Picture 3.18. shows part of the Arduino software that contains the program's instructions. For the required energy need during the first operation, since the Arduino should be fed with at least 6 volts and the valves should be work at around minimum 6 volts, Lithium-Polymer batteries with a capacity of 7.4 V and 2-cell were preferred.



4. RESULTS AND DISCUSSION

4.1. Characterization Analyses of BFS Catalysts

4.1.1. XRD characterization analyses

The purpose of characterizing BFS supported catalysts by the XRD is to verify the presence of minerals in their content. The different peaks that occur in the diffraction peak profiles during each process can be observed in the below Figures. The Figures.4.1. XRD pattern figure show the Raw BFS powder. The impacts of acid treatment and Co loading on the formation of new compounds and amorphous structure in slag-based catalysts upon the change of synthesis parameters are remarkable. The X-ray diffraction peak values of the raw BFS examined in this thesis ($2\theta = 29.73, 38.26, 44.5, 51.84, 64.91, 78.05^\circ$) indicate the presence of crystal structures in BFS content. The slag catalysts exhibit highly crystalline phases containing CaCO_3 (calcite), Ca(OH)_2 (portlandite), SiO_2 , Al_2O_3 , Fe_2O_3 and TiO_2 (rutile) [75]. However, the XRD peak profiles of the samples are showed the same strong peaks at $2\theta = 38.26^\circ$ and 44.5° in Figures.4.1.

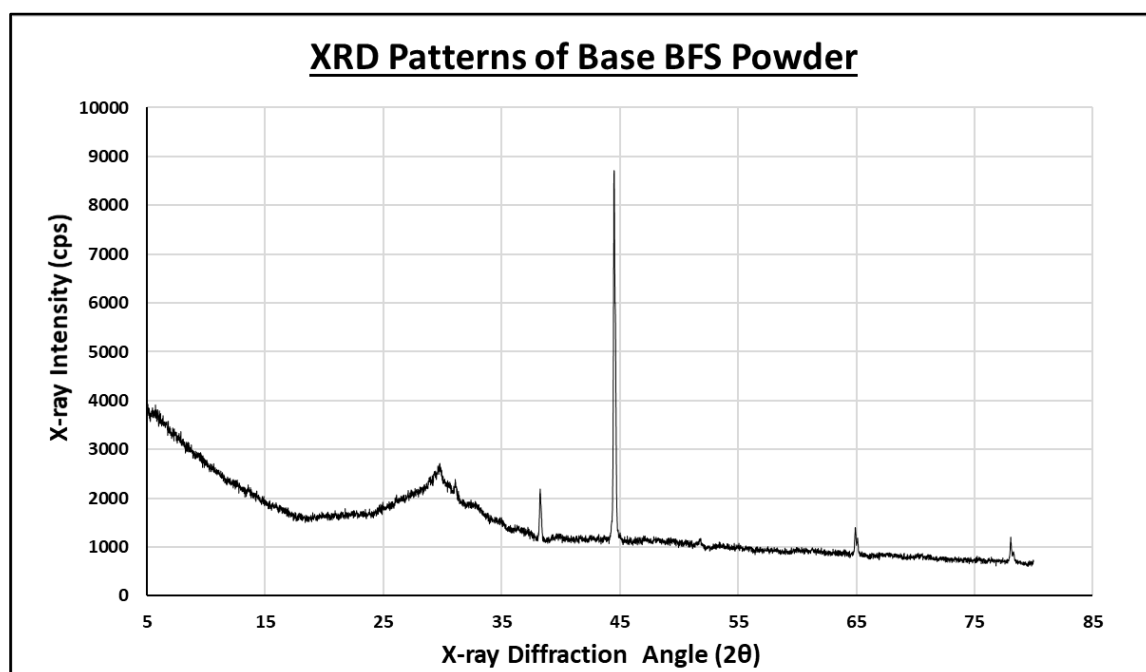


Figure 4.1. XRD peak profiles of the Raw BFS powder

Considering the XRD peak profiles of the raw BFS powder, the XRD peak profiles of the 40% Co-B-BFS catalyst obtained after loading 40% Co metal on the raw BFS powder are given in Figure 4.2. The density and intensity of the peaks in the XRD peak profile of this catalyst sample decreased according to the XRD analysis of the raw BFS powder, also some new weak peaks occurred in the Co nano species.

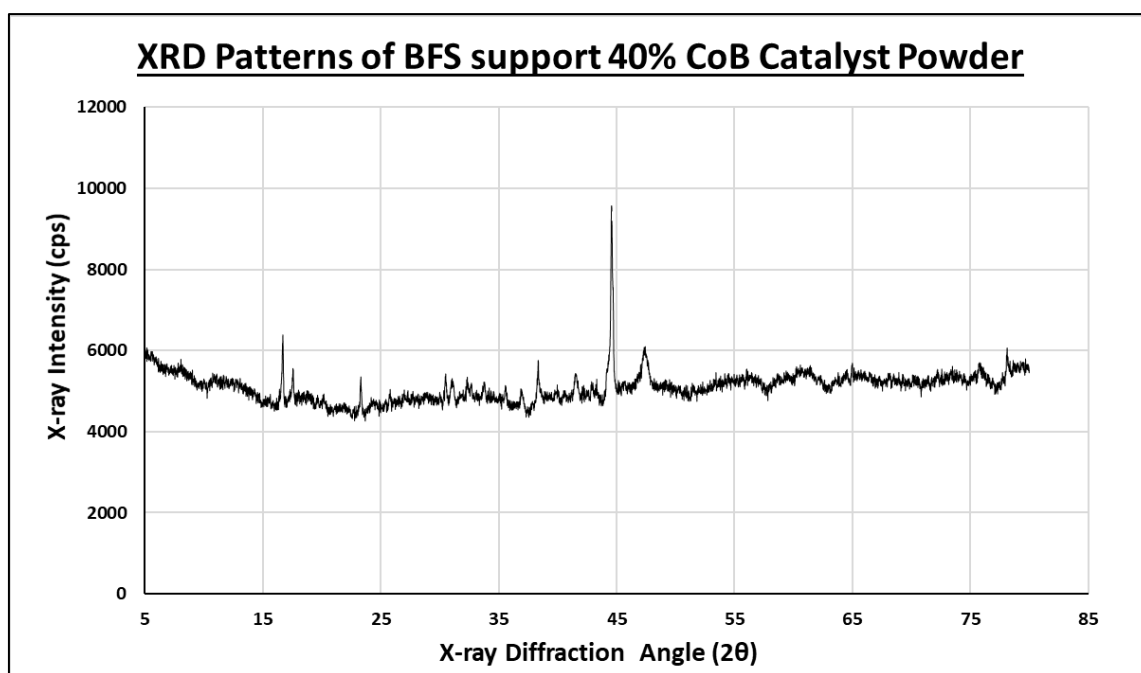


Figure 4.2. XRD peak profiles of the 40% Co-B-BFS catalyst

Considering the XRD peak profiles of the Raw BFS (BFS(-)) powder, the XRD peak profiles of the BFS(+) powder obtained by acid treatment of the raw BFS powder with 1M HCl are given in Figure 4.3. As a result of treating BFS powder with acid, the chemical composition and structure of BFS powder changes. This process ensures the separation of slag particles, removes mineral impurities in the slag content, removes metal exchange and proton exchange cations from the content of the chemical compound. As a result of this process, the improvements on the catalytic properties and surface reactivity of BFS powder were investigated. The density and intensity of the peaks in the XRD peak profile of this powder sample decreased compared to the XRD analysis of the raw BFS powder, but some of the crystalline peaks converted to amorphous structure. However, comparing the XRD analysis of raw BFS powder and the XRD analysis of BFS(+) powder, it is seen that there are still some peaks in the peak profile of BFS(+) powder.

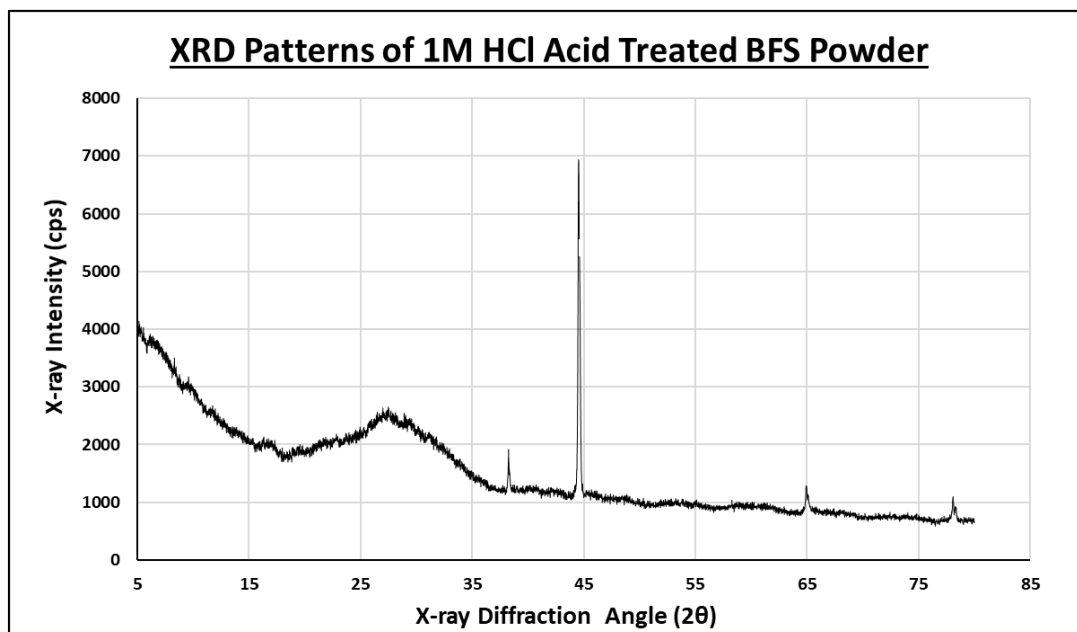


Figure 4.3. XRD pattern of 1M HCl acid treated BFS sample

Considering the XRD peak profiles of the BFS(+) powder, the XRD peak profiles of the 40% Co-B-BFS(+) catalyst obtained after loading 40% Co metal on the BFS(+) powder are given in Figure 4.4. The peaks intensity in the XRD peak profile of this catalyst sample are shown to differ according to the XRD analysis of the BFS(+) powder, also more new weak peaks occurred in the Co nano species.

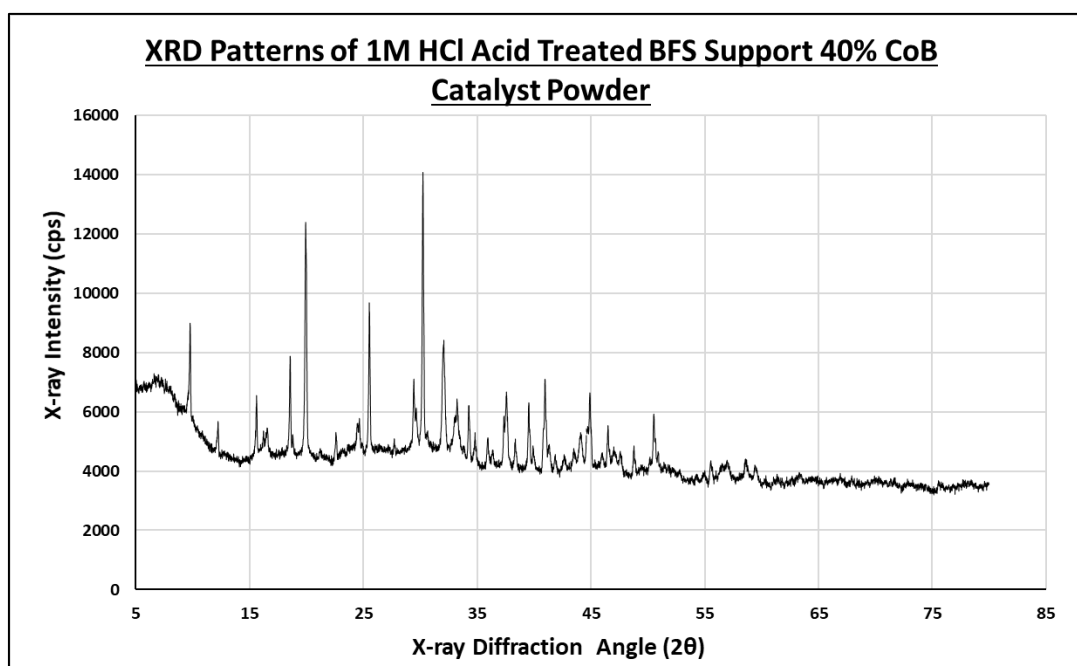


Figure 4.4. XRD peak profiles of the 40% Co-B-BFS(+) catalyst

When the structure of materials such as acid-treated clay in the literature is examined, it is observed that silica formation and degradation in octahedral layers occur. The dissolution of the plates of the support material after this acid treatment, the increase in the porosity of the plates and the observation of amorphous silica formation have been supported by many studies [49]. In addition, depending on the acidity in acid applications, there is a change in the direction of reduction in micro and mesopores. These results are confirmed by the changes in XRD peak profiles shown in Figure 4.1 and Figure 4.3. Deformations and amorphous silica formations occurring in the BFS(+) structure indicate a decrease in the peak intensity occurring in the characteristic peaks of the material. Protons in the interlayer spaces are cations of the material and with this process, they start to move around the edges of the sample particles. As a result of acid treatment of BFS powder, new bridges form OH^- groups and this increases the acidity of the material. In addition, as a result of dehydroxylation of OH groups, Al, Mg and Fe ions begin to be released from some material layers such as octahedral and tetrahedral [100].

4.1.2. SEM characterization analyses

SEM imaging technique shows the surface morphologies of the sample crystals; was used to examine in more detail in terms of shape, size and distribution changes. The raw BFS, the BFS(+), the Co-B-BFS(-) and Co-B-BFS(+) catalysts are used. Figure 4.5 and Figure 4.6, there are SEM image at (2.00 kV, spot: 8.00 and mag.:1000- 5000) various scales. The surface morphology of Raw BFS powder changes after being treated with acid, becoming a more homogeneous surface morphology. However, the size of the particles decreased and their surface area increased. In addition, while the Co-B-BFS(+) catalysts were being synthesized, the surfaces of the BFS(+) powder were coated with Co metal powder almost homogeneously.

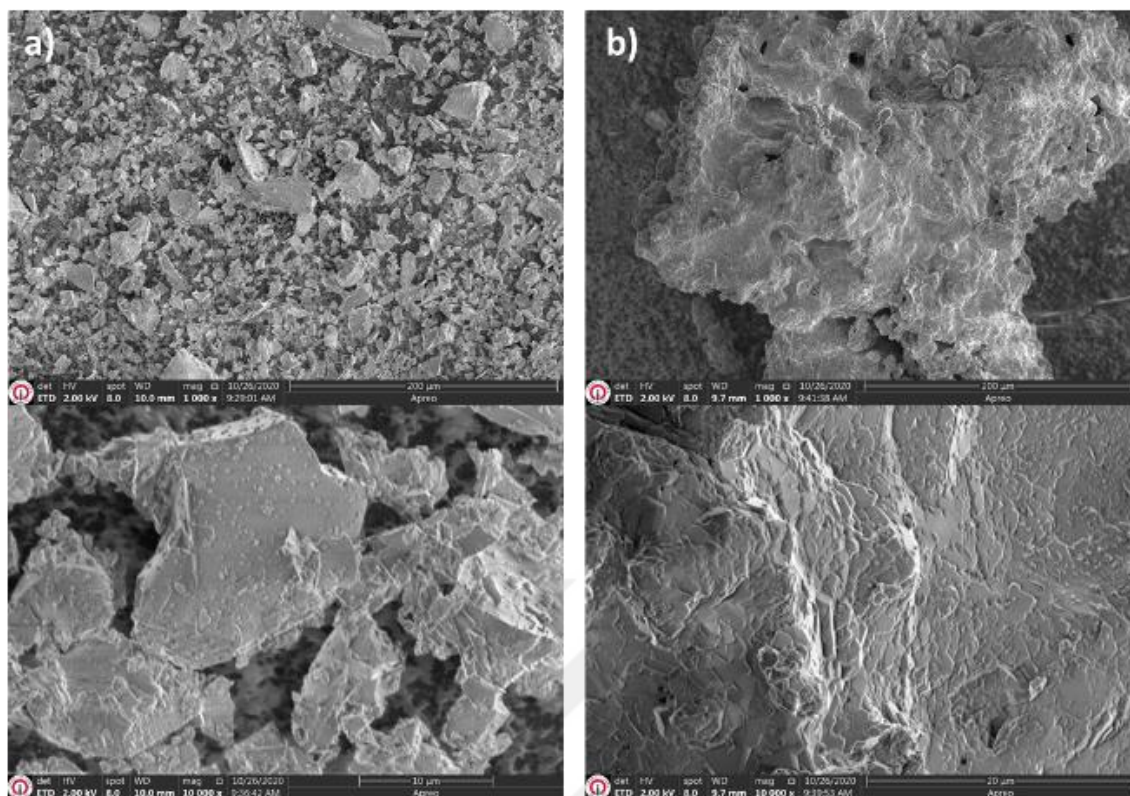


Figure 4.5. (a) SEM image of the Raw BFS powder,
(b) SEM image of the Raw BFS- Co-B catalyst

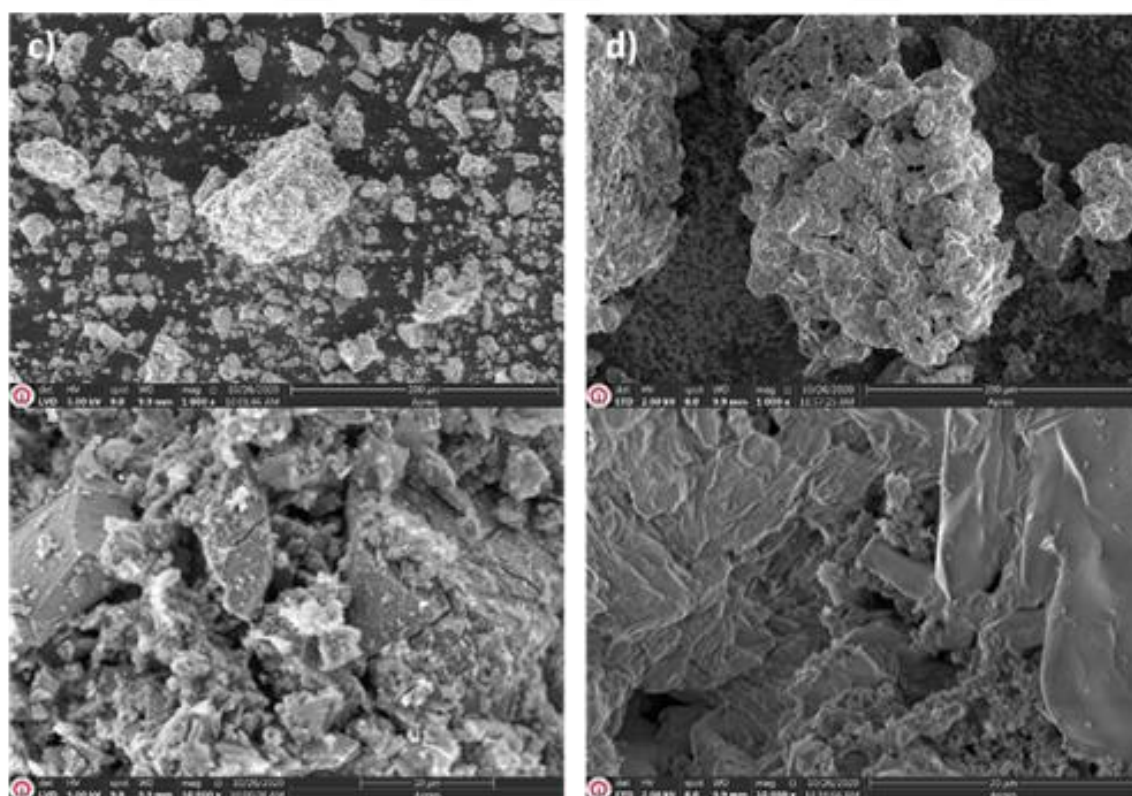


Figure 4.6. (c) SEM image of the HCl acid-treated BFS powder,
(d) SEM image of the acid-treated BFS- Co-B catalyst

4.2. Performance Analyses of BFS Catalysts

4.2.1. Performance impact of HCl acid on BFS powder and BFS catalysts on hydrolysis reaction performance

The performances of the catalyst samples prepared using BFS for the purpose of using in NaBH_4 hydrolysis were tested experimentally. The raw BFS, %20 Co-B-BFS(+) and %20 Co-B-BFS(-) catalysts were used to do the experiments. The raw BFS and %20 Co-B-BFS(+) are showed higher performance in experiments. However, both the Raw BFS and %20 Co-B-BFS(+) was better than %20 Co-B-BFS(-) catalysts. As shown in Figure 4.7., the %20 Co-B-BFS(+) were had a high performance for hydrogen production than the raw BFS. The hydrolysis reaction that using BFS catalysts untreated with acid was completed in about the same time.

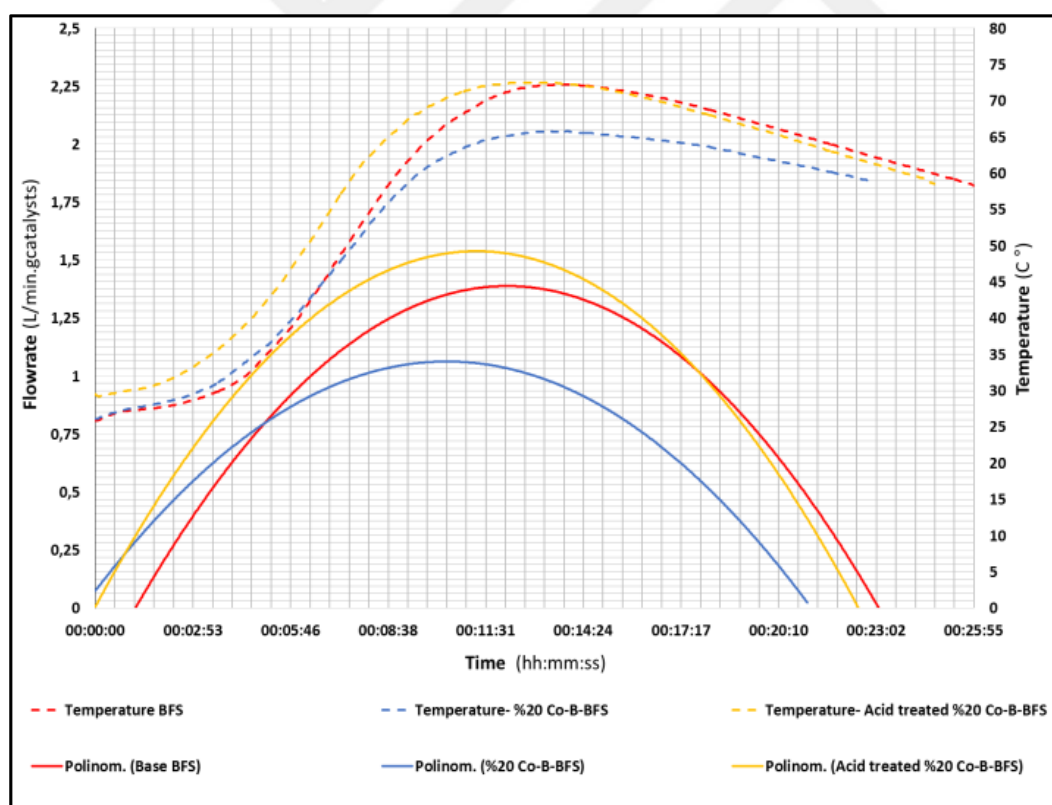


Figure 4.7. The hydrolysis reaction performance analyses of the Raw BFS, the Co -B-BFS(-) and the Co-B-BFS(+) catalysts samples

In addition, total hydrogen production volume and the hydrogen gas production average flowrate of the Raw BFS is approximately 240 L and 54.63 L/min.g.catalyst, respectively.

These values of %20 Co-B-BFS(-) are approximately 183 L and 48.06 L/min.g_{catalyst}, respectively. These values of %20 Co-B-BFS(+) are approximately 277 L and 65.99 L/min.g_{catalyst}, respectively. In line with these results, it can be said that the reason for this increase in the catalytic activity of BFS powder by acid treatment is the attachment of more Co ions to the increased surface area as a result of acid treatment.

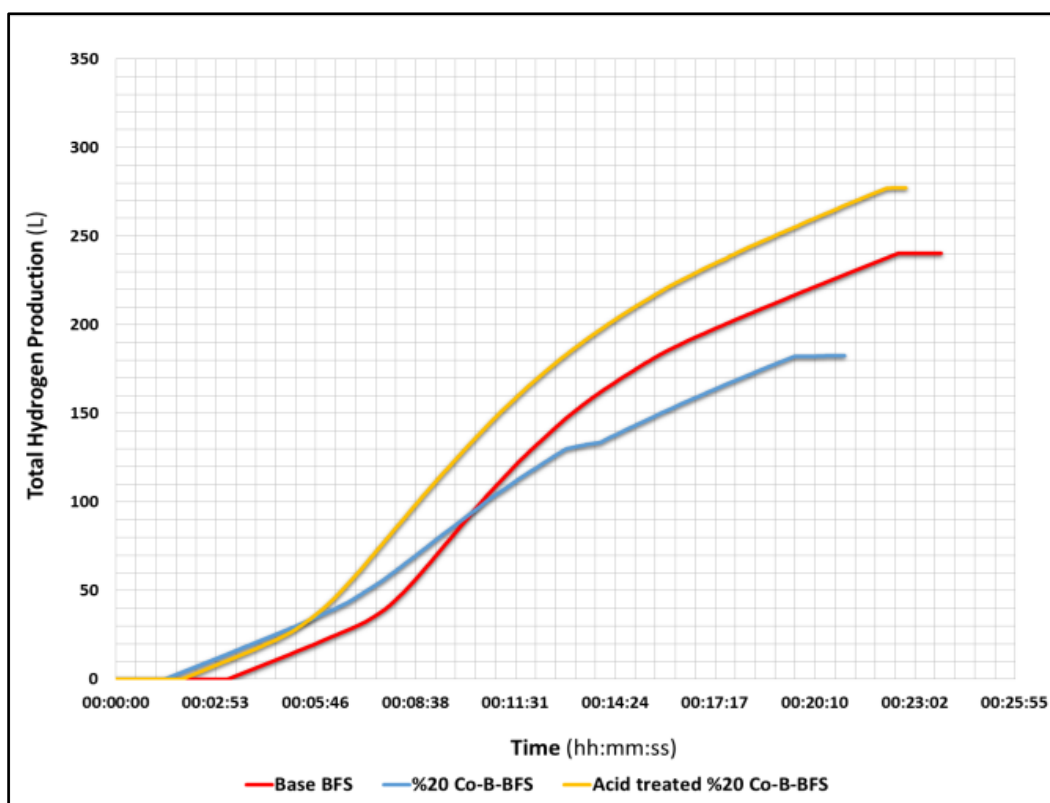


Figure 4.8. The total volume of hydrogen gas of the Raw BFS powder, the Co-B-BFS(-) and the Co-B-BFS(+) catalysts samples

4.2.2. Performance impact of Co nano powder % quantity on hydrolysis reaction performance

When the literature studies are compared, it is seen that the effect of Co metal addition on Co-B-BFS(+) catalysts is more effective than the sepiolite clay supported Co-B catalyst [49]. Catalyst samples were prepared by loading different percentages of Co nano powder into BFS(-) and BFS(+) powders. In these experiments, the effect of these Co nano powder percentages on the catalytic performances will be investigated. Experiments were made by adhering to the experiment method in the experiment setup section. In the experiments, 20%, 30%, 40% and 50% Co-B-BFS(-) catalyst samples and 20%, 30%, 40% and 50% Co-

B-BFS(+) catalyst samples were used. For this reason, the experimental results were analyzed in the different sections.

Impact of different % quantity Co nano powder addition on the Raw BFS catalysts samples

Average hydrogen gas production rates of the 20%, 30%, 40% and 50% Co-B-BFS(-) catalysts samples are approximately 48.06, 65.71, 61.73 and 44.4 L/min.g_{catalysts}, respectively. As shown in Figure 4.9, the 30% Co-B-BFS(-) and 40% Co-B-BFS(-) catalysts samples results showed high performances in hydrogen gas production reaction. The Co-B-BFS(-) catalyst samples create a noticeable change in reaction temperature.

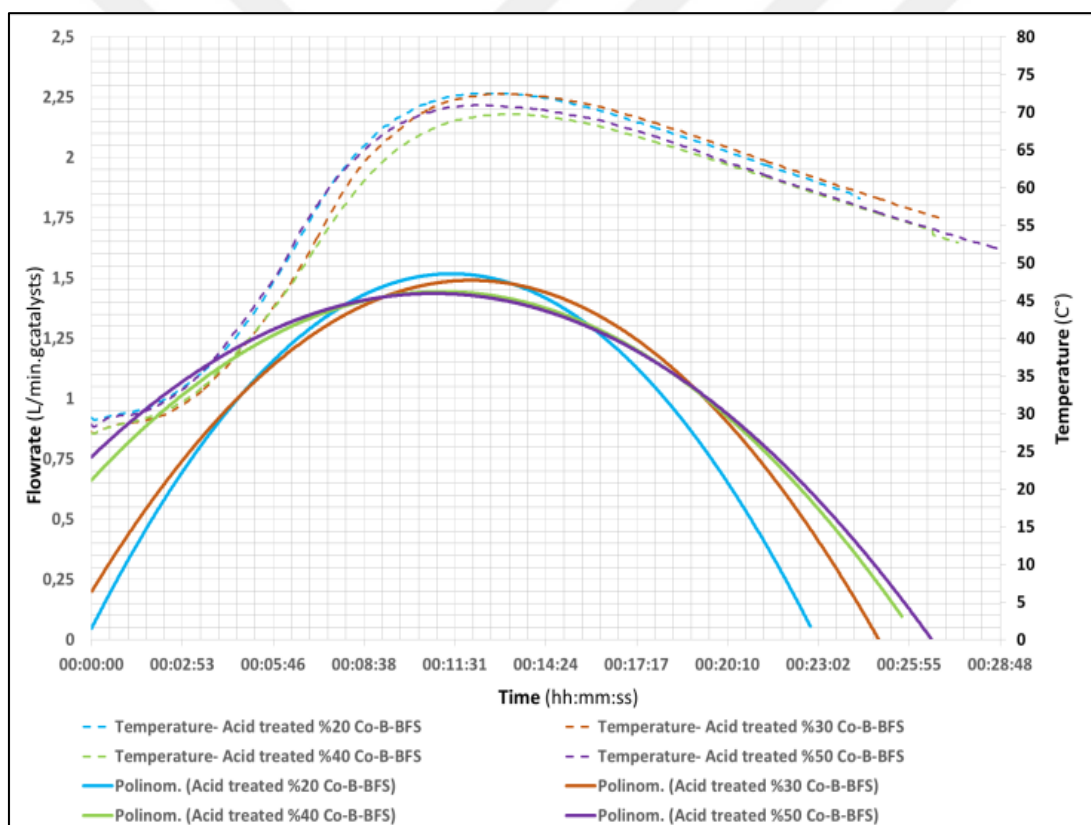


Figure 4.9. The hydrolysis reaction performance analyses of the 20% Co-B-BFS(-), 30% Co-B-BFS(-), 40% Co-B-BFS(-) and 50% Co-B-BFS(-) catalysts samples

The completion times of these hydrolysis reactions are shown in Figure 4.10. Hydrolysis reactions using the 20%, 30%, 40% and 50% Co-B-BFS powder catalysts samples were completed in approximately 20, 26, 28 and 24 minutes, respectively. The highest total hydrogen gas production amount of the 20%, 30%, 40% and 50% Co-B-BFS powder

catalysts samples is approximately 341.70 L. These experiments show us the importance of the amount used in Co nano powder loading on the outcome of the hydrolysis reaction. Looking at the graph, it will be seen that hydrogen production reached the highest peak when the amount of Co nano powder was 30%. Therefore, using less or more than 30% of Co reduces the catalytic activity.

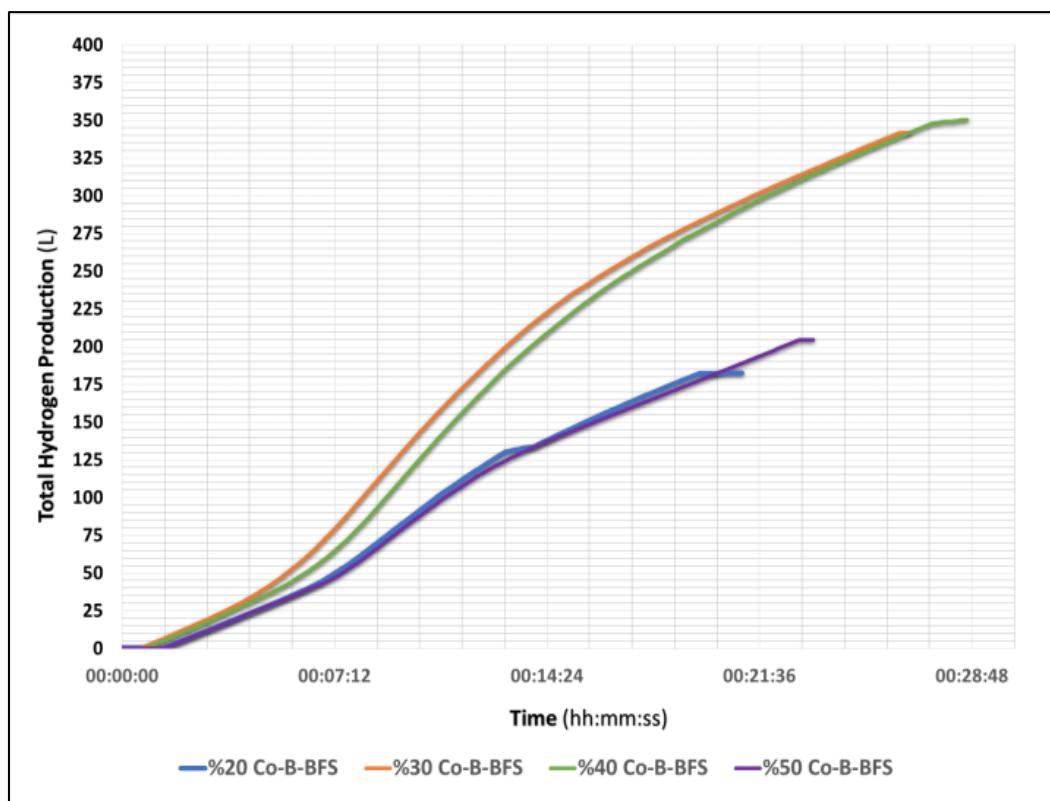


Figure 4.10. The total volume of hydrogen gas of the 20% Co-B-BFS(-), 30% Co-B-BFS(-), 40% Co-B-BFS(-) and 50% Co-B-BFS(-) catalysts samples

Impact of different % quantity Co nano powder addition on the BFS(+) catalysts samples

The average hydrogen gas production rates of the 20%, 30%, 40% and 50% Co-B-BFS(+) catalysts samples are approximately 66.98, 61.4, 66.36 and 65.16 L/min.g_{catalysts}, respectively. As shown in Figure 4.11, the 40% and 50% Co-B-BFS(+) powder catalysts samples had higher performances in the hydrogen gas production reaction. The catalyst samples, which show a linear increase in hydrolysis reactions, show the same linear effect on the temperature of the reaction, while creating a noticeable effect on both the average hydrogen gas production rate and the efficiency of hydrogen gas production.

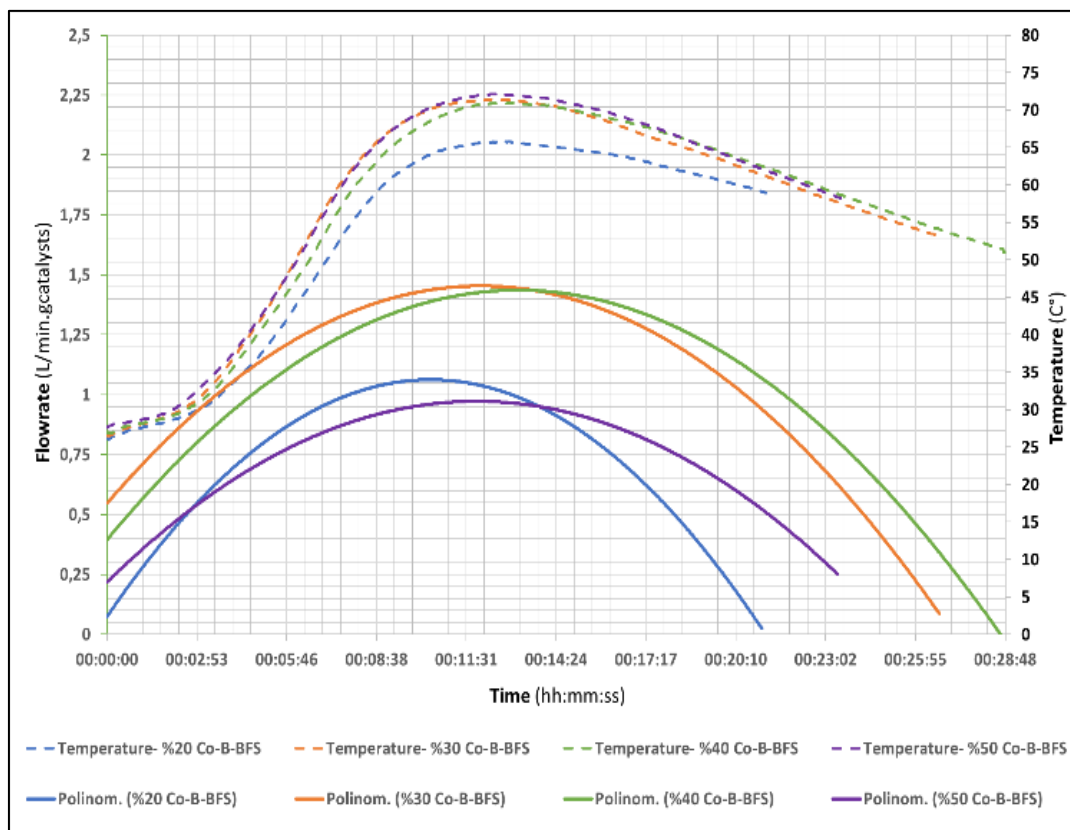


Figure 4.11. The hydrolysis reaction performance analyses of the 20% Co-B-BFS(+), 30% Co-B-BFS(+), 40% Co-B-BFS(+) and 50% Co-B-BFS(+) catalysts samples

The highest total hydrogen gas production amount of the 20%, 30%, 40% and 50% Co-B-BFS(+) powder catalysts samples is approximately 338.81 L. These experiments show us the importance of the amount used in Co nano powder loading on the outcome of the hydrolysis reaction. Looking at the graph, all samples will be seen that hydrogen production reached the linear peaks. Therefore, Co nano powder adding has created a noitable effect on the efficiency of the hydrolysis reaction. Also, 40% Co nano adding has created big effect on catalytic activity and the total hydrogen production value was increased higher than %10.

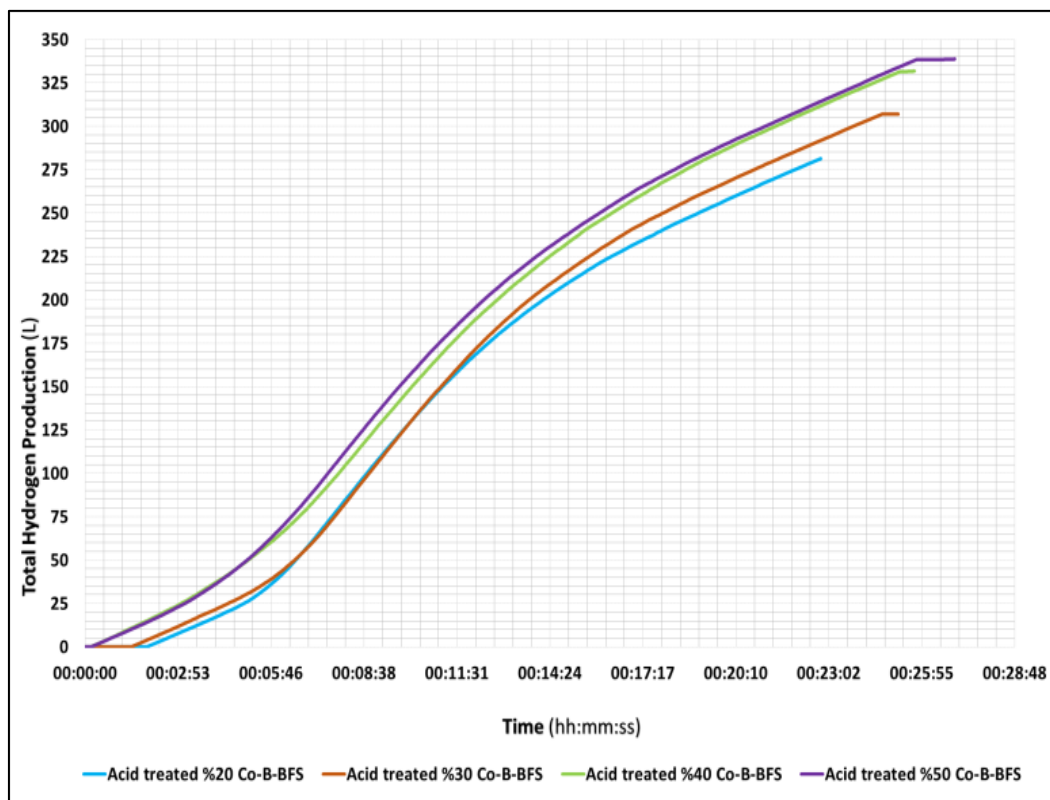


Figure 4.12. The total volume of hydrogen gas of the 20% Co-B-BFS(+), 30% Co-B-BFS(+), 40% Co-B-BFS(+), and 50% Co-B-BFS(+) catalysts samples

4.2.3. Performance impact of the catalyst quantity on hydrolysis reaction performance

In this section, the effect of the change in the amount of catalyst on the catalytic activity was investigated with the addition of 40% Co-B-BFS(+) powder catalyst sample used in 3 different amounts such as 0.2 g, 0.3 g and 0.5 g. the results of the experiment are showed in Figure 4.13. As can be seen in the Figure 4.13 and Figure 4.14, with the increase in the quantity of catalyst, the reaction time shortened.

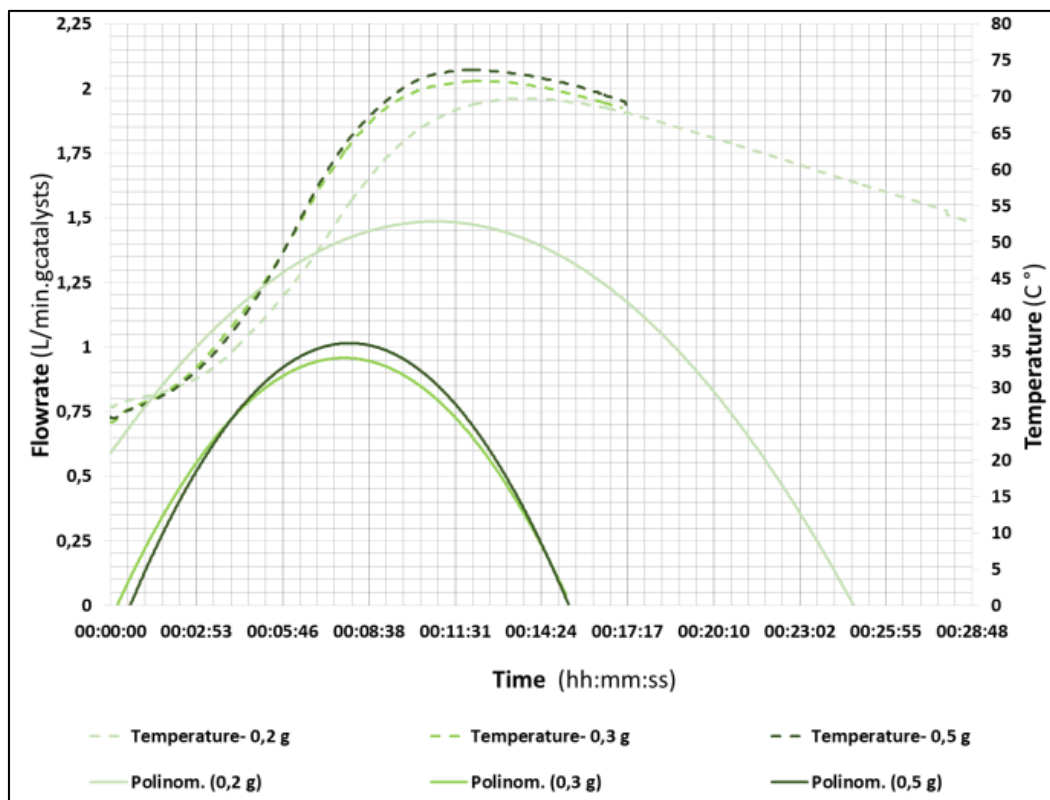


Figure 4.13. The performance analysis of the impact of the catalyst quantity on hydrolysis reaction

Although, based on the test results, it is observed that the hydrogen gas production rate decreases. When 0.2 g catalyst was used, the experiment took about 25 minutes and the hydrogen gas production reached 319.86 L and the highest hydrogen gas production rate was 2.1 L/min.g_{catalyst}. The reaction was completed in less than 15 minutes and the quantity of hydrogen produced was 174.04 L and the highest hydrogen gas production rate was measured 1.23 L / min.g_{catalyst}, when the 0.3 g catalyst quantity was used. When the 0.5 g catalyst quantity was used, the reaction time is approximately 15 minutes, the quantity of hydrogen produced was 177.33 L and the highest hydrogen gas production rate was measured 1.23 L / min.g_{catalyst}. The reaction time was shortened, but the quantity of hydrogen gas production decreased during the reaction, when the quantity of the 40% Co-B-BFS(+) powder catalyst sample was increased. According to the results of the literature studies and these experiments in the thesis, the hydrogen gas production rate in applications can be controlled by changing the amount of catalyst.

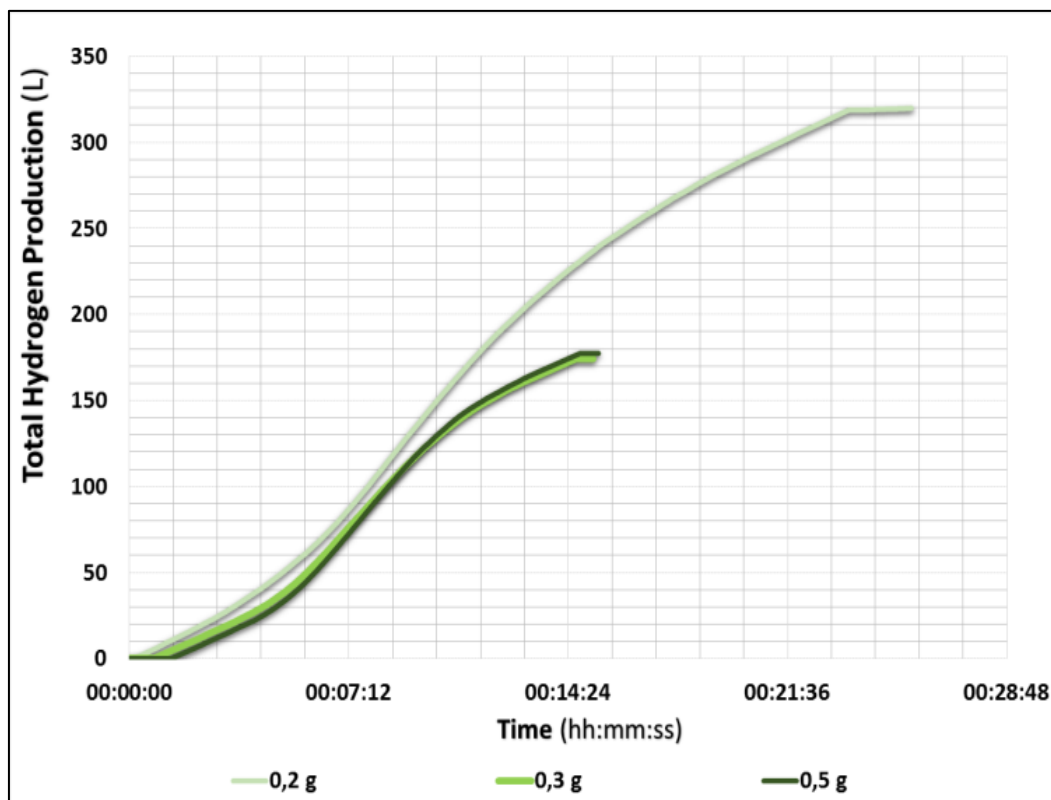


Figure 4.14. The performance impact of the catalyst quantity on the total volume of hydrogen gas

4.2.4. Performance impacts of the NaBH_4 quantity on hydrolysis reaction performance

In this section, hydrolysis reaction experiments were carried out using 0.2 g 50% Co-B-BFS(+) powder catalyst sample and 3 different concentrations (7.5%, 10% and 15%) NaBH_4 solution. The effect of the amount of NaBH_4 powder on hydrogen gas production was investigated.

As shown in Figure 4.15., the average and maximum flowrates of hydrogen produced from this hydrolysis reaction increase linearly due to the change in NaBH_4 concentration. The total volume of hydrogen gas production obtained are 168.48, 337.88 and 232.17 L respectively. Additionally, the average rates are 56.14, 67.58 and 72.55 $\text{L}/\text{min.g}_{\text{catalyst}}$, the maximum rates are 1.85, 2.25 and 2.60 $\text{L}/\text{min.g}_{\text{catalyst}}$, respectively.

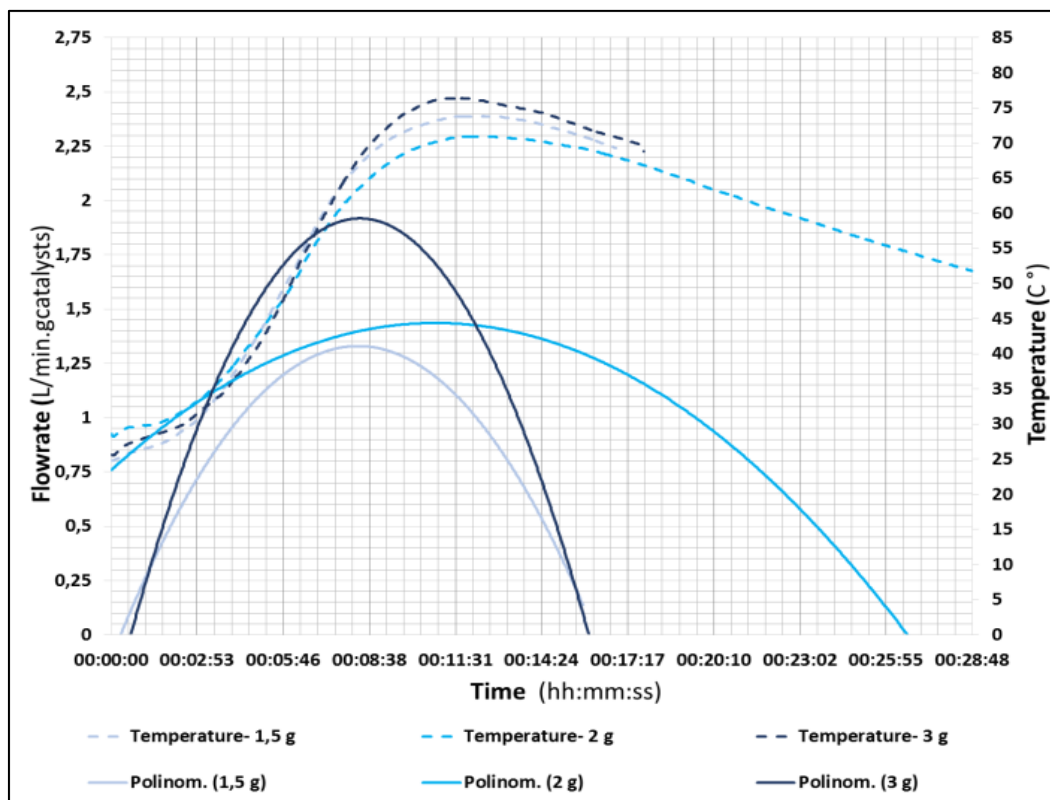


Figure 4.15. The performance analysis of the impact of the NaBH_4 quantity on hydrolysis reaction

As shown in Figure 4.16., the total volume of hydrogen gas production reached optimum value when the %10 NaBH_4 concentration was used. This may be due to the blocking of the catalytic activity, both by coating the active sites on the surface of Co-B-BFS catalysts by sodium metaborate crystals that are formed as a result of the hydrolysis reaction, and the adsorption saturation that induced with BH_4^- ions [31]. In the literature, this situation is similarly observed in other studies using many various catalyst samples [101,102]. In applications, very low concentrations are not preferred because they cannot provide sufficient hydrogen gas to the system [103]. Because they cannot supply enough hydrogen gas to the system, low reactant concentrations are not preferred in applications [36].

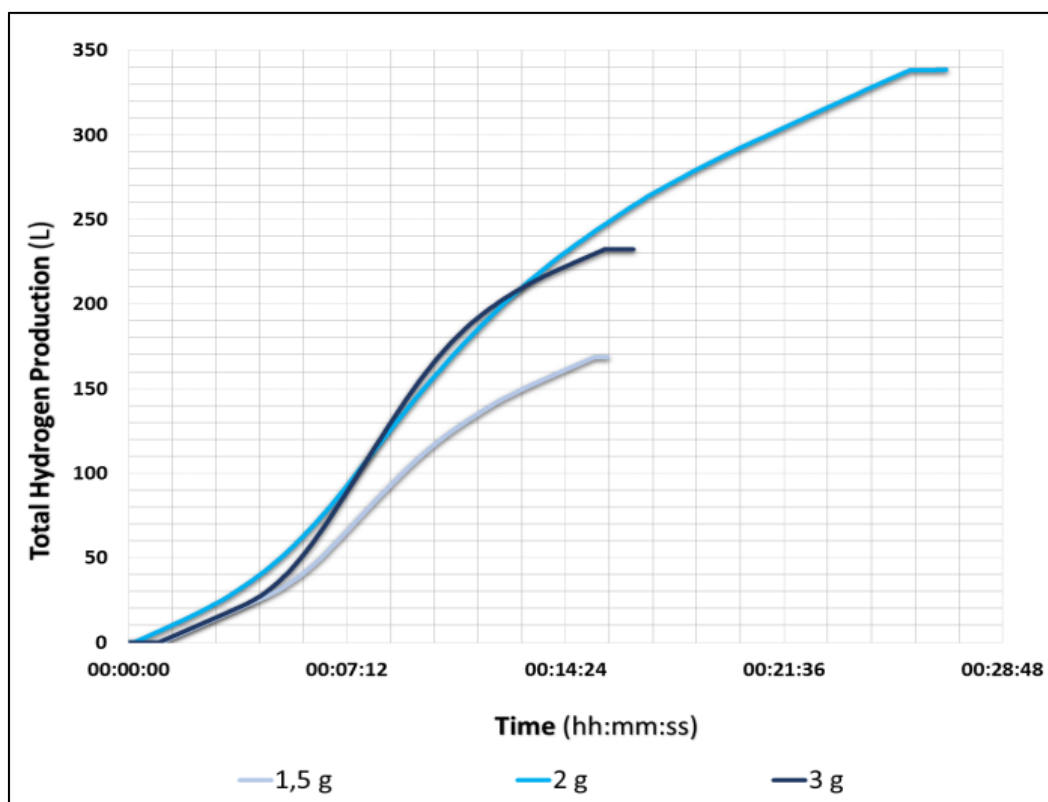


Figure 4.16. The performance impact of the NaBH₄ quantity on the total volume of hydrogen gas

4.2.5. Performance impacts of the temperature on hydrolysis reaction performance

The number of molecular collisions in catalytic reactions increases with temperature. As a result, high reaction rates are observed in catalytic reactions [104–106]. In order to make hydrogen gas production measurements more accurate and easier, the optimum temperature is preferred [26,107,108]. The quantity of hydrogen gas production increases in direct proportion to the temperature in all the experiments. Therefore, the effect of preheating temperature on the hydrolysis reaction was investigated using 20% Co-B-BFS(+) catalyst sample. The variation of hydrogen gas production rates with time is shown in Figure 4.17. Looking at the graph, it is observed with the activation of hydrogen formation that the catalysts are activated at temperatures above 30 °C. As a result, it can be said that there is a need for preheating or an induction time in catalytic reactions.

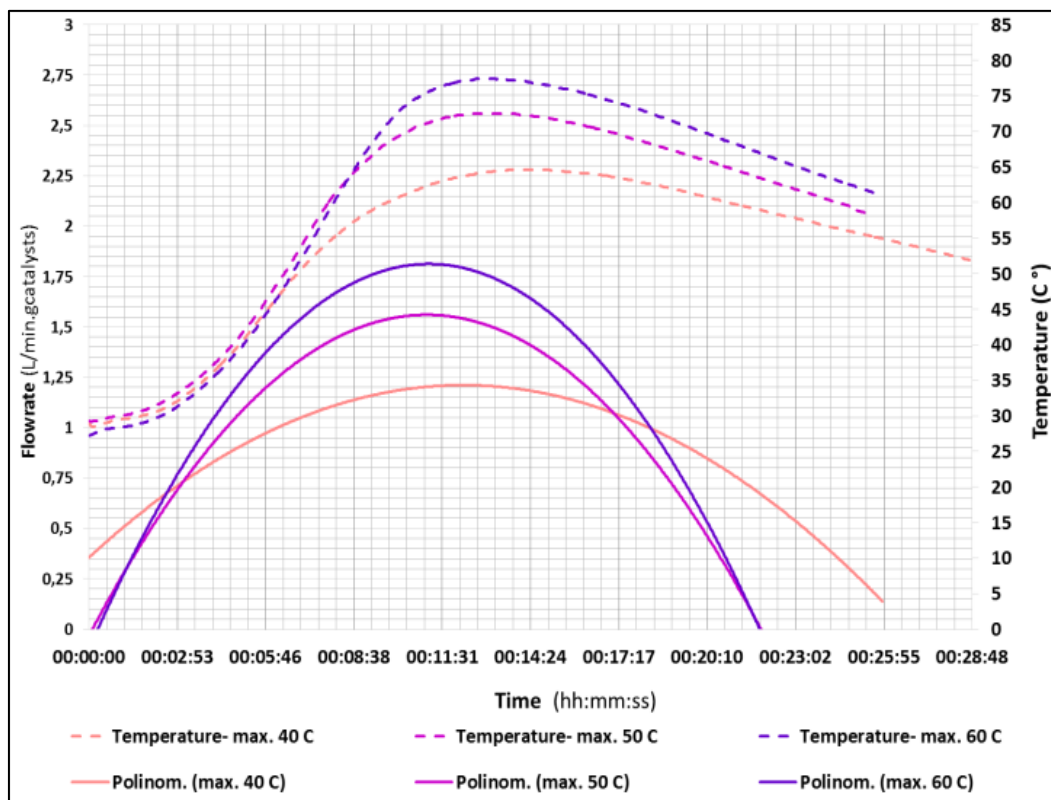


Figure 4.17. The performance analysis of the impact of the preheating temperature on hydrolysis reaction

The 20 % Co-B-BFS(+) catalyst samples were used to investigate the temperature impact of hydrolysis reactions containing 10 % NaBH_4 on hydrogen gas production rate at preheating temperature 40°C , 50°C and 60°C and is shown in Figure 4.17. As can be seen in the figures, the preheating temperature has a great influence as catalysts in this hydrolysis reaction. The maximum hydrogen gas production rates were measured as 1.85, 2.1 and 2.85 L /min.g_{catalyst}, respectively. The linear increase in the preheat temperature is likewise observed at the maximum and average flow rate of the hydrogen gas produced. According to these data, a linear increase is observed in the hydrogen gas production rate obtained with preheating temperature at 40 to 60°C . In Table 2.6, the comparison of hydrogen gas production rates, that produced at different preheating temperatures in the literature studies, are given [49,52,60–62]. As shown in Figure 4.18, the total hydrogen gas production volumes of hydrolysis reactions, that are with reaction times of approximately 23 minutes and were preheating up to 40, 50 and 60°C , are 275.64, 270.80 and 309.82 L, respectively.

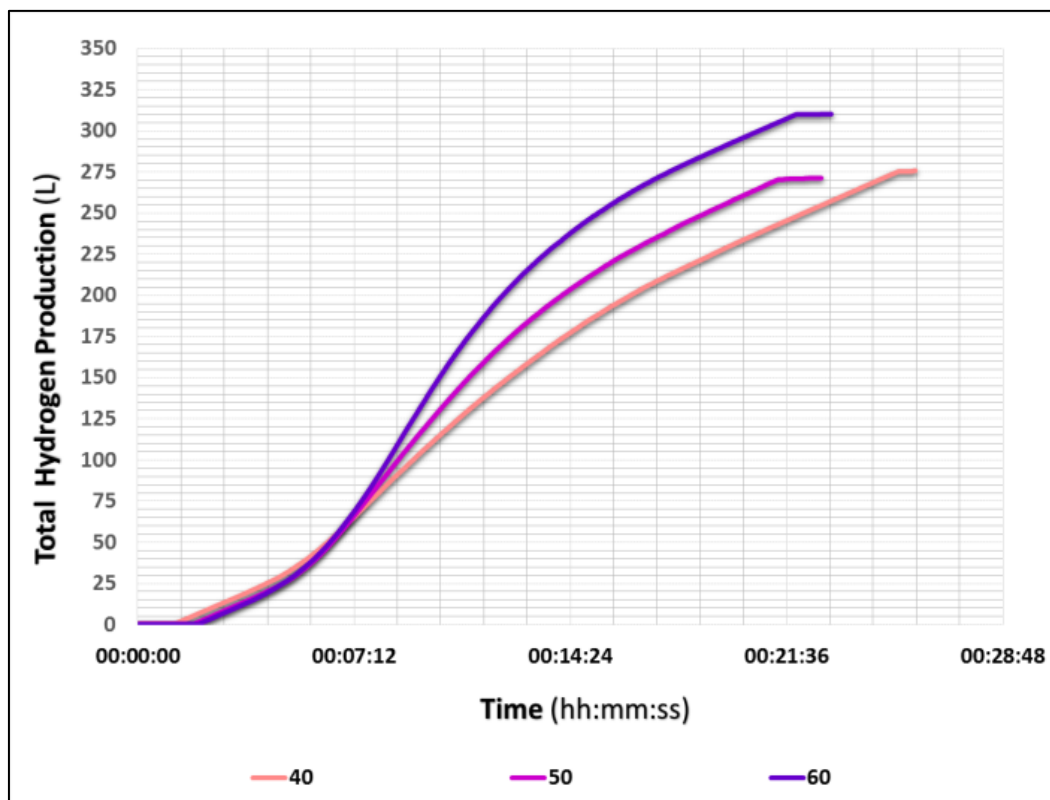


Figure 4.18. The impact of the preheating temperature on the total hydrogen gas

4.2.6. Performance impacts of the PVA film on hydrolysis reaction performance

In this section, the effect of PVA film coating on the hydrolysis reaction is investigated. The powder mixture consisting of 2 gr NaBH_4 powder and 0.2 gr 30% Co-B-BFS(+) catalyst sample was coated with PVA film and turned into a tablet. Afterwards, the experiment was completed by using the hydrolysis reaction test method used in the thesis. The reaction of both 30% Co-B-BFS(+) catalyst/ NaBH_4 powder mixture uncoated with PVA film and 30% Co-B-BFS catalyst/ NaBH_4 powder mixture coated with PVA film was completed in equal time. As shown in Figure 4.19, the uncoated sample showed high catalytic performance than the coated sample in the hydrolysis reaction.

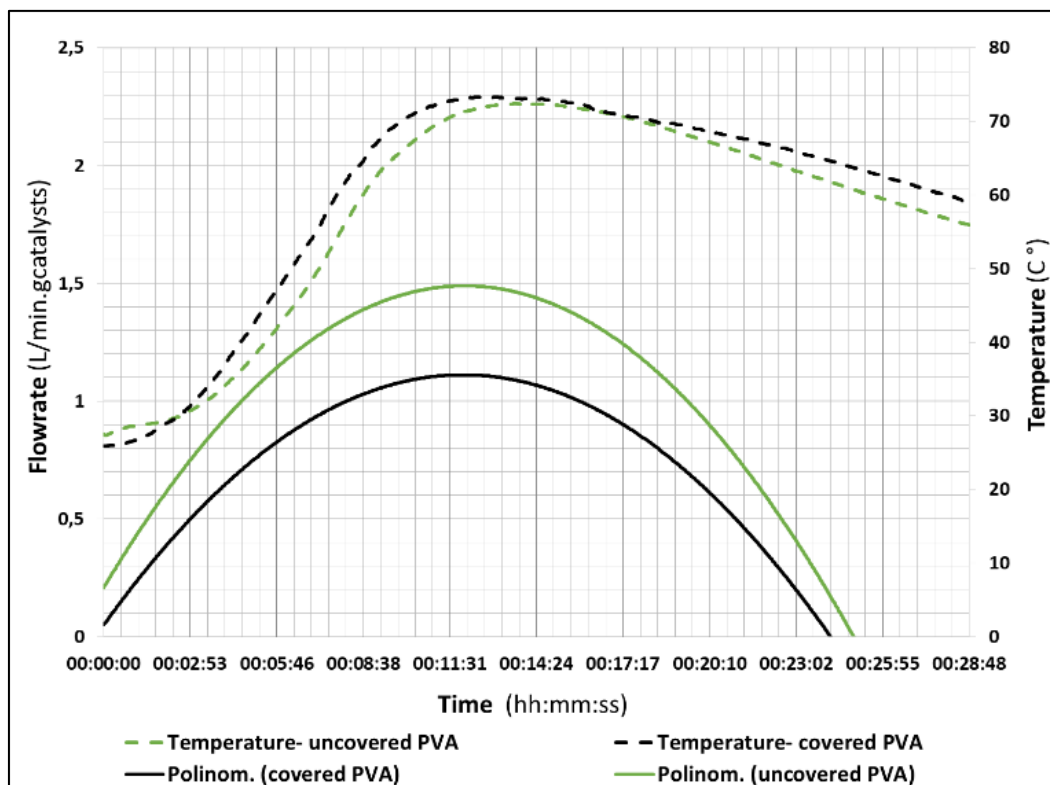


Figure 4.19. The performance analysis of the impact of the PVA coating on hydrolysis reaction

The maximum hydrogen gas production rates of the uncoated and the coated samples are 2.35 and 1.40 L/min.gcatalyst, respectively. Additionally, the average rates and total volumes of the uncoated and the coated samples are 61.43 and 51.50 L/min.gcatalyst; 307.13 and 216.29 L, respectively. As a result of the hydrogen gas production started after 40 seconds than the uncoated sample and their production starting temperature and reaction times were same, but their production quantities were decreased. The reason for this is that when the PVA film dissolves, it reduces the fluidity of water. The quantity of PVA film and the quantity of NaBH_4 were equal in this experiment. This impact would be reduced when using the big quantity of NaBH_4 and water.

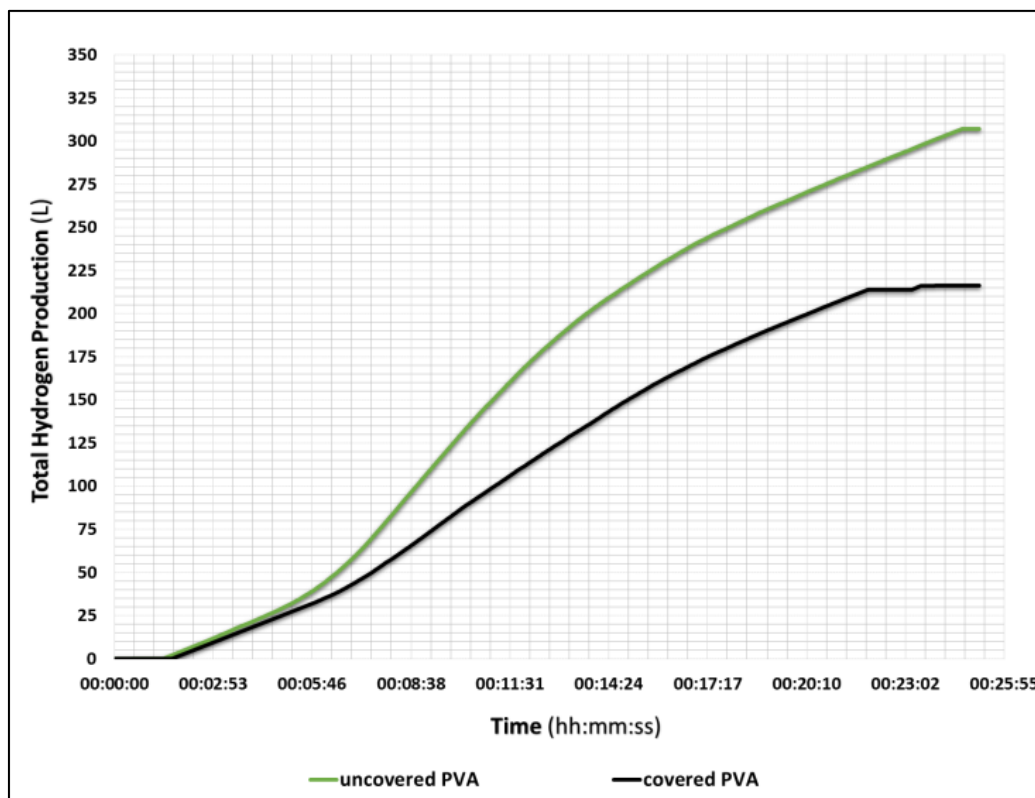
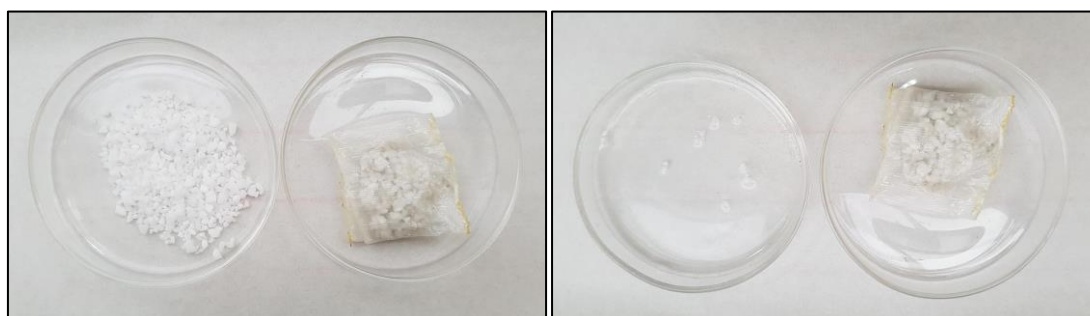


Figure 4.20. The impact of the PVA coating on the total hydrogen gas

Picture 4.3 shows powder samples coated and uncoated with PVA film. At the end of the 36-hour waiting period, the sample that was not covered with PVA film completely turned into gas form, but no change occurred in the PVA-coated sample. According to the reaction results, although coating with PVA film had negative effects, it prevented the contact of the sample mixture with moisture and oxygen in the environment, making it more durable. Thus, the dosage adjustment problem of the user in portable applications and the effects of adverse environmental conditions are eliminated.



Picture 4.3. The impact of environmental conditions on the uncoated NaBH_4 powder and on the NaBH_4/BFS catalyst powder coated with PVA

4.3. Performance Results of Prototype Design

Firstly, manual experiments have been carried out in order to record hydrogen gas production and reaction conditions such as hydrogen flow, generator' temperature, generator' pressure and to evaluate the prototype's feasibility, sealing, efficiency and performance. The sealing and the performing experiments were made using Co nano powder instead of a small quantity of synthesized Co-B-BFSs catalyst sample in this part. After then, the Co-B-BFSs catalyst samples were used in autonomous experiments of prototype.

4.3.1. Manual performance experiments of the prototype

The manual experiments of prototype were carried out using 2 g of NaBH_4 , 20 ml of distilled water and Co nano powder as a catalyst was used in 2 different amounts as 0,2 g and 0,5 g. A series of experiments were carried out until the sealing of the prototype was optimized. That is the sealing of the prototype was increased until the quantity of hydrogen gas produced by the Co nano powder in the glass reactor vessel and the quantity of hydrogen gas produced in the prototype were approximately the same.

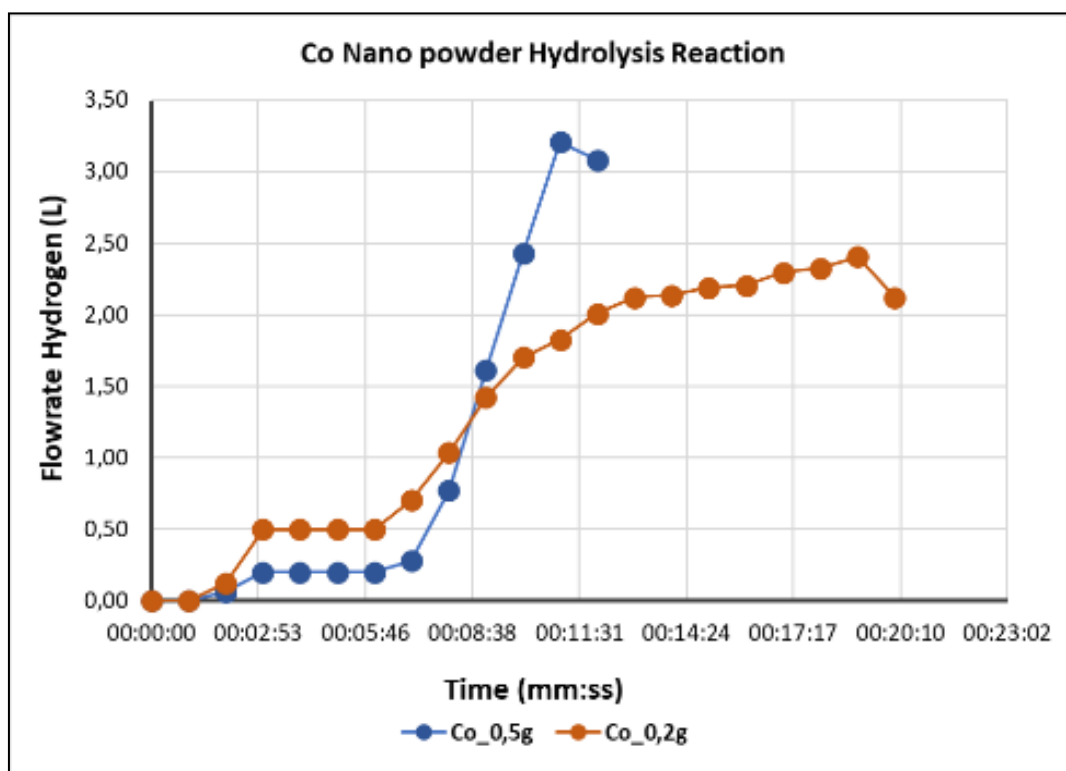


Figure 4.21. The hydrogen gas production flowrate of the Co Nano powder hydrolysis reaction

In the experiments with 0,2 g and 0,5 g of Co nano powder, the total flow rates are approximately 340 L and 360 L, respectively. The total hydrogen amounts of the 0,2 g and 0,5 g Co powders are very close to each other, but the reaction using 0,5 g of Co powder ends 2 times faster. As can be seen in Figure 4.21 and 4.22, the reaction time shortened with the increase in the quantity of catalyst, however, the hydrogen gas production rate decreased. Figure 4.21. is show relatively constant hydrogen flow (of about 17,5 L/min) along 20 min.

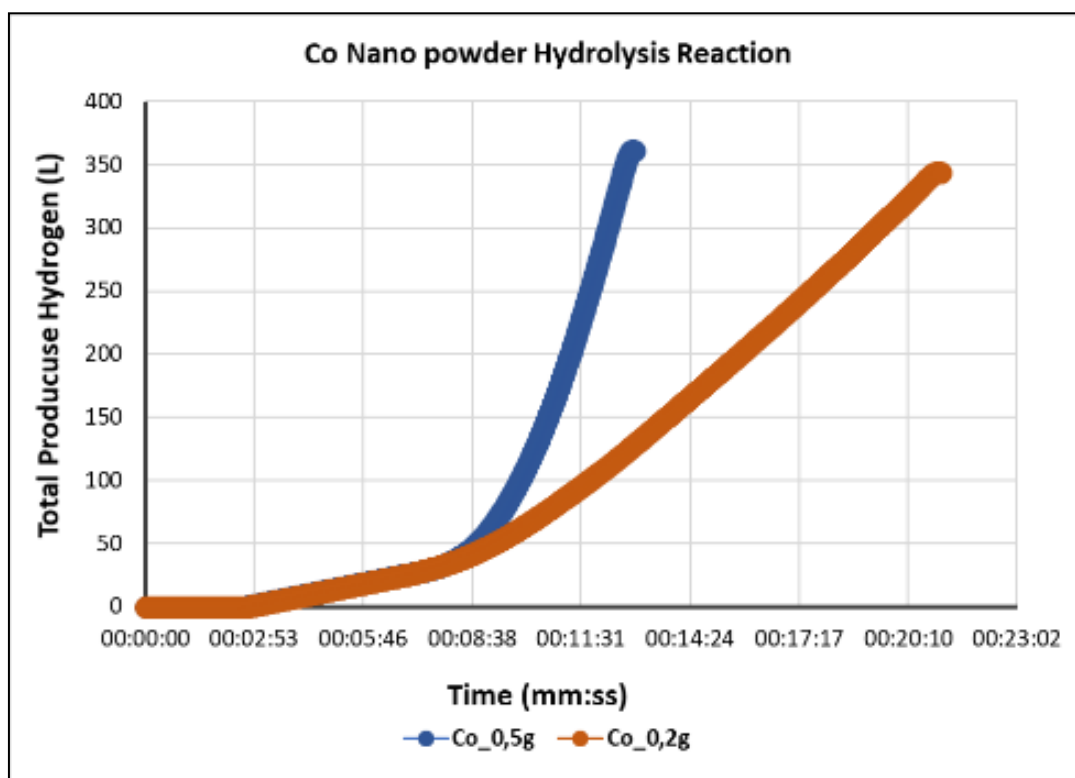


Figure 4.22. The total hydrogen production of the Co Nano powder hydrolysis reaction

4.3.2. Autonomous performance experiments of the prototype

Lastly, each part of the 4-segment generator prototype was started at end of previous segment's hydrolysis reaction. The hydrolysis reactions of the Co nano powder end suddenly, therefore, using Co nano powder was not efficient in manual 4-segment experiments. Depending on the decrease in hydrogen gas in the system, it may be considered to change the algorithm to be used for activating the next segment for some special cases. The autonomous experiments of prototype were carried out using 2 g of NaBH_4 , 20 ml of distilled water and 0,5 g Co nano powder and the %40 Co-B-BFS(+) catalyst powder as catalyst were used. Hydrogen production performance graphs of the %40 Co-B-BFS(+) catalyst powder

and the Co nano powder were given in the performance results of catalysts in other parts of this thesis. A series of performances experiments were carried out until the autonomous controlling of the prototype was optimized.

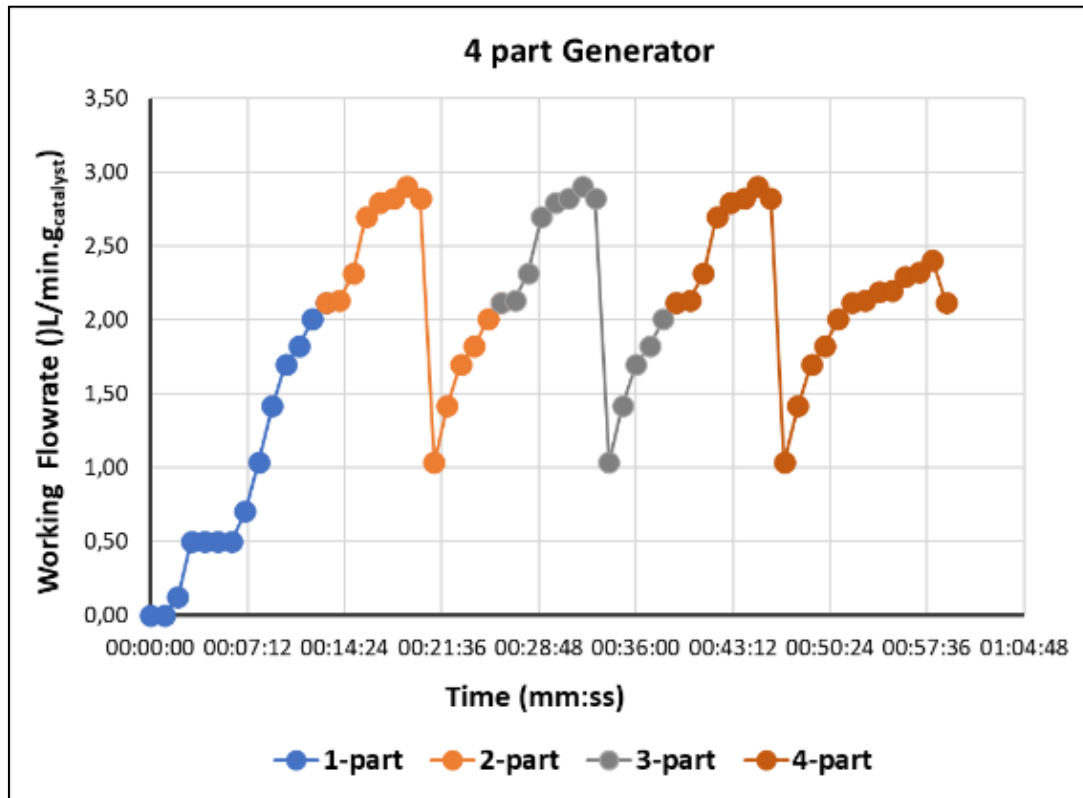


Figure 4.23. The working flowrate performance of the Co nano powder catalyst in the 4-part autonomous hydrogen generator

The results of the Co nano powder performance experiments were shown in Figure 4.23. The results of this experiment such as the working time the maximum flow rate of the reaction, the average flow rate and the maximum flow rate of the 4-part autonomous generator were almost 58 minutes, 2.15 L/min.g_{catalyst} and 2.90 L/min.g_{catalyst}, respectively. Each part of the 4-part generator was started when the rate of the previous segment's hydrolysis reaction to decrease. A working time is designed to have a maximum instantaneous hydrogen production of almost 3 L / min.g_{catalyst} continuously for 1 hour. In this working cycle, the quantity of hydrogen produced instantaneously decreases to 1 L / min.g_{catalyst} from time to time.

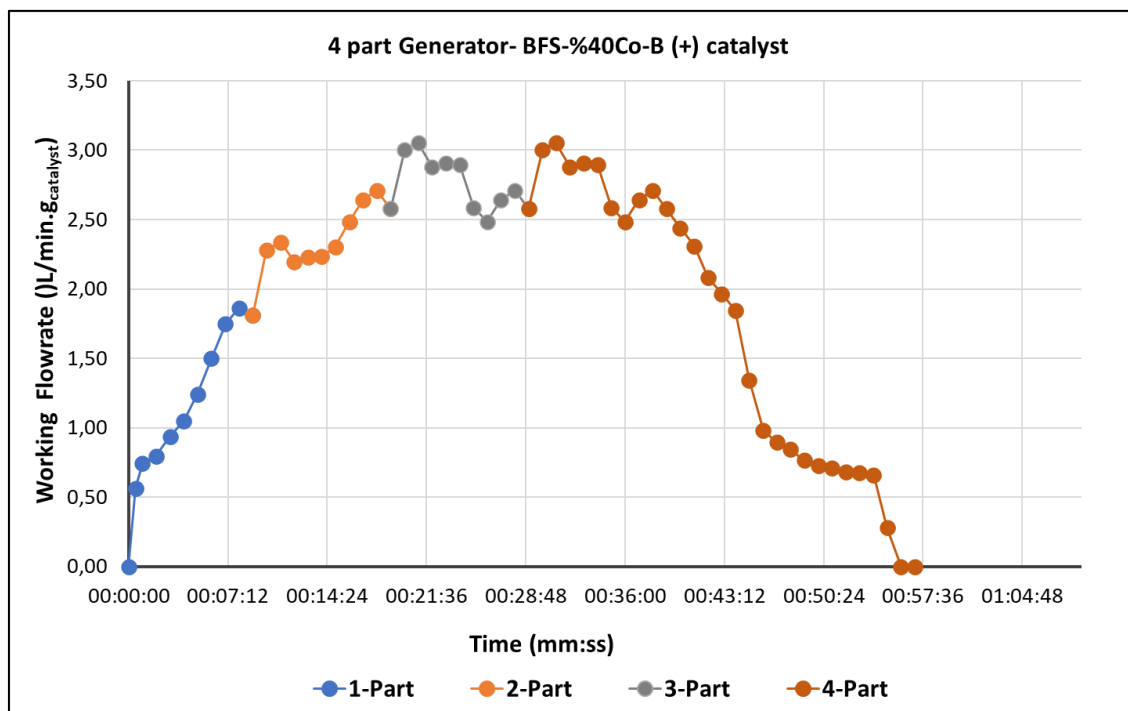


Figure 4.24. The working flowrate performance of the Co-B-BFS(+) catalyst in the 4-part autonomous hydrogen generator

The results of the %40 Co-B-BFS(+) catalyst performance experiments were shown in Figure 4.24. The results of this experiment such as the working time the maximum flow rate of the reaction, the average flow rate and the maximum flow rate of the 4-part autonomous generator were almost 57 minutes, 2.33 L/min.g_{catalyst} and 3.05 L/min.g_{catalyst}, respectively. Each part of the 4-part generator was started when the rate of the previous segment's hydrolysis reaction to decrease. A working time is designed to have a maximum instantaneous hydrogen production of almost 2.33 L / min.g_{catalyst} continuously for 1 hour. In this working cycle, the soft ripples are spied on the hydrogen-produced quantity from time to time. These ripple situations can be adjusted by increasing the quantity of NaBH₄ used according to the instantaneous hydrogen requirement of the system to which the generator will be connected.

5. DISCUSSIONS

5.1. Discussions of BFS Catalysts

The hydrogen gas production rates of Co-based catalysts that are given in Table 5.1., are lower than the hydrogen gas production rates of these catalysts. Consequently, these catalysts with high catalytic activity can be an alternative catalyst for hydrolysis applications.

Table 5.1. The comparison of some Co-based catalysts' hydrogen gas production performance

<i>Catalyst's type</i>	<i>Support Material</i>	<i>NaBH₄ (wt %)</i>	<i>Hydrolysis temperature (°C)</i>	<i>Hydrogen production rate (L/min.g_{catlayst})</i>	<i>References</i>
<i>Co powder</i>	-	1	25	0,13	[30]
<i>Co -B</i>	-	20	30	2,75	[60]
<i>Co -B</i>	<i>Graphane</i>	8	50	56,61	[63]
<i>Co -B</i>	<i>Acid treated sepiolite clay</i>	5	30	1,49	[49]
<i>Raw BFS</i>	-	10	50	54,63	This thesis
<i>Co -B</i>	<i>Raw BFS</i>	10	50	48,05	This thesis
<i>Co -B</i>	<i>Acid treated BFS</i>	10	50	65,99	This thesis

In line with the results obtained from the experiments, the study successfully achieved the two main objectives aimed at the beginning of the project.

Table 5.2. Comparing of the BFS catalysts samples experimental analysis

<i>Hydrogen Production Properties</i>	<i>Catalyst Type</i>		<i>Flowrate (L/min.g_{catalyst})</i>
	<i>Acid treated BFS</i>	<i>% Co-B</i>	
<i>Optimum H₂ production</i>	+	40	66,3
<i>Instant maximum H₂ production</i>	+	20	65,9
<i>Total H₂ production</i>	-	30	65,7
<i>Maximum H₂ production at low temperature</i>	-	20	48,05
<i>Easy production process</i>	-	30	65,7
<i>Efficient H₂ production</i>	-	30	65,7
	+	50	65,15

Firstly; alternative cheap catalysts were produced instead of the expensive noble metal catalysts that are used in the NaBH₄ hydrolysis reaction. However;

- i. A new usage area of the slag by-product has occurred with the synthesis of these catalysts. In this way, a new alternative method has been found for slag waste recycling, which is the main problem of the iron and steel industry. Waste recovery was achieved by using slag by-products produced in large quantities in iron and steel industry processes. By recycling the slag, the quantity of waste, the cost of waste disposal and energy use will be reduced. As a result, both environmental and economic gains are expected to be achieved.

- ii. The use of by-products with high metal content in the hydrolysis reaction of the chemical NaBH_4 has been paved.
- iii. The availability of NaBH_4 in solid form in the hydrolysis reaction has been increased.

5.2. Discussion of Hydrogen Generator Prototype

Secondly; It is the development of an autonomous and portable Hydrogen generator.

In the results of working;

- i. The BFS by-product is deposited in hydrochloric acid solutions and activated. Supported catalysts were synthesized using Co nano powder.
- ii. Slag powder supplemented using Co nano powder has been tested in a series of experiments. The impact of each method on the hydrogen gas production rate and the characteristics of the slag supported catalysts in the hydrolysis reaction were extracted.
- iii. The impacts of different component ratios, catalyst concentration, reaction temperature, water flow rate on the production performance of hydrogen gas were determined.
- iv. In this hydrogen generator prototype, the chemical material NaBH_4 was used in solid form. There are examples of hydrogen generator designs or prototype works in the world. However, in these designs, NaBH_4 solution is used as fuel.
- v. It is seen that there are problems such as the continuity of the system, durability and low gravimetric Hydrogen storage capacity in the designs of the solution-used Hydrogen generators. It is planned to solve the problems of solution supported designs with the use of solid-state boron hydrides.
- vi. The use of solution increases the weight of the systems and requires the transport of the liquid solution to sustain hydrogen gas production. With the use of solid-state boron hydride, the weight of the system decreased. In addition, the extra load weight is reduced by the volume of water, with the fuel material transported in powder form instead of solution.
- vii. Since the fuel will be in solid form, it has been easily transported, but the user will have a dosage adjustment problem in applications.
- viii. The use of stabilizers required to stop the low hydrolysis of NaBH_4 aqueous solutions

is expected to disappear.

- ix. The shelf life of the storage system is increased by adding solid NaBH_4 to the reactor.



6. CONCLUSION

In recent years, although there has been an increased interest in solid-state NaBH_4 hydrolysis, limited studies have been conducted on this subject in the literature. Studies are generally based on catalyst synthesis and focus on hydrogen gas production. With the catalyst synthesis made in the first part of this study, a cheap and efficient catalyst has been added to the literature and a new waste recycling alternative has been introduced for the iron and steel industry, which has a high potential in our country. The supported Co-B catalyst on the BFS treated with hydrochloric acid was synthesized by the impregnation method for hydrogen generation from catalytic hydrolysis of NaBH_4 . This result indicates that the acid treatment on slag is quite successful. As a result of the mutual effects of the reactions of NaBH_4 with these materials, the combination of these materials has various advantages such as hydrogen gas production rate and fuel conversion. The hydrogen generation amount and rate analyzed regulated by changing chemicals weight ratios, amounts, reaction temperature, water types etc. The impacts of component ratios, catalyst concentration and water content on the hydrogen gas production performance of the system have been explained.

The best performance of these powder mixture is showed the acid treated BFS catalyst sample supported 40% and 50 % Co-B/ NaBH_4 mixture when average hydrogen gas production rate approximately $65 \text{ L/min.g}_{\text{catalyst}}$ with high efficiency within 25 min at maximum preheating $50 \text{ }^\circ\text{C}$. The acid treated BFS catalyst/ NaBH_4 mixture may be applied as a portable hydrogen generation material. A new field of research has been opened regarding the use of by-products with high metal content. In addition, the use of solid-state NaBH_4 hydride in studies where hydrogen generator design is carried out is very low. With this study, it is aimed to close the gap related to solid state NaBH_4 hydrolysis in the literature.

In addition to solid state NaBH_4 hydrolysis, the energy needed by portable systems such as radios, telephones, night vision devices used in defence technologies is met by traditional energy storage technologies, which are large in volume and heavy in mass. For these systems, it is of great importance to develop lighter and more efficient alternative applications such as hydrogen generators instead of heavy energy storage technologies. With the outputs obtained as a result of the prototype work, the problems in the insufficient energy capacity of the batteries used as the traditional method have been solved. The weight and

volume of the systems have been reduced, thus increasing their duty times. This project is expected to be of great strategic importance for applications used in the defence industry, camping and mountaineering activities. In terms of military defence systems, the development and production of systems locally is important for national security. Given the requirements in military or civilian life worldwide, it is important both academically and commercially to lead the development and manufacture of these systems, which are of high strategic importance due to the large gaps that exist in this market.



REFERENCES

1. An, L., Zhao, T., Yan, X., Zhou, X., Tan, P. (2015). The dual role of hydrogen peroxide in fuel cells. *In Science Bulletin*, 60(1), 55-64. <https://doi.org/10.1007/s11434-014-0694-7>
2. Barbir, F. (2005). Fuel Cell Electrochemistry. *In PEM Fuel Cells Theory and Practice* (pp. 33-72). Location: Elsevier. <https://doi.org/10.1016/B978-0-12-078142-3.X5000-9>
3. Weydahl, H., Gilljam, M., Lian, T., Johannessen, T. C., Holm, S. I., Hasvold, J. Ø. (2019). Fuel cell systems for long-endurance autonomous underwater vehicles – challenges and benefits. *International Journal of Hydrogen Energy*, 45(8), 5543-5553. <https://doi.org/10.1016/j.ijhydene.2019.05.035>
4. Kim, J. H., Lee, H., Han, S. C., Kim, H. S., Song, M. S., Lee, J. Y. (2004). Production of hydrogen from sodium borohydride in alkaline solution: Development of catalyst with high performance. *International Journal of Hydrogen Energy*. [https://doi.org/10.1016/S0360-3199\(03\)00128-9](https://doi.org/10.1016/S0360-3199(03)00128-9)
5. Kojima, Y., Kawai, Y., Nakanishi, H., Matsumoto, S. (2004). Compressed hydrogen generation using chemical hydride. *Journal of Power Sources*. <https://doi.org/10.1016/j.jpowsour.2004.03.079>
6. IEA. (2015). *International Energy Agency (IEA) - World Energy Outlook 2015*. France: International Energy Agency.
7. Kim, J., Kim, T. (2015). Compact PEM fuel cell system combined with all-in-one hydrogen generator using chemical hydride as a hydrogen source. *Applied Energy*, 160, 945–953. <https://doi.org/10.1016/j.apenergy.2015.03.084>
8. Kordesch, K., Taucher-Mautner, W. (2009). History Primary Batteries. *Encyclopedia of Electrochemical Power Sources*, 555–564. <https://doi.org/10.1016/B978-044452745-5.00003-4>
9. Winter, M., Brodd, R.J. (2004). What Are Batteries, Fuel Cells, and Supercapacitors? *Chemical Reviews*, 104(10), 4245-4270. <https://doi.org/10.1021/cr020730k>
10. Peng, B., Chen, J. (2009). Functional materials with high-efficiency energy storage and conversion for batteries and fuel cells. *Coordination Chemistry Reviews*, 253(23–24), 2805–2813. <https://doi.org/10.1016/J.CCR.2009.04.008>
11. Larminie, J., Dicks, A. (2003). *Fuel Cell Systems Explained: Second Edition*. Published: Wiley Online Library. <https://doi.org/10.1002/9781118878330>
12. URL 1: “Battery”. <https://www.eaton.com/content/dam/eaton/products/backup-power-ups-surge-it-power-distribution/backup-power-ups/ups-batteries-resources/eaton-12v-200w-battery-brochure-BAT08FXA.pdf%0A> Last Access Date: 04.01.2022
13. URL 2: “PEMFC”. <https://www.fuelcellstore.com/g-hfcs-200w15v-200w-hydrogen-fuel-cell-power-generator> Last Access Date: 04.01.2022

14. Hansu, T. A., Caglar, A., Sahin, O., Kivrak, H. (2020). Hydrolysis and electrooxidation of sodium borohydride on novel CNT supported CoBi fuel cell catalyst. *Materials Chemistry and Physics*, 239, 122031. <https://doi.org/10.1016/j.matchemphys.2019.122031>
15. Badwal, S. P. S., Giddey, S. S., Munnings, C., Bhatt, A. I., Hollenkamp, A. F. (2014). Emerging electrochemical energy conversion and storage technologies. *Frontiers in Chemistry*, 2, 79. <https://doi.org/10.3389/fchem.2014.00079>
16. Wilberforce, T., Alaswad, A., Palumbo, A., Dassisti, M., Olabi, A. G. (2016). Advances in stationary and portable fuel cell applications. *International Journal of Hydrogen Energy*, 41(37), 16509–16522. <https://doi.org/10.1016/j.ijhydene.2016.02.057>
17. Arat, H. T., Sürer, M. G. (2019). Experimental investigation of fuel cell usage on an air Vehicle's hybrid propulsion system. *International Journal of Hydrogen Energy*, 45(49), 26370-26378. <https://doi.org/10.1016/j.ijhydene.2019.09.242>
18. Rosen, M. A., Koohi-Fayegh, S. (n.d.). The prospects for hydrogen as an energy carrier: an overview of hydrogen energy and hydrogen energy systems. *Energy, Ecology and Environment*, 1, 10–29. <https://doi.org/10.1007/s40974-016-0005-z>
19. URL 3: “Energy-Carrier”. <https://www.energy.gov/eere/articles/hydrogen-clean-flexible-energy-carrier> Last Access Date: 04.01.2022
20. Arnan, E. (2019). Development of catalyst for catalytic hydrogen production from sodium borohydride. (Master Thesis). Gazi University, Ankara.
21. Colozza, A. J. (2002). Hydrogen Storage for Aircraft. In Nasa/Cr—2002-211867 (Issue September). <http://gltrs.grc.nasa.gov> Last Access Date: 04.01.2022
22. Nour, U. M., Awad, S., Yusup, S., Sufian, S. (2010). Technical evaluation of current hydrogen storage technologies for vehicles. *Journal of Applied Sciences*, 10(12), 1200–1203. <https://doi.org/10.3923/jas.2010.1200.1203>
23. Li, M., Bai, Y., Zhang, C., Song, Y., Jiang, S., Grouset, D., Zhang, M. (2019). Review on the research of hydrogen storage system fast refueling in fuel cell vehicle. *International Journal of Hydrogen Energy*, 44(21), 10677–10693. <https://doi.org/10.1016/J.IJHYDENE.2019.02.208>
24. Motyka, T., Zidan, R., Summers, W. A., Zidan, R. (2004). Hydrogen Storage: The Key Challenge Facing a Hydrogen Economy. *World Hydrogen Energy Conference*, March 2004, USA.
25. URL 4: “NaBH₄”. <https://www.etiproducts.com/boron-in-turkey/> Last Access Date: 04.01.2022
26. Ould-Amara, H., Alligier, D., Petit, E., Yot, P. G., Demirci, U. B. (2018). Sodium borohydride and propylene glycol, an effective combination for the generation of 2.3 wt% of hydrogen. *International Journal of Hydrogen Energy*, 43(15), 7237-7244. <https://doi.org/10.1016/j.ijhydene.2018.02.169>

27. Boran, Asli, Erkan, S., Eroglu, I. (2019). Hydrogen generation from solid state NaBH₄ by using FeCl₃ catalyst for portable proton exchange membrane fuel cell applications. *International Journal of Hydrogen Energy*, 44(34), 18915–18926. <https://doi.org/10.1016/j.ijhydene.2018.11.033>
28. Chen, Y., Kim, H. (2010). Preparation and application of sodium borohydride composites for portable hydrogen production. *Energy*, 35(2), 960–963. <https://doi.org/10.1016/j.energy.2009.06.053>
29. Awada, H., Daneault, C. (2015). Chemical modification of poly(vinyl alcohol) in water. *Applied Sciences (Switzerland)*, 5(4), 840–850. <https://doi.org/10.3390/app5040840>
30. Liu, B. H., Li, Q. (2008). A highly active Co-B catalyst for hydrogen generation from sodium borohydride hydrolysis. *International Journal of Hydrogen Energy*, 33(24), 7385-7391. <https://doi.org/10.1016/j.ijhydene.2008.09.055>
31. Patel, N., Fernandes, R., Miotello, A. (2009). Hydrogen generation by hydrolysis of NaBH₄ with efficient Co-P-B catalyst: A kinetic study. *Journal of Power Sources*, 188(2), 411-420. <https://doi.org/10.1016/j.jpowsour.2008.11.121>
32. Oliveira, R. C. P., Milikić, J., Daş, E., Yurtcan, A. B., Santos, D. M. F., Šljukić, B. (2018). Platinum/polypyrrole-carbon electrocatalysts for direct borohydride-peroxide fuel cells. *Applied Catalysis B: Environmental*, 238, 454-464. <https://doi.org/10.1016/j.apcatb.2018.06.057>
33. Wei, Y., Wang, Y., Wei, L., Zhao, X., Zhou, X., Liu, H. (2018). Highly efficient and reactivated electrocatalyst of ruthenium electrodeposited on nickel foam for hydrogen evolution from NaBH₄ alkaline solution. *International Journal of Hydrogen Energy*, 43(2), 592-600. <https://doi.org/10.1016/j.ijhydene.2017.11.010>
34. Baydaroğlu, F. O. (2013). Sodyum Borhidrürün Hidrolizinden Hidrojen Eldesi İçin Etkin Katalizörlerin Geliştirilmesi, (Master Thesis). Gebze Technical University, Gebze.
35. Öztürk, E. (2019). Synthesis of metallic catalysts with various support materials for hydrogen generation from sodium borohydride. (Master Thesis). Ondokuz Mayıs University, Samsun.
36. Zhang, X., Li, C., Qu, J., Guo, Q., Huang, K. (2019). Cotton stalk activated carbon-supported Co–Ce–B nanoparticles as efficient catalysts for hydrogen generation through hydrolysis of sodium borohydride. *Carbon Resources Conversion*, 2(3), 225-232. <https://doi.org/10.1016/j.crcon.2019.11.001>
37. Guo, S., Sun, J., Zhang, Z., Sheng, A., Gao, M., Wang, Z., Zhao, B., Ding, W. (2017). Study of the electrooxidation of borohydride on a directly formed CoB/Ni-foam electrode and its application in membraneless direct borohydride fuel cells. *Journal of Materials Chemistry A*, 5, 15879-15890. <https://doi.org/10.1039/c7ta03464d>
38. Zhang, D., Ye, K., Cheng, K., Cao, D., Yin, J., Xu, Y., Wang, G. (2014). High electrocatalytic activity of cobalt-multiwalled carbon nanotubes-cosmetic cotton nanostructures for sodium borohydride electrooxidation. *International Journal of Hydrogen Energy*, 39(18), 9651-9657. <https://doi.org/10.1016/j.ijhydene.2014.04.113>

39. Zhang, D., Ye, K., Cao, D., Wang, B., Cheng, K., Li, Y., Wang, G., Xu, Y. (2015). Co@MWNTs-Plastic: A novel electrode for NaBH₄ oxidation. *Electrochimica Acta*, 156, 102-107. <https://doi.org/10.1016/j.electacta.2015.01.011>
40. Minkina, V. G., Shabunya, S. I., Kalinin, V. I., Smirnova, A. (2016). Hydrogen generation from sodium borohydride solutions for stationary applications. *International Journal of Hydrogen Energy*, 41(22), 9227–9233. <https://doi.org/10.1016/j.ijhydene.2016.03.063>
41. Braesch, G., Bonnefont, A., Martin, V., Savinova, E. R., Chatenet, M. (2018). Borohydride oxidation reaction mechanisms and poisoning effects on Au, Pt and Pd bulk electrodes: From model (low) to direct borohydride fuel cell operating (high) concentrations. *Electrochimica Acta*, 273, 483-494. <https://doi.org/10.1016/j.electacta.2018.04.068>
42. Cheng, Kui, Jiang, J., Kong, S., Gao, Y., Ye, K., Wang, G., Zhang, W., Cao, D. (2017). Pd nanoparticles support on rGO-C@TiC coaxial nanowires as a novel 3D electrode for NaBH₄ electrooxidation. *International Journal of Hydrogen Energy*, 42(5), 2943-2951. <https://doi.org/10.1016/j.ijhydene.2016.11.156>
43. Cheng, K., Xu, Y., Miao, R. R., Yang, F., Yin, J. L., Wang, G. L., Cao, D. X. (2012). Pd modified MmNi_{50.6}Co_{10.2}Mn_{5.4}Al_{1.2} alloy as the catalyst of NaBH₄ electrooxidation. *Fuel Cells*, 12(5), 869-875. <https://doi.org/10.1002/fuce.201100199>
44. Šljukić, B., Milikić, J., Santos, D. M. F., Sequeira, C. A. C., Macciò, D., Saccone, A. (2014). Electrocatalytic performance of Pt-Dy alloys for direct borohydride fuel cells. *Journal of Power Sources*, 272, 335-343. <https://doi.org/10.1016/j.jpowsour.2014.08.080>
45. Tian, H., Guo, Q., Xu, D. (2010). Hydrogen generation from catalytic hydrolysis of alkaline sodium borohydride solution using attapulgite clay-supported Co-B catalyst. *Journal of Power Sources*, 195(8), 2136-2142. <https://doi.org/10.1016/j.jpowsour.2009.10.006>
46. Zhai, Y., Zhu, Z., Zhu, C., Chen, K., Zhang, X., Tang, J., Chen, J. (2020). Single-atom catalysts boost nitrogen electroreduction reaction. *In Materials Today*, 38, 99-113. <https://doi.org/10.1016/j.mattod.2020.03.022>
47. Lv, L., Zha, D., Ruan, Y., Li, Z., Ao, X., Zheng, J., Jiang, J., Chen, H. M., Chiang, W. H., Chen, J., Wang, C. (2018). A Universal Method to Engineer Metal Oxide-Metal-Carbon Interface for Highly Efficient Oxygen Reduction. *ACS Nano*, 12(3), 3042–3051. <https://doi.org/10.1021/acsnano.8b01056>
48. Chang, X., Wang, T., Zhao, Z. J., Yang, P., Greeley, J., Mu, R., Zhang, G., Gong, Z., Luo, Z., Chen, J., Cui, Y., Ozin, G. A., Gong, J. (2018). Tuning Cu/Cu₂O Interfaces for the Reduction of Carbon Dioxide to Methanol in Aqueous Solutions. *Angewandte Chemie - International Edition*, 57(47), 15415-15419. <https://doi.org/10.1002/anie.201805256>

49. Selvitepe, N., Balbay, A., Saka, C. (2019). Optimisation of sepiolite clay with phosphoric acid treatment as support material for CoB catalyst and application to produce hydrogen from the NaBH₄ hydrolysis. *International Journal of Hydrogen Energy*, 44(31), 16387-16399. <https://doi.org/10.1016/j.ijhydene.2019.04.254>
50. Dai, P., Zhao, X., Xu, D., Wang, C., Tao, X., Liu, X., Gao, J. (2019). Preparation, characterization, and properties of Pt/Al₂O₃/cordierite monolith catalyst for hydrogen generation from hydrolysis of sodium borohydride in a flow reactor. *International Journal of Hydrogen Energy*, 44(53), 28463-28470. <https://doi.org/10.1016/j.ijhydene.2019.02.013>
51. Yang, C. C., Chen, M. S., Chen, Y. W. (2011). Hydrogen generation by hydrolysis of sodium borohydride on CoB/SiO₂ catalyst. *International Journal of Hydrogen Energy*, 36(2), 1418-1423. <https://doi.org/10.1016/j.ijhydene.2010.11.006>
52. Kılınc, D., Şahin, Ö. (2019). Effective TiO₂ supported Cu-Complex catalyst in NaBH₄ hydrolysis reaction to hydrogen generation. *International Journal of Hydrogen Energy*, 44(34), 18858-18865. <https://doi.org/10.1016/j.ijhydene.2018.12.225>
53. Lu, Y. C., Chen, M. S., Chen, Y. W. (2012). Hydrogen generation by sodium borohydride hydrolysis on nanosized CoB catalysts supported on TiO₂, Al₂O₃ and CeO₂. *International Journal of Hydrogen Energy*, 37(5), 4254-4258. <https://doi.org/10.1016/j.ijhydene.2011.11.105>
54. Şahin, Ö., Izgi, M. S., Onat, E., Saka, C. (2016). Influence of the using of methanol instead of water in the preparation of Co-B-TiO₂ catalyst for hydrogen production by NaBH₄ hydrolysis and plasma treatment effect on the Co-B-TiO₂ catalyst. *International Journal of Hydrogen Energy*, 41(4), 2539-2546. <https://doi.org/10.1016/j.ijhydene.2015.11.094>
55. Balbay, A., Selvitepe, N., Saka, C. (2021). Fe doped-CoB catalysts with phosphoric acid-activated montmorillonite as support for efficient hydrogen production via NaBH₄ hydrolysis. *International Journal of Hydrogen Energy*, 46(1), 425-438. <https://doi.org/10.1016/j.ijhydene.2020.09.181>
56. Saka, C., Salih Eygi, M., Balbay, A. (2020). CoB doped acid modified zeolite catalyst for enhanced hydrogen release from sodium borohydride hydrolysis. *International Journal of Hydrogen Energy*, 45(30), 15086-15099. <https://doi.org/10.1016/j.ijhydene.2020.03.238>
57. Joydev, M., Binayak, R., Pratibha, S. (2014). Zeolite supported cobalt catalysts for sodium borohydride hydrolysis. *Applied Mechanics and Materials*, (Vols. 490–491, pp. 213–217). Trans Tech Publications, Ltd. <https://doi.org/10.4028/www.scientific.net/AMM.490-491.213>
58. Balkanlı, E., Figen, H. E. (2019). Sodium borohydride hydrolysis by using ceramic foam supported bimetallic and trimetallic catalysts. *International Journal of Hydrogen Energy*, 44(20), 9959-9969. <https://doi.org/10.1016/j.ijhydene.2018.12.010>

59. Ding, X. L., Yuan, X., Jia, C., Ma, Z. F. (2010). Hydrogen generation from catalytic hydrolysis of sodium borohydride solution using Cobalt-Copper-Boride (Co-Cu-B) catalysts. *International Journal of Hydrogen Energy*, 35(20), 11077-11084. <https://doi.org/10.1016/j.ijhydene.2010.07.030>
60. Netskina, O. V., Tayban, E. S., Ozerova, A. M., Komova, O. V., Simagina, V. I. (2019). Solid-state NaBH₄/Co composite as hydrogen storage material: Effect of the pressing pressure on hydrogen generation rate. *Energies*, 12(7), 1184. <https://doi.org/10.3390/en12071184>
61. Shih, Y. J., Su, C. C., Huang, Y. H., Lu, M. C. (2013). SiO₂-supported ferromagnetic catalysts for hydrogen generation from alkaline NaBH₄ (sodium borohydride) solution. *Energy*, 54, 263-270. <https://doi.org/10.1016/j.energy.2013.01.063>
62. Huang, Y., Wang, Y., Zhao, R., Shen, P. K., Wei, Z. (2008). Accurately measuring the hydrogen generation rate for hydrolysis of sodium borohydride on multiwalled carbon nanotubes/Co-B catalysts. *International Journal of Hydrogen Energy*, 33(23), 7110–7115. <https://doi.org/10.1016/j.ijhydene.2008.09.046>
63. Aydin, M., Hasimoglu, A., Ozdemir, O. K. (2016). Kinetic properties of Cobalt-Titanium-Boride (Co-Ti-B) catalysts for sodium borohydride hydrolysis reaction. *International Journal of Hydrogen Energy*, 41(1), 239-248. <https://doi.org/10.1016/j.ijhydene.2015.09.105>
64. Baydaroglu, F., Özdemir, E., Hasimoglu, A. (2014). An effective synthesis route for improving the catalytic activity of carbon-supported Co-B catalyst for hydrogen generation through hydrolysis of NaBH₄. *International Journal of Hydrogen Energy*, 39(3), 1516-1522. <https://doi.org/10.1016/j.ijhydene.2013.04.111>
65. Niu, W., Ren, D., Han, Y., Wu, Y., Gou, X. (2012). Optimizing preparation of carbon supported cobalt catalyst for hydrogen generation from NaBH₄ hydrolysis. *Journal of Alloys and Compounds*, 543, 159-166. <https://doi.org/10.1016/j.jallcom.2012.07.099>
66. Şimşek, T., Barış, M. (2017). Synthesis of Co₂B nanostructures and their catalytic properties for hydrogen generation. *Bor Dergisi*, 2(1), 28–36. <https://dergipark.org.tr/tr/pub/boron/issue/28112/298507>
67. Fan, M. Q., Liu, S., Sun, W. Q., Fei, Y., Pan, H., Lv, C. J., Chen, D., Shu, K. Y. (2011). Hydrogen generation from Al/NaBH₄ hydrolysis promoted by Li-NiCl₂ additives. *International Journal of Hydrogen Energy*, 36(24), 15673–15680. <https://doi.org/10.1016/j.ijhydene.2011.08.114>
68. Li, Z., Li, H., Wang, L., Liu, T., Zhang, T., Wang, G., Xie, G. (2014). Hydrogen generation from catalytic hydrolysis of sodium borohydride solution using supported amorphous alloy catalysts (Ni-Co-P/γ-Al₂O₃). *International Journal of Hydrogen Energy*, 39(27), 14935–14941. <https://doi.org/10.1016/j.ijhydene.2014.07.063>
69. Uysal, F. F., Bahar, S. (2018). Cüruf çeşitleri ve kullanım alanlari. *Trakya University Journal of Engineering Sciences*, 19(1), 37–52.

70. Balçıkanlı, M. (2016). Alkalilerle Aktive Edilmiş Çimentosuz Cürüflu Betonların Mekanik ve Geçirimsizlik Özellikleri ve Üretim Optimizasyonu. (Master Thesis). Iskenderun Technical University, Hatay.
71. Huang, X., Huang, T., Li, S., Muhammad, F., Xu, G., Zhao, Z., Yu, L., Yan, Y., Li, D., Jiao, B. (2016). Immobilization of chromite ore processing residue with alkali-activated blast furnace slag-based geopolymer. *Ceramics International*, 42(8), 9538–9549. <https://doi.org/10.1016/j.ceramint.2016.03.033>
72. Nkinamubanzi, P.C., Baalbaki, M., Bickley, J., Aitcin, P.C. (1998). The use of slag for making high performance concrete. *Sixth NCB International Seminar on Cement and Building Materials*, (pp. 13-39). Place: New Delhi: NCB.
73. Pal, S. C., Mukherjee, A., Pathak, S. R. (2003). Investigation of hydraulic activity of ground granulated blast furnace slag in concrete. *Cement and Concrete Research*, 33(9), 1481–1486. [https://doi.org/10.1016/S0008-8846\(03\)00062-0](https://doi.org/10.1016/S0008-8846(03)00062-0)
74. Balcikanli, M., Ozbay, E. (2016). Optimum design of alkali activated slag concretes for the low oxygen/chloride ion permeability and thermal conductivity. *Composites Part B: Engineering*, 91, 243-256. <https://doi.org/10.1016/j.compositesb.2016.01.047>
75. Yazici, H., Yardimci, M. Y., Yiğiter, H., Aydin, S., Türkel, S. (2010). Mechanical properties of reactive powder concrete containing high volumes of ground granulated blast furnace slag. *Cement and Concrete Composites*, 32(8), 639-648. <https://doi.org/10.1016/j.cemconcomp.2010.07.005>
76. Kwon, S. M., Kang, S., Kim, T. (2019). Development of NaBH₄-based hydrogen generator for fuel cell unmanned aerial vehicles with movable fuel cartridge. *Energy Procedia*, 158, 1930-1935. <https://doi.org/10.1016/j.egypro.2019.01.443>
77. Okumus, E., Boyaci San, F. G., Okur, O., Turk, B. E., Cengelci, E., Kilic, M., Karadag, C., Cavdar, M., Turkmen, A., Yazici, M. S. (2017). Development of boron-based hydrogen and fuel cell system for small unmanned aerial vehicle. *International Journal of Hydrogen Energy*, 42(4), 2691-2697. <https://doi.org/10.1016/j.ijhydene.2016.09.009>
78. Lee, C. J., Kim, T. (2015). Hydrogen supply system employing direct decomposition of solid-state NaBH₄. *International Journal of Hydrogen Energy*, 40(5), 2274–2282. <https://doi.org/10.1016/j.ijhydene.2014.12.032>
79. Türker, H. T., Balçıkanli, M., Durmuş, I. H., Özbay, E., Erdemir, M. (2016). Microstructural alteration of alkali activated slag mortars depend on exposed high temperature level. *Construction and Building Materials*, 104, 169-180. <https://doi.org/10.1016/j.conbuildmat.2015.12.070>
80. İskenderoğlu, F. C., Baltacıoğlu, M. K. (2021). Effects of blast furnace slag (BFS) and cobalt-boron (Co-B) on hydrogen production from sodium boron hydride. *International Journal of Hydrogen Energy*, 46(57), 29230-29242. <https://doi.org/10.1016/j.ijhydene.2020.12.219>
81. URL 5: “Alicat M-series gas mass flow meter”. https://www.alicat.com/product/mass-flow-meters/#g_device-selection Last Access Date: 04.01.2022

82. Müller, M. (2019). Heat transfer in bioreactors. *Comprehensive Biotechnology (Third Edition)*, 2, (p. 133–150). Publisher: Elsevier. <https://doi.org/10.1016/B978-0-444-64046-8.00140-3>
83. Ulaganathan, M. K. D., Saravanan, C., Chitranjan, O. R. (2014). Cost-effective perturb and observe mppt method using arduino microcontroller for a standalone photo voltaic system. *International Journal of Engineering Trends and Technology*, 8(1), 24–28. <https://doi.org/10.14445/22315381/ijett-v8p205>
84. Biansoongnern, S., Plungkang, B., Susuk, S. (2016). Development of low cost vibration sensor network for early warning system of landslides. *Energy Procedia*, 89, 417–420. <https://doi.org/10.1016/J.EGYPRO.2016.05.055>
85. Robles-Ocampo, J. B., Medoza-Gonzalez, C., Balboa-Ríos, J., Peña-Gomar, G., Palacios, M. J., Sevilla-Camacho, P. Y. (2014). Solar plane collector for dehydration of chamomile. *Energy Procedia*, 57, 2249–2254. <https://doi.org/10.1016/j.egypro.2014.10.232>
86. URL 6: “Arduino uno rev3”. <https://store.arduino.cc/arduino-uno-rev3> Last Access Date: 04.01.2022
87. URL 7: “Water solenoid valve”. <https://www.robotistan.com/solenoid-water-valve-12v-12inch> Last Access Date: 04.01.2022
88. URL 8: “Nozzle”. https://www.zavlazovaci-systemy.net/tryska-rain-bird-van-4-rozprasovaci-0-330_z1029/ Last Access Date: 04.01.2022
89. URL 9: “Relay”. <https://www.robotistan.com/1-way-5v-relay-module-tekli-5v-role-karti> Last Access Date: 04.01.2022
90. URL 10: “Buzzer”. <https://www.farnell.com/datasheets/2891560.pdf> Last Access Date: 04.01.2022
91. URL 11: “Regulator”. <https://www.robotistan.com/voltage-regulator-33v-voltaj-regulatoru-lf33abv> Last Access Date: 04.01.2022
92. URL 12: “Gas sensor”. <https://www.robotistan.com/gas-sensor-11028> Last Access Date: 04.01.2022
93. URL 13: “Temp sensor”. <https://www.robotistan.com/gas-sensor-11028> Last Access Date: 04.01.2022
94. URL 14: “XRD”. <https://iste.edu.tr/iste-btm/xrd-lab> Last Access Date: 04.01.2022
95. URL 15: “XRD Device”. <https://www.malvernpanalytical.com/es/products/product-range/empyrean-range/empyrean> Last Access Date: 04.01.2022
96. URL 16: “SEM”. <https://iste.edu.tr/iste-btm/sem-lab> Last Access Date: 04.01.2022
97. URL 17: “SEM Device”. <https://snsf.stanford.edu/facilities/eim/apreo> Last Access Date: 04.01.2022

98. Coban, S., Bilgic, H. H., Akan, E. (2020). Improving autonomous performance of a passive morphing fixed wing UAV. *Information Technology and Control*, 49(1). <https://doi.org/10.5755/j01.itc.49.1.23275>
99. Conker, C., Baltacioglu, M. K. (2020). Fuzzy self-adaptive PID control technique for driving HHO dry cell systems. *International Journal of Hydrogen Energy*, 45(49), 26059-26069. <https://doi.org/10.1016/j.ijhydene.2020.01.136>
100. Kumar, S., Panda, A. K., Singh, R. K. (2013). Preparation and characterization of acids and alkali treated kaolin clay. *Bulletin of Chemical Reaction Engineering and Catalysis*, 8(1), 61-69. <https://doi.org/10.9767/bcrec.8.1.4530.61-69>
101. Zhang, Q., Wu, Y., Sun, X., Ortega, J. (2007). Kinetics of catalytic hydrolysis of stabilized sodium borohydride solutions. *Industrial and Engineering Chemistry Research*, 46(4), 1120–1124. <https://doi.org/10.1021/ie061086t>
102. Amendola, S. C., Sharp-Goldman, S. L., Saleem Janjua, M., Kelly, M. T., Petillo, P. J., Binder, M. (2000). An ultrasafe hydrogen generator: Aqueous, alkaline borohydride solutions and Ru catalyst. *Journal of Power Sources*, 85(2), 186-189. [https://doi.org/10.1016/S0378-7753\(99\)00301-8](https://doi.org/10.1016/S0378-7753(99)00301-8)
103. Boran, Asli, Erkan, S., Ozkar, S., Eroglu, I. (2013). Kinetics of hydrogen generation from hydrolysis of sodium borohydride on Pt/C catalyst in a flow reactor. *International Journal of Energy Research*, 37(5), 443-448. <https://doi.org/10.1002/er.3007>
104. Guo, J., Hou, Y., Li, B., Liu, Y. (2018). Novel Ni–Co–B hollow nanospheres promote hydrogen generation from the hydrolysis of sodium borohydride. *International Journal of Hydrogen Energy*, 43(32), 15245-15254. <https://doi.org/10.1016/j.ijhydene.2018.06.117>
105. Saha, S., Basak, V., Dasgupta, A., Ganguly, S., Banerjee, D., Kargupta, K. (2014). Graphene supported bimetallic G-Co-Pt nanohybrid catalyst for enhanced and cost effective hydrogen generation. *International Journal of Hydrogen Energy*, 39(22), 11566-11577. <https://doi.org/10.1016/j.ijhydene.2014.05.131>
106. Hua, D., Hanxi, Y., Xinping, A., Chuansin, C. (2003). Hydrogen production from catalytic hydrolysis of sodium borohydride solution using nickel boride catalyst. *International Journal of Hydrogen Energy*, 28(10), 1095-1100. [https://doi.org/10.1016/S0360-3199\(02\)00235-5](https://doi.org/10.1016/S0360-3199(02)00235-5)
107. Didehban, A., Zabihi, M., Shahrouzi, J. R. (2018). Experimental studies on the catalytic behavior of alloy and core-shell supported Co-Ni bimetallic nano-catalysts for hydrogen generation by hydrolysis of sodium borohydride. *International Journal of Hydrogen Energy*, 43(45), 20645-20660. <https://doi.org/10.1016/j.ijhydene.2018.09.127>
108. Hung, A. J., Tsai, S. F., Hsu, Y. Y., Ku, J. R., Chen, Y. H., Yu, C. C. (2008). Kinetics of sodium borohydride hydrolysis reaction for hydrogen generation. *International Journal of Hydrogen Energy*, 33(21), 6205-6215. <https://doi.org/10.1016/j.ijhydene.2008.07.109>

INDEX

4

4 Reaction Chambers · 51

A

Abstract · İ, İv
 Acid-Treated BFS · İ, Xv, 43, 47,
 60, 62, 64, 65, 66
 Adunio Uno · İ, İi
 Aqueous Solution · 28, 45
 Autonomous Control · İ, Xiv, 49,
 50, 52, 53
 Autonomous Hydrogen
 Generator · 3, 77, 78
 Autonomous Performance · Vi,
 76
 Autonomous Systems · 1, 2, 5, 8,
 9, 49
 Auxiliary Equipment · 2, 50

B

Batteries · 1, 6, 8, 54, 83, 86

Battery Technologies · Vii, 6, 7,
 8
 BFS Katalizör · İi
 BFS · İv, Xiv, İv, 25, 98
 By-Products · 27, 80, 81, 83

C

Carbon Black · 24
 Catalysts Synthesized · İ
 Catalytic Structure · 23
 Chemical compound · Vii, 26, 31
 Chemical compounds · 26
Chemical Hydride · 18
 Chemical Materials · V
 Clay · 23, 24
 Climate Change · 5, 6
 Co Micron Powder · Vii, 30
 Co-B Catalyst · İ, Xiv, Xv, 3, 22,
 43, 44, 45, 47, 56, 57, 59, 60,
 62, 69, 70, 71, 77, 83, 88, 90,
 92
 Cobalt · V, Vii, 24, 28, 62, 79,
 89, 91, 92, 94, 98
 Conclusions · Vi
 Control Card · V, 4, 49, 52, 53

Control System Algorithms · V,
 52, 53
 Control Unit · 4, 50
 Cost-Effective · 13, 20
 Cüruf · İi, 93

D

Discussions · Vi, 79
 Distilled Water · İ, 43, 44, 45, 47,
 66, 75, 77
 Duty Times · 7, 10, 83

E

Efficiently · İ, 3, 5
 Electronic · V, 1, 8, 9, 35, 39, 49
 Energy Carrier · Xiv, 14, 87
 Energy Demand · 1, 6
Energy Density · 7
 Energy Production · İv, 5
 Energy Required · 1, 3, 10
 Energy Storage · İv, 1, 6, 15, 16,
 20, 21, 83, 86
 Experimental Methods · V, 29

Experimental Setup · V, 46, 47,
48, 50, 51, 52

F

Fuel Cell Applications · İv, 13
Fuel Cells · 1, 3, 7, 8, 9, 15, 85,
86, 88, 89, 90

G

Gas Barrier · 3, 48
Gas Sensor · Xiv, 40
GBFS · İv, 30, 31, 43, 44, 45
Global Warming · 6
Granulated · Xiv, 30, 93
Greenhouse Gas · 6

H

Hcl Acid · V, Xiv, Xv, 29, 43,
45, 47, 56, 57, 60, 62, 66, 72
Hidrojen Gazı · İi
High Applicability · 4
High Energy Density · 4
High Metal Content · İ, 2, 81, 83
Hydrogen Production
Performance · V
Hydrogen Flow Rates · İ, 98
Hydrogen Gas · İ, 3, 14, 17, 22,
32, 40, 46, 47, 48, 49, 50, 52,
62, 64, 66, 69, 70, 71, 75, 76,
81, 83
Hydrogen Gas · Xiv, 13, 14
Hydrogen Generator System ·
Xiv, 28, 49, 50, 51
Hydrogen Generators · İ, 28, 83
Hydrogen Generators · İv, 27
Hydrogen Production · İ, V, Vi,
Vii, Xv, Xvi, 1, 2, 4, 15, 20,
21, 22, 23, 24, 25, 27, 28, 49,
60, 61, 62, 63, 64, 66, 67, 68,
69, 70, 71, 72, 73, 75, 76, 77,
79, 81, 83, 88, 91, 94, 98

Hydrogen Storage · Vii, 1, 2, 3,
4, 13, 15, 16, 18, 20, 21, 28,
87, 92

Hydrogen Tank · Vii, 1, 9

Hydrolysis · İ, V, Xv, Xvi, 2, 3,
21, 22, 23, 24, 25, 43, 46, 47,
48, 52, 60, 61, 63, 64, 65, 66,
67, 68, 69, 70, 71, 72, 73, 75,
76, 77, 79, 81, 82, 83, 88, 89,
90, 91, 92, 95, 96

Hydrolysis Reaction · İ, Xvi, 2,
3, 21, 22, 24, 25, 43, 46, 47,
48, 60, 61, 62, 63, 65, 66, 67,
68, 69, 71, 73, 75, 76, 77, 80,
81, 91, 92, 96

I

İnexpensive · 2, 4, 24
Iron-Steel Factory · Xiv, 25

L

Leakage · 4
Literature · İv, 5
Low Cost · 4, 39

M

Magnetic Stirrer · 32
Manual Performance · Vi, 75
Materials · V, 29
Microcontroller · 4, 34, 36, 37,
48, 49

N

NaBH₄ · İ, İi, İv, V, Vi, Vii, Xv,
İv, 1, 2, 3, 4, 12, 18, 20, 21,
22, 23, 24, 25, 27, 28, 29, 30,
43, 44, 45, 46, 47, 48, 50, 60,
61, 62, 63, 64, 65, 66, 67, 68,
69, 70, 71, 72, 73, 74, 75, 77,

79, 80, 81, 82, 83, 88, 89, 90,
91, 92, 93, 94

NaBH₄ Hydrolysis · 2, 22, 25,
46, 60, 62, 63, 64, 71, 72, 80,
83

Noble Metal Catalysts · İ, 22, 80

Nozzle · Vii, 36, 37, 50

O

O₂ · İv, 8, 12

Objectives · İv, 2

ÖZET · İi, İv

P

Parameter Tests · 4
PEMFC · İv, 7, 9, 13, 86
Performance Effect · V, Vi, 60,
62, 66
Performance Tests · İ, 49, 50
Piezo Buzzer · Vii, Xiv, 39
Plexiglass · Vii, 4, 35, 51
Portable · İ, İv, 6, 98
Portable Technologies · 1, 5, 7, 9
Power Supply · 1, 7, 9
Power Supply · İv, 6
Principles · İv, 2
Product · 2, 5, 8, 24, 25, 26, 27,
80, 81, 94
Production Flowrate · Xv, Xvi,
75
Prototype · İ, V, Vi, 1, 3, 4, 29,
30, 35, 48, 49, 50, 52, 75, 76,
77, 81, 83
Prototype Application · İ, İi, İ
Prototype Design · V, Vi, 49, 75
Prototype Design · V, 29
PT-100 Thermocouple · Xiv, 33
PVA · Vi, Xv, 48, 72, 73, 74

R

Raw BFS · Xiv, Xv, Xiv, 3, 43,
44, 45, 47, 55, 59, 60, 61, 62,
63, 64, 79

Reaction Chamber · 4, 49

Reaction Temperature · I, 46, 47,
63, 70, 81, 83

Reaction Vessel · 46, 47, 52, 62,
66, 68

References · Vi, 85

Refilling · 4

Relay · Xiv, 37, 38, 94

Renewable Energy · 6, 9, 15

Resistor · Xiv, 38

Result · I, 3, 4, 5, 6, 24, 25, 31,
32, 48, 56, 58, 61, 69, 73, 80,
83

S

Scanning Electron Microscopy ·
42

Self-Decision Mechanism · 4

SEM · V, Xv, 3, 41, 42, 58, 59,
60

SEM Characterization · V

Slag · I, Vii, Xiv, 2, 24, 25, 26,
27, 29, 30, 31, 41, 42, 45, 55,
56, 59, 60, 80, 81, 83, 93, 94,
98

Sodium Boron Hydride · 1, 3, 94,
98

Solid-State Nabh₄ · 2, 47, 83

Storage System · 4, 82, 87

Storage Techniques · 15, 17

Support Materials · 22

Surface Area · 23, 31, 45, 59, 61

T

Technical features · Vii, 35, 36,
37, 39

Temperature Sensor · Xiv, 40, 41

Temperature Variation · Xv

Test Results · I, 49, 50, 52

Test Rig · V, Xiv, 46, 47, 48, 49

Thermocouples · 33

Tools · V, 32

Total Hydrogen Production · Xv,
Xvi, 61, 63, 65, 71, 72, 73, 74,
76

Transportation · 1, 7, 9, 15, 21

U

UAV · Vii, 2, 5, 13, 15, 28, 95

V

Voltage Regulator · Xiv, 39, 40

W

Water Solenoid Valve · Vii, 36

Working Algorithm · Xiv, 4, 53

X

X-Ray Diffraction · 41

X-Ray Fluorescence Analysis ·
31

XRD · V, Xiv, Xv, Xiv, 3, 41,
42, 55, 56, 57, 95

XRD Characterization · V, 55

XRD Pattern · Xiv, 55, 56, 57



TEKNOVERSİTE



teknoversite **AYRICALIĞINDASINIZ**

İSTE

